STUDIES ON SOME FLUORESCENT SYSTEMS WITH INTRAMOLECULAR CHARGE TRANSFER EMITTING STATES

A THESIS
SUBMITTED FOR THE DEGREE OF
DOCTOR OF PHILOSOPHY

BY

G. SAROJA

SCHOOL OF CHEMISTRY
UNIVERSITY OF HYDERABAD
HYDERABAD 500 046
INDIA

APRIL 1998

to

my parents

CONTENTS

Chapter 4   **Photophysical Behaviour of n-(4-aminophthalimido)aIkanes in Polar Media and its Implications**

Chapter 5   **4-N,N-Diniethylaminophthalimide and its Fatty Acid Derivative as Sensors in Micellar Media**

Chapter 6   Photophysical Studies on Two Carbostyril Dyes and N,N'-bis(4-Carbomethoxyphenyl)piperazine

STATEMENT

I hereby declare that the matter embodied in this thesis is the result of investigation carried out by me in School of Chemistry, University of Hyderabad, India under the supervision of **Dr. Anunay Samanta**.

In keeping with the general practice of reporting scientific observations, due acknowledgements has been made wherever the work described is based on the findings of other investigators. Any omission which might have occurred by oversight or error is regretted.

G. Saroja

CERTIFICATE

Certified that the work contained in the thesis entitled *"Studies on Some Fluorescent Systems With Intramolecular Charge Transfer Emitting States"* has been carried out by Ms. G. Saroja under my supervision and the same has not been submitted elsewhere for any degree.
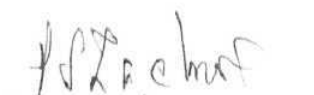
Hyderabad

May 1998

Anunay Samanta

(Thesis Supervisor)

Dean

School of Chemistry

ACKNOWLEDGEMENTS

Finally, I am thankful to my parents, who brought me to the stage where I stand and for their inspiring encouragement to my higher education without which my research would have been impossible. I am also thankful to my all cousins who have inspired me from their excellent academic record and higher education, which has given me a proper direction to pursue my education. Lastly, but not leastly, I thank my brothers for their love and co-operation.

G. Saroja

Research Publications

1. Polarity of the micelle-water interface as seen by 4-aminophthalimide, a solvent sensitive fluorescence probe

   G. Saroja and A. Samanta, *Chem. Phys. Lett.,* 246, 506, 1995.

2. Photophysical study of two Carbostyril dyes: investigation of the possible role of a rotary decay mechanism

   G. Saroja, N. B. Sankaran and A. Samanta, *Chem. Phys. Lett.,* 249, 392, **1996**.

3. Photophysical studies on a fluorescence probe labelled fatty acid: Chain folding in a micellar environment

   G. Saroja and A. Samanta, *J. Chem. Soc, Faraday Trans.,* 92, 2697, **1996.**

4. Ground and excited state dipole moments of N-N'-bis(4-carbomethoxyphenyl)piperazine and its Implications

   G. Saroja, N. P. Rath and A. Samanta, *J. Chem. Res.,* 332, 1997.

5. Photophysical behaviour of some Pyrenylethylene derivatives and its Implication on Trans-->Cis Photoisomerisation Reactions

   V. Raj Gopal, V. Jayathirtha Rao, G. Saroja and A. Samanta, *Chem. Phys. Lett.,* 270, 593, 1997.

iv

6. Steady state and time-resolved studies on the redox behaviour of 1,8-naphthalimide in excited state

    A. Samanta and G.Saroja, *J. Photochem. Photobiol, A: Chem.,* 84, 19, 1994.

7. AMI study of the twisted intramolecular charge transfer phenomenon in p-(N,N-dimethylamino)benzonitrile

    T. Soujanya, G. Saroja and A. Samanta, *Chem. Phys. Lett.,* 236, 503, 1995.

8. An investigation of the triplet state properties of 1,8-naphthalimide: a laser flash photolysis study

    A. Samanta, B. Ramachandram and G. Saroja, *J. Photochem. Photobiol., A: Chem.,* 101,29, 1996.

9. 4-Aminophthalimide derivatives as environment sensitive probes

    G. Saroja, T. Soujanya, B. Ramachandram and A. Samanta, communicated.

10. Hydrophobicity induced aggregation of N-alkyl-4-aminophthalimide derivatives in aqueous media

    G. Saroja and A. Samanta, to be communicated.

11. The fluorescence response of a structurally modified 4-aminophthalimide derivative covalently attached to a fatty acid in homogeneous and micellar environment

    G. Saroja, B. Ramachandram and A. Samanta, to be communicated.

CHAPTER 1

INTRODUCTION

This chapter gives a brief introduction on the photoinduced charge separation process with emphasis on twisted intramolecular charge transfer (TICT) phenomenon. Subsequently, fluorescence studies on the micellar media are summarised briefly. The chapter ends with a description of the motivation of the present work and the layout of the thesis.

1.1. Photoinduced Charge Separation at Molecular Level

Photoinduced charge separation (PECS) reactions occupy a central position in the chemistry of life. Over the past decades, a significant effort has been devoted to the study of PECS as a means of capturing and storing solar energy.[1] Photoinduced energy and electron transfer processes in artificial multicomponent systems are currently the object of extensive studies.[2] The interest on these processes can be related to the following goals: i) a better understanding of natural photosynthesis;[3] ii) the design of supramolecular luminescent systems capable of sensing environments;[4] iii) the construction of nanometer scale wires,[5a] switches,[5b] logic gates,[5c] and other components for

the development of molecular electronic devices.[6] The development of non-linear optical materials is also primarily based on charge-transfer phenomenon.[7]

Mulliken introduced the concept of the charge transfer transition to describe the spectral and bonding interactions of molecular complexes formed between an electron donor and acceptor[8] Weller was first to show that a charge-transfer complex can be formed between an excited and a ground state species,[9] even though no complex formation could be detected in the ground state. Such an excited molecular complex is termed as exciplex.[9] In systems involving flexible spacers, the charge transfer complex or exciplex is often formed by conformational changes occurring in the spacer, where the donor (D) and the acceptor (A) moieties come closer, thus allowing charge transfer to occur by D-A orbital overlap.[10] In systems with limited conformational flexibility, where through-space interaction of the D and A orbitals is not possible, the charge separation can take place as a result of through-bond interaction of the D and A orbitals. There has been considerable effort thorough model systems comprising electron D and A groups linked covalently through π or σ bond to investigate the dependence of the electron transfer rates on the free energy of reaction, D-A distance, orientation and solvent.[2,11] PECS has also been studied in great detail in an attempt to minimise the back electron transfer steps so that these materials could be useful for molecular devices.[12] Many systems are reported in the literature to demonstrate that efficient PECS can occur over large distances.[13] One of the most spectacular of which is to be

found in the photosynthetic reactions centres of certain photosynthetic bacteria. [14]

Since charge separation on a molecular level is often involved, the study of the model systems displaying charge separation is essential to understand the mechanisms involved. In the fortuitous case of luminescent charge transfer (CT) state, the CT emission provides an excellent opportunity to monitor their dynamics because internal and environmental influences affect this luminescence in characteristic way yielding detailed information on their thennodynamic, kinetic and other Photophysical and even photochemical properties of such species. The Photophysical techniques such as steady-state, time-resolved fluorescence and transient absorption studies are useful to detect the CT states. Luminescent molecules are also known for their extensive utility in the study of molecular organisation and dynamics in macromolecules [15,23] and organised assemblies such as proteins, [16,19,23] micelles, [17-22,23] cyclodextrins and membranes etc. [16-23]

1.2. Twisted Intramolecular Charge Transfer Phenomenon

Over past three decades there has been considerable interest in the Photophysical properties of the D-A compounds formally linked by a single bond. [23-26,28] Since the first report by Lippert [26] on dual fluorescence exhibited by p-(dimethylamino)benzonitrile (DMABN), a vast number of studies have been devoted to elucidation of the mechanism of the intramolecular charge

transfer (ICT) emission in systems where the D and A moieties are linked by a single bond.[23-26,28] Lippert originally proposed that there are two excited states, a highly polar state (A band, ^1L_a state in Platt's notation[27]) and relatively nonpolar state (B band, ^1L_b, state), responsible for the long and short wavelength emission, respectively. Later Grabowski et al, [28] on the basis of experimental studies on model compounds such as 1-4, proposed the TICT concept to account for the dual-luminescence. According to this hypothesis, the primary excited

1   **2**   **3**   **4**
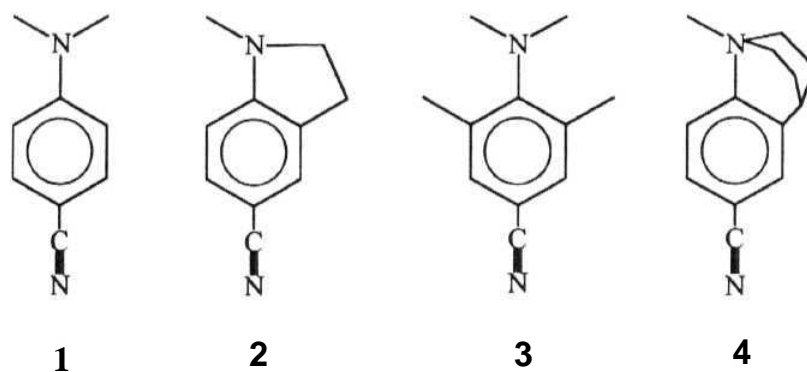
state of D-A molecules (for e.g., p-dialkylamino derivatives of benzonitrile) converts to a highly polar fluorescent state with a mutually perpendicular confirmation of the D^+ and A^- moieties. The π-electronic decoupling of the D^+ and A^- moieties leads to a full charge separation and consequently, to a large dipole moment and a considerable solvent reorientational energy.[23-26,28] Dual luminescence is believed to be due to the emission from the substrate

locally excited (LE) state (planar conformation) and the product TICT state (twisted conformation). The energetic situation, as can be extracted from the spectra of DMABN and related compounds, is depicted in Fig 1.1.
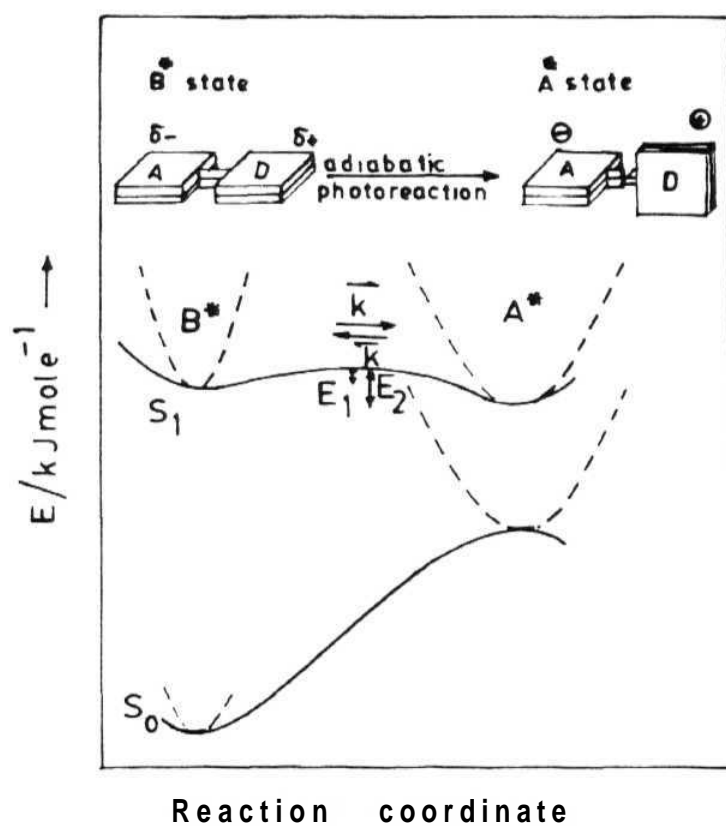
Fig. 1.1. A schematic representation of the TICT phenomenon.

There have been numerous studies, on a wide variety of systems, primarily for the verification of the TICT mechanism. Observation of TICT like emission from the molecules already twisted in the ground state, absence of the second emission in rigidized systems,[29] consistency of the excited state dipole moment with a large degree of intramolecular separation of charge,[30] observation of radical anion in transient absorption spectroscopic measurements,[31] observation of dual fluorescence in vapour phase[32] and many others[23,24] have given this mechanism a strong basis. Apart from molecules containing dialkylamino or arylamino groups, TICT is reported for a host of other molecules, e.g. biaryls, amides etc.[1,2] and recently for 3H-indoles.[33] Even though dual emission is observed for many compounds, a non-emissive TICT has also been proposed in many cases.[34,35,127]

Several other models have been offered in the literature to account for the dual emission in DMABN and its derivatives, e.g. solute-solvent exciplex formation,[36] the so called pseudo-Jahn-Teller coupling effect and/or change in pyramidalisation of the amino nitrogen[37] and the recently proposed model that assumes a bending of the cyano group.[38] Some of these models have been criticised.[39,40]

The most important feature of the TICT states is the transfer of exactly one unit of electronic charge from D to A which can be verified by experimental measurement of the dipole moment of charge separated species. A number of external and internal factors influence the TICT formation rate. The electron

donor and the acceptor strength of the substituents,[24,28] ground state twist angle,[29a,d,41] rotating volume of the twisting group[42] and molecular shape are some of the factors which determine the rate of TICT formation. An increase in the polarity is expected to stabilise the TICT state by solvation and hence should favour the TICT process.[23,24] To account for the observation of an increase in the TICT rate increase with increase in the polarity of the medium, Eisenthal et al[43] proposed a polarity dependent activation barrier (Eg) which decreases linearly with increase in polarity as in equn. 1.1, where $E_T(30)$ is the microscopic polarity parameter (defined in sec. 2.1.1) and E_B^0 is the barrier in a hydrocarbon having an $E_T(30)$ value of 30 kcal/mol.

$$E_B = E_B^0 - A\left[E_T(30) - 30\right] \qquad 1.1$$

Thus the overall rate, k_T is given by equn. 1.2.

$$k_T = k_T^0 \exp\left(-E_B^0 \big/ RT\right)\exp\left[A\left\{E_T(30) - 30\right\}\big/ RT\right] \qquad 1.2$$

This relation accounts for a linear relation between $\log k_T$ and $E_T(30)$. Increase in viscosity is likely to hinder the twisting motion, thereby retarding the TICT process.[44] Pressure also affects the rate of TICT process as it changes the solvent viscosity and dielectric constant which play a vital role in determining the rate.[45,46]

7

The dramatic dependence of the TICT process on solvent polarity has attracted a large number of theoretical studies on the solvents effects on TICT, classified as stochastic models and quantum chemical methods.[23] In the stochastic models, the overall rate is obtained by statistical treatment or mechanical model (e.g. Langevin equations) incorporating the solvent effect as a friction term.[47] The second approach is based on quantum chemical calculation of the potential energy surface with twist angle as the reaction co-ordinate for isolated molecules and in the presence of solvents.[39,48-53] The semi-empirical calculation based on various methods such as INDO[48], MNDO,[49] CNDO[50] and AMI methods[33b, 39, 51,52] *and ab initio* studies,[38,40] have been performed to describe the anomalous behaviour of DMABN and similar systems. Most of the calculations support the TICT mechanism.

1.3. An Introduction to Micelles

The organised systems can be broadly classified into three types: 1) organised assemblies composed of surfactants and lipids such as micelles, vesicles, liposomes, mono and multilayers, microemulsions, and liquid crystals; 2) supramolecular host systems with large cavities capable of accommodating small guest molecules and ions such as zeolites, clays and cyclodextrins etc.; 3) adsorbed molecules on reactive and non-reactive surfaces e.g. silica, porous glass etc. These systems are generally called 'microheterogeneous' to indicate their heterogeneous character at the microscopic level with the presence of

interfaces separating distinct hydrophobic and hydrophilic domains. A good majority of these systems provide optically clear solutions readily amenable to photochemical studies. [54] Organised surfactant aggregates, micelles, microemulsions etc. have been extensively exploited for developing chemistry based on membrane-mediated processes. [54] Micelles have been proposed as simple model systems for a variety of important two-phase systems such as monolayers, colloids, proteins, enzymes and membranes. [54-56] Micelle-water interface incorporates the dielectric asymmetry and microenvironments typical of other interfacial systems, thus extremely useful for posing and answering problems regarding microenvironments encountered in interfacial systems of other complex systems of biological interest. The formation of micelles is one of the most spectacular example of hydrophobic interactions. [55] Therefore, simple micelles provide models for the investigation of hydrophobic interactions, a crucial problem in understanding the stability of biologically important molecules such as protein. Organisation and compartmentalisation in membrane mimetic systems have been exploited for reactivity control, [54] molecular transport, [54,57] recognition, [54,58] artificial photosynthesis [54,59] and target-directed drug deliveries. [54,60] Lastly, but not leastly, organised surfactant assemblies, as the term membrane mimetic implies, can be considered to mode structures and interactions in real membranes. [61]

Micelles refer to aggregates of surfactant molecules of colloidal dimensions and implies a situation in which these aggregates are in mobile

equilibrium with the molecules or ions from which they are formed, i.e. a micelle is a dynamic structure which exists in equilibrium with its monomer. Depending on the chemical composition, micelles can be non-ionic, ionic or ampholytic. Aggregation behaviour depends on the nature and length of the hydrocarbon chain, the head group, concentration, temperature and other additives.[54, 55] A schematic sketch of different possible structures of micelles is shown in Fig. 1.2.
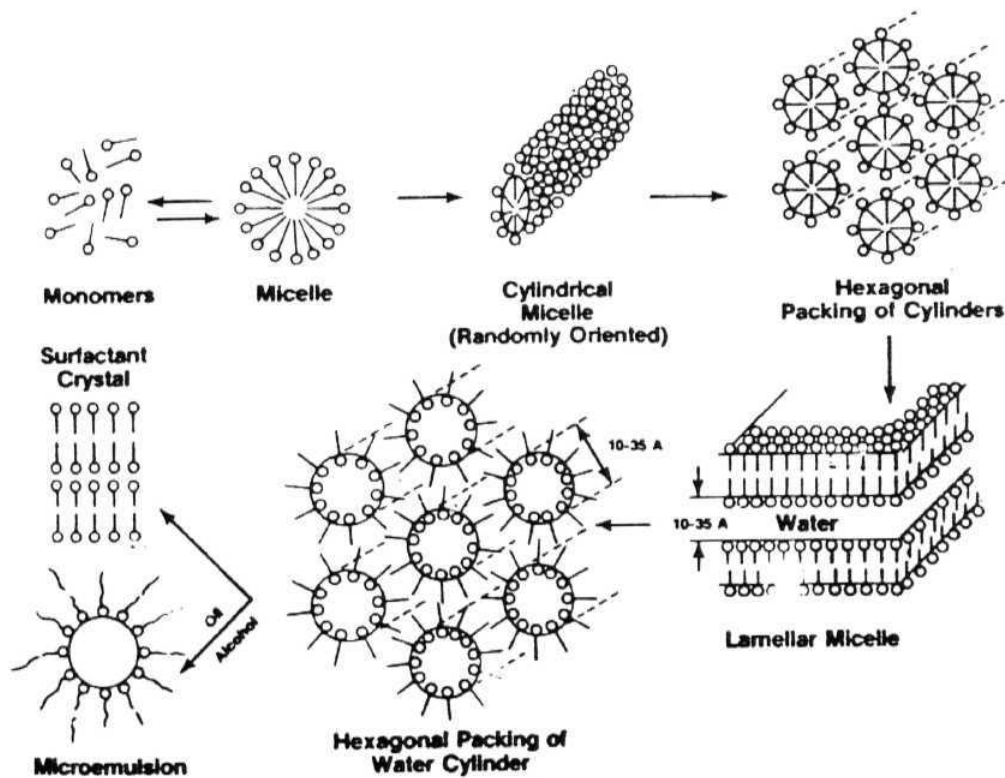
Fig. 1.2. Different structures of micelles and mesophase.

The concentration at which micelles appear corresponds to the critical micelle concentration (CMC). However, the change occurs, over a narrow concentration range rather than a precise point and the magnitude of the range depends somewhat on the physical property being measured. For detergents containing long-chain hydrocarbon groups, the CMC value is usually between 10^{-4} and 10^{-2} M.[54] The addition of strong electrolytes reduces the CMC *of* ionic surfactants but only slightly alters that of nonionic surfactants. Effects of temperature and other factors which alter the CMC are helpful in investigation of micellar catalysis, inhibition, or hydrophobic interactions.[20, 54] The number of monomers in the aggregate, the aggregation number (N) determines the size and the geometry of the micelle and hence an important quantity.[20,54] N ranges for surfactants of 10-18 carbon atoms in *aq* medium generally between 10-150 Like CMC, N is also dependent on the concentration of the surfactant, additives and on the temperature. The conventional methods for the determination of N are light scattering, diffusion, viscosity, NMR and fluorescence techniques.[20,54]

The common picture of a micelle is quite similar to Hartley's original notion of an *oil droplet in a polar coat.*[62] At CMC, the aggregation begins which grow rapidly over a very limited concentration range to a size which for a given surfactant remains approximately constant with further increase in surfactant concentration. Fig. 1.3. shows the conventional representation of the micelle formed by ionic detergents. Typically such micelles have an average radii of 12-13 A containing 20-100 monomers. Depending on the head group

structure, concentration and other experimental variables, the micelle may be roughly spherical, ellipsoidal, disk-like or **rod-shaped**.[54,55,56] Spherical at low concentration and rod-shaped at high concentrations is found to be the case for a wide variety of ionic surfactants. The hydrophobic part of the aggregate forms the *'core'* of the micelle which is liquid-paraffin like in character while the polar
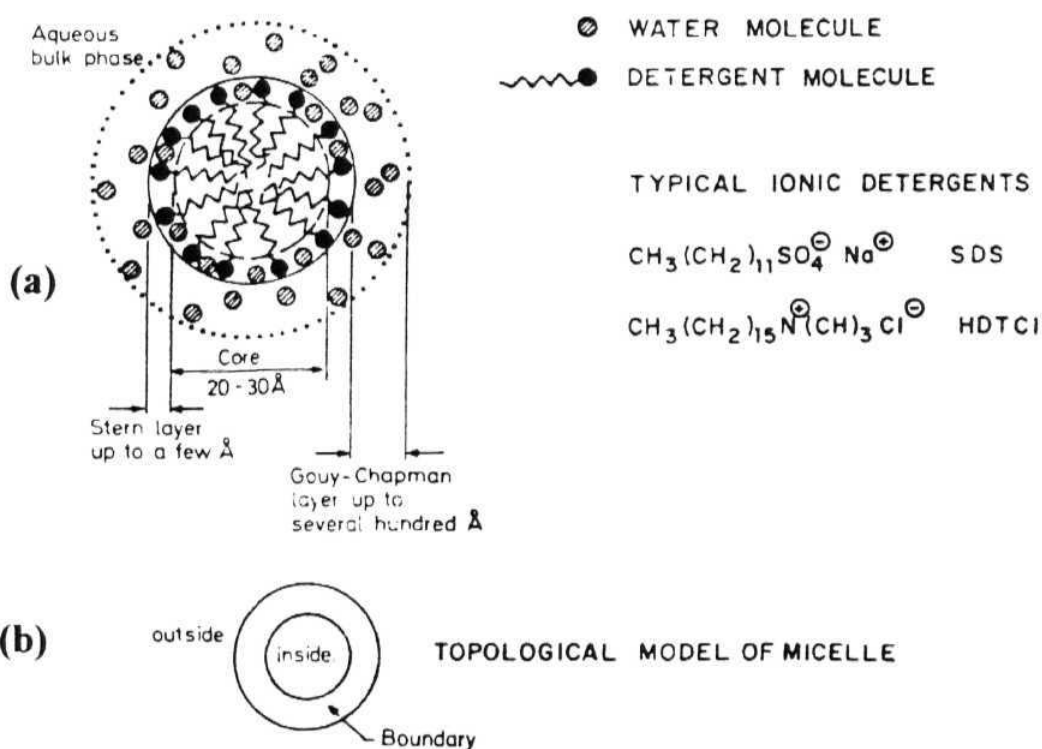
Fig. 1.3. la **and** b. Schematic representation of a typical ionic micelle.

12

head groups are located at micelle-water interface in contact with and hydrated by a number of water molecules. The charged head groups and the small counterions of the ionic micelle are located in a compact region known as the *'Stern layer'*, which extends from the core to a few angstroms beyond the shear surface of the micelle. The compactness of the Stern layer is responsible for the reduction of the net charge on the micelle and is an extremely anisotropic region with properties intermediate between those of water and hydrocarbon (alcohol-like is the common description of its polarity).[54,55] The remaining counterions are however, located outside the shear surface forming diffuse *'Gouy-Chapman'* electrical double layer where they are completely dissociated from the charged aggregate and are able to exchange with the ions in the bulk of the solution. The structure of the small globular micelles formed at low surfactant concentrations is a matter of on going and lively debate[63"69] especially with regard to the question of water penetration in the micelle. Hartley's model cannot be reconciled with any appreciable water-to-hydrocarbon contact. Experimental studies do indicate that depending on the micelle type, water appears to penetrate the micelle to various depths.[65] There have been other models from Dill and Flory,[66] Fromherz,[67] and recently Menger's *reef model* which proposes a loose, porous, and highly disordered cluster comprising of hydrocarbon chains and water.[65] Molecular dynamics simulation method is also being used to investigate the microstructure of micelles theoretically.[70]

Formation of association colloids is not **restricted** to aqueous solutions. In non-aqueous **media,** certain amphiphilic molecules, such as sodium bis(2-**ethylhexyl)sulfosuccinate** (AOT), assemble to form reverse micelles aggregation
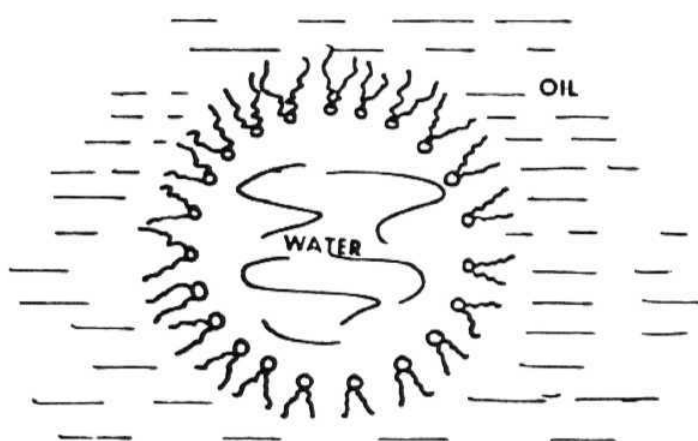
Fig. 1.4. Structure of reversed **micelle.**

in which the polar heads of the **amphiphile** cluster to form a micellar core and the hydrophobic tails extend into the organic bulk **phase.**[54,55,71] Thestructure of a reverse micelle in a nonpolar media is shown in Fig. 1.4. The distinguishing feature of these inverted micelles is their ability to solubilize large amounts of water in the inner core. The ability to control the size of the water pool and the properties of the water present therein itself is a unique feature that a good

14

majority of studies in reversed micelles are devoted to the characterisation of waterpools (size, polarity, viscosity, etc.) and exploitation of various chemical reactions in these waterpools. The waterpool is an interesting model candidate to mimic the water pockets that are often found in various bioaggregates such as proteins, membranes, etc.[71]

1.3.1. Fluorescent Systems for Study of Micellar Media

A considerable amount of effort has been directed over the past decades in determining the physio-chemical properties of self-assembled surfactant aggregates using physical methods such as X-ray, small angle neutron spectroscopy, nuclear magnetic resonance spectroscopy, light scattering etc. Photophysical methods stand apart for their wide scope and extreme sensitivity at very low solute concentrations which is necessary for least perturbation of the host system by the guest molecules.[15-23,56,71,72] Luminescence probes can be thought of as sensors of microenvironments. The photons emitted by such probes are reporters of the local structure in the vicinity of the probe at the time of emission. The basic notion behind the use of a luminescent probe is that luminescence parameters, sensitive to changes in the microenvironments will display experimentally distinct luminescence properties which will characterize uniquely each environment. The various luminescence parameters that are used in this context are the location (λ_{max}), intensity (ϕ), lifetime (τ) and polarisation (P) of the emission. The measured changes in a luminescence probe have been

related to the properties of the environment of the probe as i) polarity; ii) viscosity; iii) diffusion; iv) partitioning between phases; v) roughness of the micelle surface; vi) degree of water penetration into these aggregates; vii) concentration of quenchers and viii) distance between groups.

A variety of probes are documented in the literature whose fluorescence characteristics are altered by the environment for a variety of reasons (polarity, viscosity, pH etc.). The structures of a few commonly used fluorescence probes are shown in Fig. 1.5. The properties or the parameters of the micelles that are most commonly measured by employing fluorescence probes are CMC, mean solvent properties such as polarity and viscosity measured in terms of effective dielectric constant (ef) or $E_T(30)$ and apparent micro viscosity, η, respectively, degree of water penetration and mean electrostatic surface potential (ψ).[15-23,72] The various commonly used fluorescence probes can be classified as follows.

1.3.1.1. *Probes Based on Ham Effect*

Condensed aromatics such as Py (1) show fairly well-resolved fluorescence spectra in solution. Variation of solvent leads to a large variation in the intensities of the vibronic bands without much spectral shift and the phenomenon is known as *Ham Effect*.[73] For Py, the peak intensity ratio of the vibronic bands I and III serves as a sensitive guide of the environmental

Fig. 1.5. Chemical structures of some commonly used fluorescence probes.

17
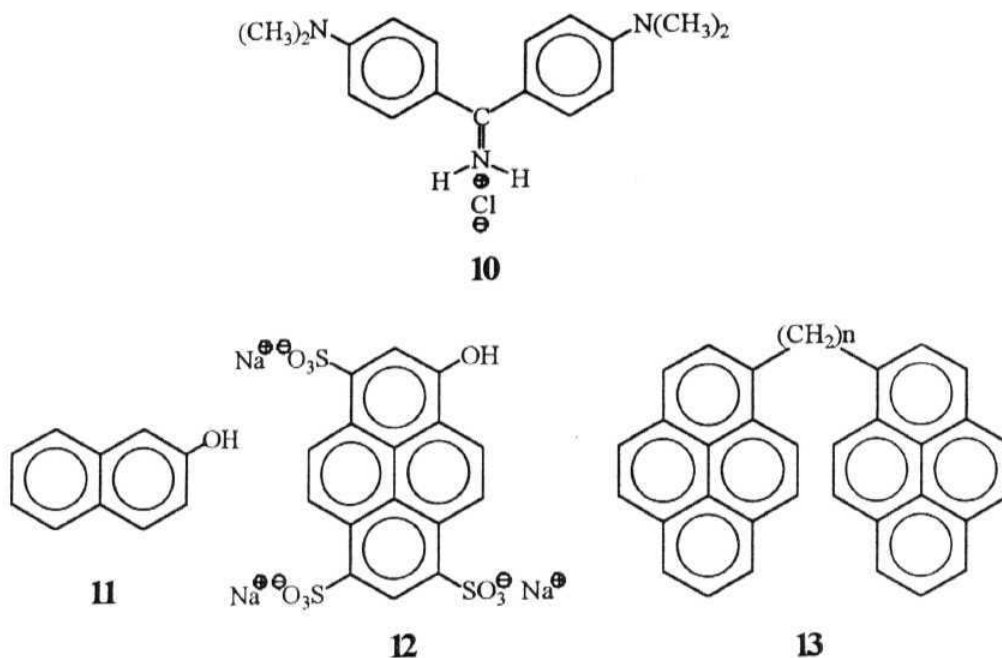
Fig. 1.5. Chemical structures of some commonly used fluorescence probes.

micropolarity and this has been used to evaluate the different parameters relating to micellar aggregates.[74, 75] Important among them are CMC values of the micelles, polarity of the interfacial region, water penetration into the micelles.[74,75] Zachariasse et al[76] employed amphiphilic molecules such as Py-(CH$_2$)$_n$-COOH and Py-(CH$_2$)$_n$-$\overset{+}{N}$(CH$_3$)$_3$Br$^-$ to show that the pyrenyl group penetrates more and more into the interior of the micelles when n increases from 3 to 15. The polarity of the direct probe environment decreases from a value somewhat larger than that of methanol for Py-(CH$_2$)$_3$-COOH solubilised in surface region of the micelle, to a value approaching that of hexadecane for the

18

central region of the micelle (e.g. SDS) for n-15. It is concluded that the water content in the micelles decreases when going from the surface region to the micellar interior and the later was found to be free of water molecules.

The bile salts are among the most important biological detergent-like molecules and aggregation in *aq* solution has been investigated using Py monomer fluorescence/^ The utility of the I/III peak ratio of Py emission as a probe for determining the pressure effect on CMC was demonstrated by Hara et al[78] at high pressures. Frindi et al[79] have found that the CMCs of amphoteric surfactants n-octyl, n-decyl DPSs are much higher than expected for surfactants with zero net charge using Py probe. The presence of polymers induces the aggregation behaviour of surfactant well below the CMC, referred to as critical aggregation concentration (CAC). Recently, this has been studied using Py probe in presence of nonionic polymer, PVA and highly co-operative nature of the aggregation has been concluded from peak ratio variation.[80a] The interfacial polarities, ε_f of the mixed systems CT AB/PPG estimated to be 17 and 13 for M.W=425 and 1000, respectively.[80b] Py fluorophore has also been used to study 1:1 CTAB/β-CD complex aggregates.[80c]

1.3.1.2. Probes Based on High Excited State Dipole Moment

In certain cases, the dipole moment of the excited state is significantly higher than that of the ground state. As a consequence, the emission maxima (λ_{emi}^{max}) and yield (ϕ_f) depend on the *polarity* of the solvent. Usually an empirical procedure of comparison of the emission spectra of the probe in

different solvents with those obtained in the organised media is used for the evaluation of microenvironmental polarity. Examples of this kind of probes are ANS (2),[81a] TNS (3),[81b] DNSC (5) and NPN (6). These probes show a large variation in λ_{emi}^{max} and ϕ_f with solvent polarity which serves as an indicator of the surrounding the microenvironment. Recently, Narang et al[81c] have introduced a new hemicyanine polarity probe whose emission behaviour is extremely sensitive to polarity. The increase in ϕ_f and blue shift of λ_{fl}^{max} of ANS with formation of micellar aggregates was monitored to estimate the CMC values of nonionic and SDS surfactants.[82] The interfacial polarity of nonionic and zwitterionic micelles was found to correspond to the polarity of 70% ethanol-30% water mixture from ANS fluorescence. This probe was also used in testing the environment of AOT reversed micelles when the volume of the water core was varied.[82c] TNS[83] has been shown to be a potential indicator for following the micellisation of different surfactants in the absence and the presence of salt. Kano et al[84] used dansyldodecylamine as probe to conclude that the fluorescing moiety could be located near the surface of the micelles.

Recently, Melo et al[85] used 12-AS to probe the water content of cationic and anionic micelles. Very recently, Sarkar et al[86] have studied the solvation dynamics of coumarin 480 in AOT/n-heptane/water, in neutral (TX-100), cationic (CTAB) and anionic (SDS) micelles showing that the dynamic properties of the water molecules in water cluster of reversed micelles and Stern layer of the normal micelles were appreciably different from those in bulk water.

The structure of the AOT reverse micelles in near-critical and supercritical fluids has sparked significant interest which has been investigated using fiuorophores such as prodan and ANS.[87]

1.3.1.3.   Probes Based on Solvent Effects on (n,n*) and (n, π*) States

Presence of low-lying closely-spaced (n, π*) and (π, π*) levels is a common feature in the photophysics of organic heterocyclics. As (π, π*) and (n, π*) states respond differently to the polarity of the medium, in molecules that have the (n, *n*)* state as the lowest energy in nonpolar solvents, there can be inversion in the nature of the lowest excited state in polar solvents leading to drastic changes in fluorescence efficiency. Fluorophores PyCHO (4),[88] and 7. alkoxycoumarin (7) show this type of behaviour. Nile red   also has recently been shown to be an excellent fluorescence probe of this class. [89]

The strong solvent polarity dependence of the fluorescence of PyCHO has been excellently exploited to probe the polarities of a number of various micelles. As this molecule was found to sit at the micelle-water interface, it served for the estimation of interfacial polarities of micelles.[88] Turro et al[88b] have studied the variation the interfacial polarities of SDS, CTAB and CTAC micelles with pressure. PyCHO was also reported to be an ideal fluorophore for CMC evaluation. [88c] Solvent dependent ϕ_f values of 7-alkoxycoumarins was found to be useful in measuring the CMCs and also the surface polarities of the micelles formed by ionic (SDS, CTAB) and non-ionic (TX-100) detergents.[90] Using picosecond emission spectroscopy, the dynamics of the ICT process of

nile red inside the water pool of AOT/n-heptane microemulsions has been studied recently. [91]

1.3.1.4. Donor-Acceptor Molecules with TICT States

A few organic molecules with D and A moieties linked by single bond exhibit dual fluorescence originating from planar ICT (short λ band) and perpendicular TICT states (long X band). Fluorescence originating from the TICT state is highly sensitive to the solvent polarity due to the large dipole moment arising from the perpendicular conformation of the D^+ and A''. Examples of probes of the this category could be found in a recent review article.[23] Systems such as DMABMN (8) display fluorescence that is remarkably sensitive to the polarity and viscosity of the microenvironment. Hence many probes of this class find application in the measurement of micropolarity as well as microviscosity.[92,93]

High surface roughness and porous nature of SDS micelles have been suggested from a study of the polarity and viscosity dependent fluorescence properties of several 3H-indole derivatives in SDS and CTAB micelles.[94a,b] These derivatives have also been employed for the study of reverse micelles. [94c] Very recently, BSA-SDS aggregates have been investigated using ED AC. [95]

1.3.1.5. Probes Sensitive to Hydrogen-Bonding Effects

There are certain fluorescent probes such as xanthene dyes (9) (e.g., rose bengal and erythrosin) whose absorption and emission properties are particularly sensitive to the hydrogen-bonding ability of the solvent.[96] These probes show a

drastic increase in τ_f in going from a protic to polar a aprotic media. The effect has been used in probing hydrogen bonding capabilities of and water penetration into the microenvironments of organised media.[97] Acridine,[98] methyl 9-anthroate,[99] 4-aminophthalimide[100] are systems belonging to this class.

Molecules undergoing excited state proton transfer (ESPT) often exhibit dual emission, with the normal one arising from an excited species similar in geometry to that in ground state while the Stoke's-shifted emission originates from a tautomer formed in the excited electronic state. The normal and tautomer emission depend crucially on the conformation of the molecule, polarity and hydrogen bonding ability of the solvents. A recent finding indicates that fluorophores which display ESPT can serve as sensitive probes for exploring microenvironment and phase transitions in micelles, and for estimation of CMCs.[101] 3-HF,[102a] HPBI (24)[102b,c] and 7-azaindole[103] are examples of this kind.

1.3.1.6. Probes for Environmental Rigidity

Stilbenes and higher polyenes in general represent a group of molecules whose fluorescence properties are very sensitive to the environmental rigidity. Trans-stilbene, for example, is only weakly fluorescent (ϕ ~ 0.05) and cis-stilbene is non-fluorescent in fluid solutions at room temperature. But in rigid environments both compounds are highly fluorescent (ϕ ~ 0.75). Whitten and co-workers have used several surfactant derivatives of stilbenes as probes.[104] Fromherz et al[104] have introduced amphiphilic stilbazonium dye and

hemicyanine dyes of similar kind. AuO (10) is another excellent example of a viscosity sensitive probe.[106] The ϕ_f of this system is sensitive to the viscosity of the medium as it affects the internal rotation of the dimethylamino groups, the main cause of the deactivation of the excited state . Rhodamine B[107] is also a viscosity sensitive probe.

As the ϕ_f of cis and trans stilbenes, in particular the surfactant stilbenes, depends on the fluidity of the environment, the effect has been studied by Suddaby et al[108a] to show that the fluidity decreases in the order of homogeneous hydrocarbons > micelles > vesicles. Similar report has been obtained from aminostilbazonium dye fluorescence.[108b] AuO is found to be a good probe for the determination of CMCs and η of various micelles.[106]

1.3.1.7. Other Fluorescent Probes

Apart from the types of probes already discussed, one can find a few other fluorescent systems which are used for studies in organised media.[20-22] Fluorescent pH indicators such as NpOH (11), PyTS (12) and proflavin have been extensively used to investigate the proton donor-acceptor character of the microenvironments and the electrical potential at the surface of the charged interfaces.[109-113]

Since excimer formation is viscosity dependent, a number of systems which form inter or intramolecular excimer are used to measure the microviscosities of micelles including bile salt micelles.[20,21,72] Probes involving Py are most commonly employed for this purpose.[72,113]

Monitoring the depolarisation of solubilised probe fluorescence often allows the determination of the microviscosity of probe environment. Both steady-state and time-resolved fluorescence depolarisation measurements have been used to measure the microviscosities of organised media.[20,22,72] Fluorescence polarisation studies of 2-MeAn, Pe,[115] n-AS,[116] rhodamine B,[117] PyTS,[118] PTC,[119] ANS,[120,121] TNS[120] and very recently SDU probe [122] in various organised media are examples of this kind.

1.4. Motivation of The Present Work

The main objective of this investigation is i) to exploit the sensitivity of the fluorescence properties of already known EDA molecules to study the microenvironments of the organised media such as micelles and to modify or design them with enhanced ability as sensors for microenvironments and ii) to study the Photophysical behaviour of some new EDA molecules which may have potential as sensors or reporter molecules. The effective use of fluorescence probes requires a detailed knowledge of the nature of the radiative and radiationless transitions and of the mechanism of the interaction of the excited state with different environments. Fluorescent EDA molecules form an important class of candidates for probing microstructural aspects of organised media.

Aminophthalimides are known for their spectral sensitivity towards minor changes in the physical properties of the environment.[123,124] During the

study of EDA molecules,[124-127] it was observed that the fluorescence properties of 4-aminophthalimide (AP) were extremely sensitive to the polarity of the media, in particular to the hydrogen bonding solvents.[124,127] The emission properties of dimethylamino derivative of AP i.e. 4-N,N-dimethylaminophthalimide (DAP) were found to be even more sensitive to the polarity of the medium when compared with those for AP. This is due to the existence of a non-fluorescent TICT state below the ICT emitting state of DAP.[127] Thus qualifying to act as probes for microstructures, we prompted to use AP and DAP as fluorophores to investigate the structural aspects of organised systems among which the micellar systems are the simplest ones of biological models. Therefore, studies have been carried out using these polarity sensitive probes. The results show that aminophthalimides can act as excellent probes for following the aggregation behaviour of the surfactants. Polarity of the binding sites have been evaluated from the spectral data. AP is found to be a good probe for the interfacial region of the micelles.

Further, to develop probes for the core region of the micelles, new amphiphilic probes , 11-(4-aminophthalimido)undecanoic acid (APL) and 11-(4-N,N-dimethyaminophthalimido)undecanoic acid (DAPL) have been synthesised where the fluorophores AP and DAP are integral part of the respective amphiphiles. Mode of binding and Solubilisation site have been examined for these probes in micellar media apart from their ability to follow micellisation.

26

While investigating the fluorescence decay behaviour of the surfactant fluorophore, APL, it was observed that the fluorescence decay of the system in aqueous medium as biexponential with long-lived component along with the expected short-lived species. It is known that in aqueous and aqueous-organic binary mixed solvents, hydrophobic interactions force molecules with long hydrocarbon chain to aggregate or self-coil. 128,129 To fi$_{nc}$j out the origin of the unusual long-lived second component a series of AP-labelled alkanes (APn) with different hydrocarbon chain length have been synthesised and their fluorescence behaviour has been observed in different media.

Among the new EDA systems, we have studied the Photophysical behaviour of two structurally related systems, Carbostyril 124 and Carbostyril 165 (C124 and C165) which are used as laser dyes.[130] The focus of this investigation is to find out the possible role of the TICT state, if any, on the fluorescence properties of these systems. This was considered necessary in view of similarity (structural and electronic) of the these systems with the extensively studied coumarin dyes C1 and C120, the latter is known to possess a low-lying non-fluorescent TICT state that affects its fluorescence properties.[34] Theoretical study based on semi-empirical AM1 method has been performed on C124 and C165 to confirm our experimental results. Despite the possibility of the existence of Carbostyrils as keto-enol tautomers, the keto form is shown to be the only absorbing and emitting species. The likely use of these systems as probes for the organised media has been investigated.

A symmetrical dimeric species, N,N'-bis(4-carbomethoxyphenyl)benzoate (BIMBP) has been synthesised and its fluorescence behaviour is studied in media of different polarities to find out whether structural changes in the excited state of this highly symmetrical system could lead to the formation of dipolar species.

1.5. **Layout** of **The Thesis**

The 2nd chapter of the thesis gives the experimental details of this investigation. The 3rd chapter presents the results of the investigation carried out on AP and APL in micellar media. Chapter 4 describes the study of the AP-labelled compounds in polar media. Chapter 5 describes the results obtained for DAP and DAPL in micellar media. Chapter 6 is divided into two sections, the first of which concerned with the study of the Carbostyril dyes and the second one describes the fluorescence behaviour of BIMBP in homogeneous media.

Glossary

ANS - 1-Anilinonaphthalene-8-sulfonate

nAS - n-(9-anthroyloxy)stearic acid, n= 2, 6, 9, 12

Au O - Auramine O

nADPS - n-Alkyl(dimethylamino)propane sulfonate

CTAC - Cetyltrimethylammonium chloride

CTAB - Cetyltrimethylammonium bromide

DMABMN - N,N-dialkylaminobenzylidene malononitrile

DNSC - Dansyl chloride

ED AC - Ethyl p-dimethylamino cinnamate

HPBI - 2-(2'-hydroxyphenyl)benzimidazole

3-HF - 3-Hydroxyflavone

2-Methylanthracene - 2-MeAn

NpOH - 2 - naphthol

Pe - Perylene

NPN - N-Phenylnaphthylamine

PVA - Poly(vinyl alcohol)

PPG - Poly(propylene glycol)

Py - Pyrene

PyCHO - Pyrene-3-carboxaldehyde

PyTS - 8-Hydroxy-l,3,6-pyrenetrisulfonate

PTC - 3, 4, 9, 10-Perylene tetracarboxylate

SDS - Sodium dodecyl Sulfate

SDU - 5(E)-Styryl-1,3-dimethyl uracil

TNS - 2-(p-Toluidinyl)-naphthalene-6-sulfonate

TX-100 - Triton X-100

1.6. References

1. a) *Photoinduced Electron Transfer*, M. A. Fox, M. Chanon, eds., Parts A-
    D, Elsevier: New York, **1988;** b) S. S. Isied In: *Electron Transfer in*

Inorganic, Organic and Biological Systems, J. R. Bolton, N. Mataga, G. McLendon, eds., Advances in Chemistry Series 228, American Chemical Society: Washington DC, **1991,** Chap. 15; c) T. J. Meyer, *Acc. Chem. Res.,* 22, 163, **1989;** d) J. R. Winkler, H. B. Gray, *Chem. Rev.,* 92, 369, **1992;** e) S. S. Isied, M. -Y. Ogawa, J. F. Wishart, *Chem. Rev.,* 92, 381, **1992;** f) D. Gust, T. A. Moore, A. L. Moore, *Acc. Chem. Res.,* 26, 198, **1993;** g) *Photoinduced Electron Transfer,* parts I-V In: *Topics in Current Chemistry,* J. Mattay, ed., Springer-Verlag: New York, **1991;** h) H. Kurreck, M. Huber, *Angew. Chem. Int. Ed. Engl.,* 34, 849, **1995.**

2. M. **R.** Wasielewski, *Chem. Rev.,* 92, 435, **1992.**

3. a) M. E. Michel-Beyerle, *The Reaction Centre of Photosynthetic Bacteria,* Springer-Verlag: Berlin, **1995.**

4. L. Fabbrizzi, A. Poggi, *Chem. Soc. Rev.,* 24, 197, **1995.**

5. a) V. Balzani, A. Juzis, M. Venturi, S. Campagna, S. Serroni, *Chem. Rev.,* 96, 759, **1996;** b) S. L. Gilat, S. M. Kawai, J. M. Lehn, *Chem. Eur. J.,* 1, 275, **1995;** c) M. **R.** Wasielewski, M. P. O'Neil, D. Gosztola, M. P. Niemczyk, W. A. Svec, *Pure Appl Chem.,* 64, 1319, **1992.**

6. *Molecular Electronic Devices,* F. L. Carter, R. E. Siatoski, H. Woltjen, eds., North-Holland: Amsterdam, **1988.**

7. a) D. B. Shelton, J. E. Rice, *Chem. Rev.,* 94, 3, **1994;** b) A. W. Sleight, *Acc. Chem. Res.,* 28, 103, **1995.**

8. R. S. Mulliken, *J. Am. Chem. Soc.*, 72, 600, **1950,** 74, 811, **1952;** *J. Phys. Chem.,* 56, 801, **1952.**

9. a) H. Leonhardt, A. Weller, *Ber. Bunsenges. Phys. Chem.,* 67, 791, **1963;** b) **R.** S. Davidson In: *Adv. Phys. Org. Chem.,* V. Gold, D. Bethell, eds., Vol 1, Academic Press: New York, **1983,** 1p; c) M. Gordon, W. Ware, *The Exciplex,* Academic Press: New York, **1975.**

10. J. B. Birks, *Photophysics of Aromatic Molecules,* Wiley: New York, 1970.

11. a) N. Mataga, S. Nishikawa, T. Asahi, *J. Phys. Chem.,* 94, 1443, **1990;** b) J. W. Verhoeven, *Pure Appl. Chem.,* 62, 1535, **1990;** c) J. W. Verhoeven, T. Scherer, R. J. Willemse, *Pure Appl. Chem.,* 65, 1717, **1993** and references therein; d) K. D. Jordan, M. N. Paddon-Row, *Chem. Rev.,* 92, 395, **1992;** e) S. Sinha and R. De, T. Ganguly, *J. Phys. Chem. A,* 101, 2852, 1997; f) M. A. Fox, E. Galoppini, *J. Am. Chem. Soc,* 119, 5277, **1997.**

12. a) R. J. Willemse, J. W. Verhoeven, A. M. Brouwer, *J. Phys. Chem.,* 99, 5753, **1995;** b) S. T. van Dijik, C. P. Groen, F. Haiti, A. M. Brouwer, J. W. Verhoeven, *J. Am. Chem. Soc, US,* 8425, **1996.**

13. **M.** N. Paddon-Row, *Acc. Chem. Res.,* 27, 18, **1994.**

14. J. Deisenhofer, H. Michel, *Angew. Chem. Int. Ed. Engl.,* 28, 829, **1989.**

15. R. P. Hauland, *Handbook of Fluorescent Probes and Research Chemicals,* Molecular Probes Inc. : Eugene, UR, **1989.**

16. a) *Spectroscopy and Dynamics of Molecular Biological Systems,* P. M. Bayley, E. R. Dale, eds., Academic Press: New York, 1986.

17. N. J. Turro, M. Gratzen, A. M. Braun, *Angew. Chem. Int. Ed. Engl.*, 19, 675, **1980.**

18. J. K. Thomas, *Acc. Chem. Res.,* 10, 133, **1977;** *Chem. Rev.,* 80, 283, **1980;** *J. Am Chem. Soc,* 91, 267, **1987.**

19. **J. R.** Lakowicz, *Principles of Fluorescence Spectroscopy,* Plenum Press: New York, **1983.**

20. K. Kalyanasundaram, *Photochemistry in Microheterogeneous Systems,* Academic Press: New York, **1987.**

21. V. Ramamurthy, *Photochemistry in Organised and Constrained Media,* VCH: New York, **1991.**

22. K. Kalyanasundaram In: *Photochemistry in Organised and Constrained Media,* V. Ramamurthy, ed., VCH: New York, **1991,** Chap. 2 and references cited therein.

23. K. Bhattacharyya, M. Chowdhury, *Chem. Rev.,* 93, 507, **1993.**

24. W. Rettig, *Angew. Chem. Int. Ed. Engl.,* 25, 971, **1986.**

25. a) W. Rettig, *Proc. Ind Acad. Sci.,* 104, 89, **1992;** b) W. Rettig, W. Baumann In: *Photochemistry and Phtophysics,* Vol 6, CRC Press: Boca Raton, **1992,** 79p; c) W. Rettig, In: *Topics in Current Chemistry,* J. Mattay, ed., Springer-Verlag: Berlin, **1994;** d) W. Rettig, D. -L. Claude, C. Jouvel, S. M. Barra, P. Szrifiger, L. Kim, F. Castano, *J. Chim. Phys., (Fr)* 92, 465, **1995.**

26. E. Lippert, Z *Natureforsch*, 10a, 541, **1955.** b) E. Lippert, W. Luder, H. Boos, In: *Advances in Molecular Spectroscopy,* A. Mangini, ed., Pergamon: New York, **1962,** 443p.

27. J. R. Platt, *J. Chem. Phys.*, 17, 484, **1949.**

28. a) K. Rotkiewicz, K. H. Grellmann, Z. R Grabowski, *Chem. Phys. Lett.*, 19, 315, **1973;** 21, 212, **1973;** b) Z. R. Grabowski, K. Rotkiewicz, A. Siemiarczuk, D. J. Cowley, W. Baumann, *Nouv. J. Chem.,* 3, 443, **1979;** c) Z. **R.** Grabowski, J. Dobkowski, *Pure Appl. Chem.,* 55, 245, **1983;** d) J. Karpluk, Z. R. Grabowski, F. C. De Schryver, *Proc. Ind. Acad. Sci.,* 104, 13, **1992.**

29. a) G. Wermuth, W. Rettig, *J. Phys. Chem.,* 87, 2729, **1984;** b) W. Rettig, R. Gleiter, *J. Phys. Chem.,* 89, 4676, **1985;** c) **M.** Vogel, W. Rettig, R. Sens, K. H. Drexhage, *Chem. Phys. Lett.,* 148, 452, **1988;** d) W. Rettig, *Ber. Bunsenges. Phys. Chem.,* 95, 259, **1991.**

30. a) S. A. Jonker, J. M. Warman, *Chem. Phys. Lett.,* 185, 36, **1991;** b) W. Baumann, H. Bischof, J. C. Frohling, C. Brittinger, W. Rettig, K. Rotkiewicz, *J. Photochem. Phobiol., A: Chem.,* 64, 49, **1992;** c) W. Liptay In: *Exited States,* E. C. Lim, ed., Vol 1, Academic Press: New York, 129, **1974;** d) H. Labhart, *Adv. Chem. Phys.,* 13, 179, **1990.**

31. a) T. Okada, N. Mataga, W. Baumann, *J. Phys. Chem.,* 91, 760, **1987;** b) C. Rulliere, Z. R. Grabowski, J. Dobkowski, *Chem. Phys. Lett.,* 137, 400,

1987; c) N. Mataga, H. Yuo, T. Okada, W. Rettig, *J. Phys. Chem.*, 93, 3383, **1989.**

32. a) Y. -P. Sun, C. -E. Bunker, *J. Chem. Soc., Chem. Commun.*, 5, **1994;** b) Y. -P. Sun, T. L. Bowen, C. -E. Bunker, *J. Phys. Chem.*, 98, 12486, **1994.**

33. a) M. Belletete, G. Durocher, *J. Phys. Chem.*, 93, 1793, **1989;** 96, 9183, **1992;** b) M. LaChapelle, M. Belletete, M. Poulin, N. Godbout, F. LeGrand, A. Heroux, F. Brisse, G. Durocher, *J. Phys. Chem.*, 95, 9764, **1991;** c) M. Belletete, R. S. Sarpal, G. Durocher, *Chem. Phys. Lett.*, 201, 145, 1993; d) M. Belletete, S. Nigam, G. Durocher, *J. Phys. Chem.*, 99, 4015, **1995.**

34. a) G. Jones II, W. R. Jackson, A. M. Halpern, *Chem. Phys. Lett.*, 72, 391, **1980;** b) G. Jones II, W. R. Jackson, C. Choi, W. R. Bergmark, *J. Phys. Chem.*, 89, 294, **1985.**

35. a) M. Vogel, W. Rettig, R. Sens, K. H. Drexhage, *Chem. Phys. Lett.*, 147, 461, **1988;** b) M. Vogel, W. Rettig, U. Fiedeldei, H. Baumgaertel, *Chem. Phys. Lett.*, 148, 347, **1988;** c) J. **D.** Siman, S. G. Su, *J. Phys. Chem.*, 92, 2395, **1988;** d) T. L. Chang, H. C. Cherung, *Chem. Phys. Lett.*, 173, 343, **1990.**

36. a) E. A. Chandross, H. T. Thomas, *Chem. Phys. Lett.*, 9, 397, **1971;** b) P. C. M. Weissenborn, A. Huizer, C. A. G. O. Varma, *Chem. Phys.*, 133, 437, 1989 and references therein. c) U. Leinhos, W. Kuhnle, K. A. Zachariasse, *J. Phys. Chem.*, 95, 2013, **1991.**

37 a) W. Schuddeboom, S. A. Jonker, J. M. Warman, U. Leinhos, W. Kuhnle, K. A. Zachariasse, *J. Phys. Chem.*, 96, 10809, **1992;** b) K. A. Zachariasse, T. von der Harr, A. Hebecker, U. Leinhos, W. Kuhnle, *Pure Appl. Chem.*, 65, 1745, **1993;** c) K. A. Zachariasse, T. von der Haar, U. Leinhos, W. Kuhnle, *J. Inf. Rec. Mats.,* 21, 561, **1994;** d) K. A. Zachariasse, M. Grobys, T. von der Harr, A. Hebecker, Y. U. Il'ichev, Y. -B. Jiang, O. Morawski, W. Kuhnle, *J. Photochem. Photobiol., A: Chem.*, 102, 59, **1996.**

38. A. L. Sobolewski, W. Domcke, *Chem. Phys. Lett.,* 250, 428, **1996.**

39. A. D. Gorse, M. Pesquer, *J. Phys. Chem.,* 99,. 4039, 1995.

40. L. S. Andres, M. Merchan, B. O. Roos, R. Lindh, *J. Am. Chem. Soc.*, 117, 3189, **1995.**

41. a) G. Wermuth, W. Rettig, E. Lippert, *Bet: Bunsenges. Phys. Chem.,* 85, 64, **1981;** b) W. Rettig, G. Wermuth, *J. Photochem.,* 28, 351, 1985; c) W. Rotkiewicz, W. Rubaszecoska, *J. Lumin.,* 27, 221, 1989.

42. S. Tazuke, R. K. Guo, R. Hayashi, *Macromolecules,* 22, 729, **1989.**

43. a) J. M. Hicks, M T. Vandersall, Z. Babarogic, K. B. Eisenthal, *Chem. Phys. Lett.,* 116, 28, 1985; b) J. M. Hicks, M. T. Vandersall, E. V. Sitzmann, K. B. Einsenthal, *Chem. Phys. Lett.,* 135, 413, 1987.

44. H. C. Chiang, H. Luckton, *J. Phys. Chem.,* 79, 1935, 1975.

45. R. Hayashi, S. Tazuke, C. W. Frank, *Chem. Phys. Lett.,* 135, 123, 1987; b) J. M. Lang, Z. A. Dreger, H. G. Drickamer, *J. Phys. Chem.,* 98, 11308, **1994.**

46. a) **D.** S. Bulgarevich, O. Kajimoto, K. Hara, *J. Phys. Chem.,* <u>99</u>, 356, **1995;** b) **K.** Hara, **W.** Rettig, <u>96</u>, 8307, **1992;** c) K. Hara, N. Kometan, O. Kajimot, *J. Phys. Chem.*, <u>100</u>, 1488, **1996.**

47. a) A. Chandra, B. Bagchi, *Ann. Rev. Phys.,* <u>80</u>, 1, **1990;** b) C. F. Chapman, F. S. Fee, M. Maroncelli, *J. Phys. Chem.,* <u>94</u>, 4929, **1990**; c) M. Maroncelli, *J. Chem. Phys.,* <u>94</u>, 2084, **1991;** d) A. Polimeno, A. Barbon, P. L. Nordio, W. Rettig, *J. Phys. Chem.,* <u>93</u>, 12158, **1994.**

48. J. Linpinsky, H. Chojnack, K. Rotkiewicz, Z. R. Grabowski, *Chem. Phys. Lett.*, <u>70</u>, 449, **1980.**

49. S. D. Majumdar, K. Sen, S. P. Bhattacharyya, K. Bhattacharyya, *J. Phys. Chem.,* <u>95</u>,4321, **1991.**

50. S. Marguet, J. C. Mialocq, G. Millic, F. Berthier, F. Momicchioli, *Chem. Phys. Lett.*, <u>160</u>, 205, **1992.**

51. P. K. McCarthy, C. J. Blanchard, *J. Phys. Chem.,* <u>97</u>, 12205, **1993.**

52. T. Soujanya, G. Saroja, A. Samanta, *Chem. Phys. Lett,* <u>236</u>, 503, **1996**.

54. a) J. H. Fendler, *Membrance Mimetic Chemistry,* Wiley, New York, **1982;** *Pure Appl. Chem.,* <u>54</u>, 1809, **1982;** *Acc. Chem. Res.,* .<u>19</u>,153, **1976;** *Ann. Rev. Phys. Chem.,* <u>35</u>, 137, **1984;** b) **J. H.** Fendler, E. J. Fendler, *Catalysis in Micellar and Macromolecular Systems,* Academic Press: New York, **1975.**

55. C. Tanford, *The Hydrophobic Effect, Formation of Micelles and Biological Membranes,* Wiley: New York, IInd edn., **1980.**

56.	K. L. Mittal, *Micellisation*, *Solubilisation and Microemulsions,* Vol 1,2, Plenum Press: New York, 1977.

57. T. H. Tien, *Bilayer Lipid Membranes Theory and Practice,* Marcel Dekker: New York, **1974.**

58. a) I. Tabushi, Y. Kobuke, J. Imuta, *Nucleic Acid Research,* 6, 175, **1979;** b) M. Shimomma, T. Kunitake,./. *Am. Chem. Soc,* 104, 1957, **1982.**

59. a) M Calvin, *Acc. Chem. Res.,* 11, 369, **1978;** b) M. Gratzel, *Acc. Chem. Res.,* 14,376, **1981.**

60. a) M. J. Lawrence, *Chem. Soc. Rev.,* 23, 417, **1994;** b) G. Gregoriads, *Drug Carriers in Biology and Medicine,* Academic Press: London, **1979.**

61. R. Radhakrishnan, C. M. Gupta, B. Eroni, R. J. Robson, W. Curatolo, A. Majumbar, A. H. Ross, Y. Takagaki, H. G. Khorama, *Ann. NY A cad. Sci.,* 346, 165, **1980.**

62. G. S. Hartley, *Aqueous solutions of Paraffin Chain Salts,* Hermann: Paris, **1936.**

63. C. A. Bunton, F. Nome , F. G. Quina, L. S. Rowsted, *Acc. Chem. Res.,* 24, 357, **1994.**

64. a) I. N. Isaelachvili, D. J. Mitchel, B. W. Ninham, *J. Chem. Soc, Faraday Trans.,* 76, 1525, **1976;** b) D. **J.** Mitchel, B. W. Ninham, *J. Chem. Soc, Faraday Trans.,* 77, 601, **1981.** c) D. W. R. Gruen, *Prog. Colloid Polymer Sci.,* 70, 6, **1980.**

65. a) F. M. Menger, *Acc. Chem. Res.,* 12, 111, **1979;** b) F. M. Menger, B. J. Boyer, *J. Am. Chem. Soc,* 102, 5936, **1980;** 108, 1297, **1986;** c) F. M. Menger, C. E. Mourier, *J. Am. Chem. Soc.,* 115, 12222, **1993.**

66. K. A. Dill, P. J. Flory, *Proc. Natl. Acad. Sci.,U. S. A.,* 78, 676, **1981.**

67. P. Formherz, *Chem. Phys. Lett.,* 77, 460, **1981.**

68. A. Ben-Shaul, W. M. Gelbart, *Ann. Rev. Phys. Chem.,* 36, 179, **1985.**

69. J. H. Fendler, *Ann. Rev. Phys. Chem.,* 35, 137, **1984.**

70. a) Jr. Bocker, J. Brickmann, P. Bopp,./. *Phys. Chem.,* 98, 712, **1994;** b) T. Bust, R. H. Schke, *J. Phys. Chem.,* 100, 12162, **1996.**

71. K. V. C. Laane, A. J. W. G. Visser, *Photochem. Photobiol.,* 45, 863, **1987** and references cited therein.

72. F. Griesser, C. J. Drummond, *J. Phys. Chem.,* 92, 5580, **1988** and references cited therein.

73. a) A. Nakajima, *Bull. Chem. Soc. Jpn.,* 44, 3272, **1971;** b) P. Lianos, S. Georghiou, *Photochem. Phobiol.,* 29, 843, **1979;** 30, 355, **1979.**

74. K. Kalyanasundaram, J. K. Thomas, *J. Am. Chem. Soc,* 99, 2039, **1977.**

75. C. A. Backer, D. G. Whitten, *J. Phys. Chem.,* 91 , 865, **1987.**

76. K. A. Zachariasse, B. Kozankiewicz, W. Kuhnle, In: *Surfactants In Solution,* K. L. Mittal, B. Lindmann, eds., Vol 1, Plenum Press: **1984,** 565p.

77. a) R. Zana, G. Guveli, *J. Phys. Chem.,* 89, 1687, **1985;** b) M. Meyerhoffer, Z. B. McGrown, *Anal Chem.,* 63, 2082, **1991.**

78. K. Hara, H. Suzuki, N. Takisama, *J. Phys. Chem.,* 93, 3710, **1989.**

79. **M. Frindi, B.** Michels, R. Zana, *J. Phys. Chem.*, 98, 6607, **1994;** 96, 6095, **1992**.

80. **a) A. K. Panda,** A. **K.** Chakraborty, *Ind. J. Chem.*, 36A, 184, **1996;** b) M. L. Sierra, E. Rodens, *J. Phys. Chem.*, 97, 12387, **1993; c) L. R.** Lim, Y. **-B. Jiang, X. -Z. Du,** X. -Z. Haung, G. -Z. Cheu, *Chem. Phys. Lett.,* 68, 179, **1991**.

81. a) J. Slavik, *Biochem. Biophys. Acta*, 1, 694, **1982;** b) G. M. Edelman, W. O. McClure, *Acc. Chem. Res.,* 1, 65, **1968;** c) V. Narang, C. F. Zhav, J. D. Bhawalkar, F. V. Bright, P. N. Prasad, *J. Phys. Chem.,* 100, 4521, **1996.**

82. a) **R.** Mast, L. V. Haynes, *J. Colloid Interface Sci.,* 53, 35, **1977;** b) P. Horowitz, *J. Colloid Interface Sci.,* 61, 197, **1977;** c) **M.** Wong, J. K. Thomas, M. Gratzel, *J. Am. Chem. Soc.,* 98, 2391, **1976**.

83. a) H. -C. Chaing, A. Lukton, *J. Phys. Chem.*, 79, 1935, **1975;** b) K. S. Birdi, H. N. Singh, S. U. Daltages, *J. Phys. Chem.,* 83, 2733, **1979; c)** A. Nag, K. Bhattacharyya, *J. Photochem. Photobiol., A: Chem.,* 47, 97, **1989**.

84. K. Kano, Y. Ueno, S. Hashimoto, *J. Phys. Chem.,* 89, 3161, **1985.**

85. E. C. C. Melo, S. M. B. Macanita, A. L. Santos, *J. Colloid Interface Sci.,* 141, 439, **1991.**

86. N. Sarkar, A. Datta, S. Das, K. Bhattacharyya, *J. Phys. Chem.,* 100, 15480, **1996**.

87. a) **P.** Yazdi, G. J. McFann, M. A. Fox, K. P. Johnston, *J. Phys. Chem.,* 94, 7224, **1990;** b) **J.** Zhang, F. V. Bright, *J. Phys. Chem.,* 96, 5633, **1992.**

88. K. Kalyanasundaram, **J. K**. Thomas, *J. Phys. Chem.,* 81, 2176, **1977;** b) N. J. Turro, T. Okubo, *J. Phys. Chem.,* 86, 159, **1982;** c) K. P. Ananthapadmanabhan, E. D. Goddard, N. J. Turro, P. L. Kuo, *J. Colloid Interface Sci.,* 1, 352, **1985.**

89. **D. L.** Sackett, J. R. Knutson, J. Wolff, *J. Biol. Chem.,* 265, 14899, 1990; b) D. L. Sackett, J. Wolff, *Anal. Biochem.,* 167, 228, **1989.**

90. a) **K. Muthuramu,** V. Ramamurthy, *J. Photochem.,* 26, 57, **1984, b) T.** Moria, *Bull. Chem. Soc. Jpn.,* 61, 585, **1988.**

91. A. Dutta, D. Mandal, S. K. Pal, K. Bhattacharyya, *J. Phys. Chem. B,* KM, 10221, 1997.

92. a) R. O. Loutfy, K. Y. Law, *J. Phys. Chem.,* 84, 2803, **1980;** b) K. Y. Law, *Photochem. Photobiol,* 33, 799, **1981.**

93. U. S. Khalil, A. T. Sonessa, *Mol. Photochem.,* 2, 399, 1977.

94. R. S. Sarpal, M. Belletete, G. Durocher, *Chem. Phys. Lett.,* 224, 1, **1994;** 97, 5007, **1993;** b) S. Nigam, M. Belletete, R. S. Sarpal, G. Durocher, *./. Chem. Soc, Faraday Trans.,* 91, 2135, 1995; c) M. Belletete, M. Lachapelle, G. Durocher, *J. Phys. Chem.,* 94, 5337, **1990.**

95. R. Das, D. Guha, S. Mitra, S. Kar, S. Lahiri, S. Mukerjee, *./. Phys. Chem., A,* 101, 4042, **1997.**

96. L. E. Cramer, **K.** G. Spears, *J. Am. Chem. Soc,* 100, 221, **1978.**

97. a) **M. A. J.** Rodgers, *J. Phys. Chem.,* 85, 3372, **1981;** *Chem. Phys. Lett.,* 78, 509, **1981;** b) W. Reed, M. A. J. Politi, J. H. Fendler, *J. Am. Chem.*

Soc, <u>103</u>, 4591, **1981;** c) M. A. J. Rodgers, In: *Reverse Micelles,* P. L. Luisi, B. E. Straub, eds., Plenum Press: New York, **1984,** 165p.

98. T. Wolff, *J. Colloid Interface Sci.,* <u>83</u>, 658, **1981.**

99. A. L. Macanita, F. P. Costa, S. M. B. Costa, E. C. Melo, H. Santos, *J. Phys. Chem.,* <u>93</u>, 336, **1989.**

100. G. Saroja, A. Samanta, *Chem. Phys. Lett.,* <u>246</u>, 506, **1995.**

101. N. Chattopadyay, R. Dutta, M. Chowdhury, *J. Photochem. Photobiol., A: Chem.,* <u>47</u>, 249, **1989.**

102. a) M. Sarkar, P. K. Sengupta, *Chem. Phys. Lett.,* <u>68</u>, 179, **1991;** b) N. Sarkar, K. Das, S. Das, A. Datta, D. Nath, K. Bhattacharyya, *J. Phys. Chem.,* <u>99</u>, 17711, **1995;** c) S. Das, S. K. Dogra, *J. Chem. Soc, Faraday Trans.,* <u>94</u>, 139, **1998.**

103. J. G. Ray, P. K. Sengupta, *Chem. Phys. Lett,* <u>230</u>, 75, **1994.**

104. D. G. Whitten, *Acc. Chem. Res.,* <u>26</u>, 502, **1996.**

105. a) P. Fromherz, H. Ephardt, *J. Phys. Chem.,* <u>93</u>, 7717, **1989;** <u>97</u>, 4750, **1993.**

106. a) S. Miyagishi, T. Asakawa, M. Nishida, *J. Collod Interface Sci.,* <u>115</u>, 199, **1987;** b) M. Hasegawa, T. Sugimura, K. Kuraishi, Y. Shindo, A. Kitahara, *Chem. Lett.,* 1373, **1992;** c) S. Miyagishi, H. Kurimoto, T. Asakawa, *Bull. Chem. Soc. Jpn.,* <u>67</u>, 2398, **1994;** d) M. Hasegawa, T. Sugimura, Y. Suzuki, Y. Shindo, *J. Phys. Chem.,* <u>98</u>, 2120, **1994; e) S.**

Miyagishi, H. Kurimoto, T. Asakawa, *Bull. Chem. Soc. Jpn.*, 68, 135, **1995**.

107. M. Vogel, W. Rettig, R. Sens, K. H. Drexhage, *Chem. Phys. Lett.*, **148,** 452, **1988**.

108. a) B. R. Suddaby, P. E. Brown, J. C. Russel, D. G. Whitten,./. *Am. Chem. Soc*, 107, 5609, **1985;** b) H. Ephardt, P. Fromherz, ./. *Phys. Chem.*, 93, 7717, **1989**.

109. G. S. Hartley, J. W. Roe, *Trans. Faraday Soc.,* 36, 101, **1940.**

110. K. Kano, J. H. Fendler, *Biochim. Biophys. Acta.,* 509, 209, **1978.**

111. a) M. S. Fernandez, P. Fromherz, *J. Phys. Chem.,* 81, 1755, **1977;** b) J. Gircia-soto, M. S. Fernandez, *Biochem. Biophys. Acta.,* 731, 275, **1983.**

112. a) H. Kondo, M. Ichivo, J. Sunamoto, *J. Phys. Chem.,* 86, 4826, **1982;** b) E. Bardez, B. -T. Goguillon, E. Iceh, B. Valeur, *J. Phys. Chem.,* 88, 1909, **1984;** c) M. J. Politi, O. Brandt, J. A. Fendler, *J. Phys. Chem.,* 89, 2345, **1985;** d) M. J. Politi, H. Chaimovich, *J. Phys. Chem.,* 90, 282, **1986.**

113. E. Bardez, E. Monnier, B. Valeur, *J. Colloid Interface Sci.,* 112, 200, **1986**.

114. a).H. **J.** Pownall, L. C. Smith, *J. Am. Chem. Soc,* 75, 3136, **1973;** b) K. A. Zachariasse, *Chem. Phys. Lett,* 57, 429, **1978;** c) K. Hara, H. Suzuki, *J. Phys. Chem.,* 94, 1079, **1990.**

115. M. Shinitzky, A. C. Dianoux, C. Gitler, G. Weber, *Biochemistry,* 10, 2106, **1971.**

116. a) E. Blatt, K. P. Ghiggino, W. H. Sawyer, *J. Phys. Chem.*, 86, 4461, **1982;** b) E. Blatt, *Aust. J. Chem.*, 40, 851, **1987;** c) E. Blatt, K. B. Ghiggino, W. H. Sawer, *Chem. Phys. Lett.*, 114, 47, **1985.**

117. M. Wong, M. Gratzel, J. K. Thomas, *J. Am. Chem. Soc,* 98, 2391, **1976.**

118. G. D. Correll, R. N. Cheser, F. Nome, J. H. Fendler, *J. Am. Chem. Soc,* 100, 1254, **1978.**

119. a) B. Valeur, E. Keh, *J. Phys. Chem.,* 85, 3305, 1979; b) E. Keh and B. Valeur *J. Colloid Interface Sci.,* 79, 465, **1981;** c) M. Zulauf, A. F. Eicke, *J. Phys. Chem.,* 83, 480, **1979.**

120. P. E. Zinsli, *J. Phys. Chem.,* 83, 3223, 1979.

121. J. Eastoe, B. H. Robinson, A. J. W. G. Visser, D. C. Steytler, *J. Chem Soc.,Fraday Trans.,* 87, 1899, 1991.

122. D. -M. Shin, S. W. Kim, S. C. Shim, *Photochem. Photobiol.,* 34, 31, **1991.**

123. a) W. R. Ware, S. K. Lee, G. J. Brant, P. P. Chow, *J. Chem. Phys.,* 54, 4729, **1971;** b) V. Nagarajan, A. M. Brearley, T. -J. Kang, P. F. Barbara, *J. Chem. Phys.,* 86, 3183, **1987;** c) N. A. Nemkovich, W. Baumann, H. Reis, N. Detzer, *J. Photochem. Photobiol., A: Chem.,* 89, 127, **1995;** d) E. Laitinen, K. Salonen, T. Harju, *J. Chem. Phys.,* 104, 6138, **1996.**

124. a) T. Soujanya, T. S. R. Krishna, A. Samanta, *J. Photochem. Photobiol., A: Chem.,* 66, 185, **1992;** b) T. Soujanya, T. S. R. Krishna, A. Samanta, *J. Phys. Chem.,* 96, 8544, **1992.**

125. S. Mukerjee, A. Chattopadhyay, A. Samanta, T. Soujanya, *J. Phys. Chem.,* 98, 2809, **1994.**

126. a) M. Ravi, A. Samanta, T. P. Radhakrishnan, *J. Phys. Chem.*, 98, 9133, **1994;** b) M. Ravi, T. Soujanya, A. Samanta, T. P. Radhadirshnan, *J. Chem. Soc, Faraday Trans.,* 9±, 2739, **1995.**

127. T. Soujanya, R. W. Fessenden, A. Samanta, *J. Phys. Chem.,* 100, 3507, **1996**.

128. X. -K. Jiang, *Acc. Chem. Res.,* 21, 362, **1988;** b) W. Blokzijl, J. B. F. W. *Angew. Chem. Int. Ed. Engl.,* 32, 1545, **1993.**

129. a) Z. Zhen, C. -H. Tung, *Chem. Phys. Lett.,* 180, 211, **1991;** b) C. -H. Tung, Y. Li, Z. -Q. Yang, *J. Chem. Soc, Faraday Trans.,* 90, 947, **1994.**

130. **J. B.** Marling, J. G. Hawley, E. M. Liston, W. B. Grant, *Appl. Optics,* 13, 2317, **1994**.

EXPERIMENTAL AND THEORETICAL DETAILS

This chapter gives a description of the experimental and theoretical procedures that have been followed at various stages of the investigation. In the experimental section, details have been provided regarding the procurement, synthesis and purification of the materials, the instruments and the methodologies for Photophysical investigations. The theoretical section outlines a brief account of various semi-empirical methods and is followed by a description of the actual procedure employed in our AMI calculations.

2.1. Experimental

2.1.1. Materials and Purification

4-Aminophthalimide (AP) was obtained from Kodak and recrystallised several times from an ethanol-water mixture for Photophysical studies but used as received for the synthesis of its derivatives. Laser grade Carbostyrils, Cl24 and Cl65 (Fisher Scientific) were used without any purification. Sodium dodecyl sulphate (SDS), Cetyltrimethylammonium bromide (CTAB) and Triton X-100 were from Aldrich and were purified thoroughly before use as follows: SDS and CTAB were recrystallised from ethanol-water and acetone-water

mixtures, respectively. Triton X-100 was purified by column chromatography using silica gel column and acetone as eluent. Quinine sulphate monohydrate (Aldrich) used for fluorescence quantum yield measurements was recrystallised several times from water-ethanol mixture before use. KI and $CuSO_4 \cdot 5H_2O$, used for quenching studies, were locally procured chemicals of analytical grade (SDS Fine Chemicals Ltd., India). Analytical grade H_2SO_4 was also received from the same source.

p-Fluorobenzoic acid, p-fluorobenzonitrile and 11-bromoundecanoic acid were from Aldrich and were used as such for synthetic purpose. Piperazine (BDH) used for synthesis was recrystallised from acetonitrile. n-Propylamine, n-butylamine and n-hexylamine were from SDS Chemicals and distilled over KOH prior to use. Dodecylamine, hexadecylamine and octylamine (Aldrich) were used as received. 70 Wt. % solution in water as ethylamine solution was used as such which was from SDS Chemicals.

Silica gel used for column chromatography (SGC) was from Acme Scientific Chemicals (India). The drying agents used at various stages of the purification procedure, anhydrous CaO, $CaCl_2$, $MgSO_4$, CaH_2, K2CO3, P_2O_5 and Mg turnings were from Indian chemicals. Other common chemicals used KOH, Na_2CO_3 were of laboratory grade from BDH (India).

$CDCl_3$ (99.8%) from Sigma and $DMSO\text{-}d_6$ from Aldrich were used for ^1H NMR measurements.

Solvents

Extremely pure and dry solvents are essential for spectroscopic investigation of compounds involving dipolar species, because any contamination of the solvent by polar impurities such as water affects the spectral behaviour of the compounds significantly. Even though the solvents (locally procured, India) were of spectral grade, extreme care was taken for the purification and drying of the solvents in view of the solvatochromic nature *of* the spectral bands of the compounds studied. Each solvent was purified by following a standard procedure [1] which is outlined below. Only freshly purified solvents were used for spectral measurements.

Toluene, 1.4-dioxane, tetrahydrofuran and diethyl ether: Preliminary drying was done over ignited $CaCl_2$ or CaH_2 depending on the solvents. The perfect dryness of solvents was attained by distilling the solvent containing the blue ketyl formed from the reaction of Na with small amounts of benzophenone.

Ethyl acetate: Preliminary drying was done over anhydrous $CaCl_2$ and again dried by shaking with $MgSO_4$. Finally, the solvent was fractionally distilled over P_2O_5.

Chloroform: Preliminary purification was done by washing with water 2 to 3 times, drying over anhydrous $CaCl_2$ overnight and distilling fractionally. Finally, the solvent was distilled over P_2O_5.

Dichloromethane: Shaken with portions of concentrated H_2SO_4 until the acid layer remained colourless, then washed successively with water, 5% aqueous

Na_2CO_3 and water. Pre-dried over anhydrous $CaCl_2$ and distilled. Perfectly dried solvent was finally obtained by distilling over P_2O_5.

Acetone: Small portions of $KMnO_4$ added to acetone at reflux, until the violet colour persisted. This was followed by distillation, drying with anhydrous K_2CO_3 and fractional distillation.

Acetonitrile. Most of the water was removed by shaking the solvent with activated silica gel. Subsequent stirring with CaH_2 until no further evolution of hydrogen gas was evolved left only traces of water. This was followed by fractional distillation over CaH_2.

Methanol (MeOH): First, dried over CaH_2 by stirring overnight. Then to 50-75 ml of methanol, clean dry Mg turnings (5 g) and iodine (0.5 g) were added and warmed until all the Mg was converted into the magnesium methoxide. To this about 1 litre of methanol was added, refluxed for 2-3 h and distilled.

Ethanol (EtOH). First, the solvent was refluxed with freshly dried CaO (250 g/lit) for 6 h, allowed to stand overnight and then it was distilled to give absolute ethanol. To 50-75 ml of absolute ethanol, clean dry Mg turnings and iodine (0.5 g) were added and warmed until all the Mg was converted to the ethoxide. To this about 1 litre of ethanol was added, refluxed for 2-3 h and fractionally distilled to give perfectly dry solvent.

n-Propanol (n-PrOH): Pre-dried with CaH_2 and distilled fractionally. Then dried further by distilling at reflux with activated Mg with iodine.

n-Butanol (n-BuOH): Pre-dried with anhydrous $MgSO_4$, followed by reflux with and distillation over activated Mg with iodine.

The solvents, N,N-dimethylformamide (DMF) and dimethyl sulfoxide (DMSO) used for synthesis were purified by the procedures mentioned in reference 1.

Water. Triply distilled water was used for all studies involving aqueous medium.

The extent of dryness of each solvent was checked by monitoring the wavelength of the absorption maximum of the betaine dye 1 in a given solvent which exhibits one of the largest solvatochromic effects.[2] 1 was introduced by Dimorth and Reichardt[3] as a polarity indicator of the solvent in view of the extreme sensitivity of the intramolecular charge transfer band of the dye. Based

1
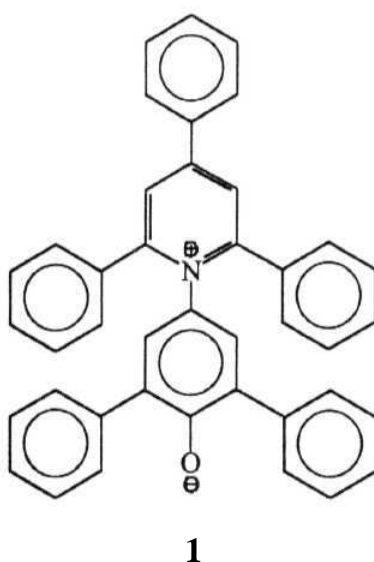
on the transition energy of the longest wavelength solvatochromic absorption band of the dye, a solvent polarity scale in terms of a polarity parameter, $E_T(30)$ was proposed. $E_T(30)$ was defined as

$$E_T(30)(\text{kcal/mol}) = 28591/\lambda_{max}(\text{nm}) \qquad 2.1$$

where $E_T(30)$ is the molar transition energy of 1 measured in kcal/mol at room temperature (25°C) and 1 atmospheric pressure and λ_{max} is the wavelength of the longest absorption band in nanometers. We measured the $E_T(30)$ values of the solvents and compared with the literature $E_T(30)$ values of the respective solvents to determine the extent of the contamination by the polar impurities. 1 was a kind gift from Prof. C. Reichardt of Philips University and used without any further purification.

2.1.2. Synthesis of the Probe Molecules

2.1.2.1. 11-(4-Aminophthalimido)undecanoic acid
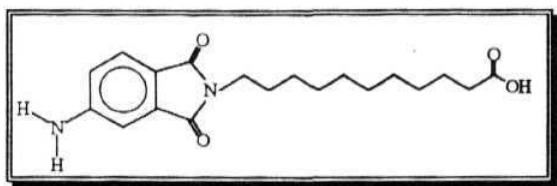
An equimolar mixture (2.2 mmol) of the potassium salt of AP and 11-bromoundecanoic acid was heated at 100 °C in dry DMF for 24 h under nitrogen atmosphere. The cooled reaction mixture was added to the water and the product was extracted with ethyl acetate. The yellowish solid obtained on

removal of ethyl acetate was purified by SGC (Hexane (HX): Ethyl acetate (EtOAc) / 60:40). The desired product was confirmed by the analysis of IR, ^{1}H NMR and Mass spectroscopy.

IR(KBr, cm"[1]): 3445, 3330, 2918, 2851, 1714, 1614, 1506, 1469.

^{1}H NMR (DMSO-d$_6$): 5 1.1-1.7 (m, 16H); 2.2 (t, 2H); 4(t, 2H); 6.8 (dd, 1H) 7.1 (d, 1H);7.5(d, 1H); 12 (s, 1H).

M[+]: 185, 162.

2.1.2.2. 11-(4-N,N-Dimethylaminophthalimido)undecanoic acid
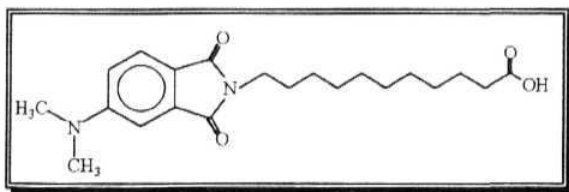
First, 4-dimethyl aminophthalimide (DAP), which was prepared from AP by following a procedure given in the literature.[4] Next, the potassium salt of DAP was prepared by heating a mixture of DAP (0.77 mmol) and KOH (0.77 mmol) in ethanol for 1 h and removing the solvent. In the second step, equimolar (0.5 mmol) mixture of the potassium salt of DAP and 11-bromoundecanoic acid was heated at 80 °C for 36 h in dry DMF. The cooled reaction mixture was added to the water and the product was extracted with ethyl acetate. The solid thus obtained was purified by SGC (HX:ETOH/70:30) to yield a yellowish crystalline material which was characterised by IR, ^{1}H NMR.

IR(KBr, cm"[1]): 3500, 2926, 2854, 1745, 1703, 1618, 1520, 1446.

^{1}H NMR (CDCl$_3$): δ 1.2-2.0 (m, 16H); 2.2 (t, 2H); 3.5 (t, 2H); 6.8 (dd, 1H); 7.1(d, 1H);7.6(d, 1H).

2.1.2.3. *N,N'-bis(4-Cyanophenyl)piperazine*
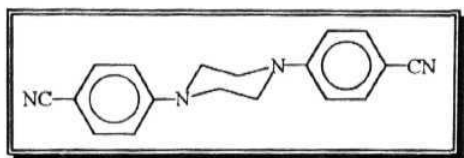
The compound was prepared by following a procedure given in the literature[5] as follows.

A mixture of piperazine (4 mmol) and p-fluorobenzonitrile (8 mmol) was taken in dry DMSO and heated at 90 °C for 24 h. The pale yellowish precipitate thus formed, after cooling reaction mixture was recrystallised from acetonitrile to obtain pale yellowish crystals. The compound was confirmed from the analytical data by comparing with the literature.

IR: (KBr, cm^{-1}): 2962, 2843, 2216, 1602, 1514.

CHN Analysis: Calculated for C$_{20}$H$_{16}$N$_4$: C=19.44, H=5.37, N=74.33; Found: C=19.44, H=5.55, N=75.0.

2.1.2.4. *N,N -bis(4-Carbomethoxyphenyl)piperazine(BIMBP)*
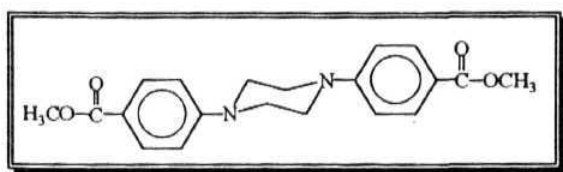
A mixture of piperazine (6.67 mmol) and p-fluoromethylbenzoate (13 mmol) was taken in dry DMSO and heated at 90 °C for 24 h. The cooled reaction mixture was added to the water and the product was extracted with ethyl acetate. The brownish solid thus obtained on evaporation of the solvent was purified by SGC (HX:EtOAc/60:40). The yellowish solid obtained was

further purified by recrystallisation using EtOH-H_2O mixture. The desired product was characterised by IR, ^{1}H NMR and CHN analysis.

IR: (KBr, cm"[1]): 2950, 1699, 1518, 1601, 1284, 1182, 1109.

^{1}H NMR (DMSO-d_6): δ 7.95 (d, J=9Hz, 4H); 6.9(d, J=9Hz, 4H); 3.85 (s, 6H); 3.5 (s, 8H).

CHN Analysis: Calculated for $C_{20}H_{22}N_2O_4$: C=67.79, H=6.21, N=7.90; Found: C=67.54, H=6.31, N=7.87.

mp: 225-229 °C.

2.1.2.5. *16-(4-Amin ophthalimido) h exadecane*
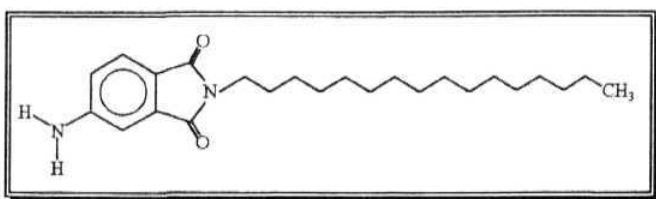
A mixture of AP (0.037 mmol) and hexadecylamine (0.037 mmol) in 1 ml of DMF was heated at 110 °C for 8 h.

After cooling the reaction mixture, H_2O was added and the compound was extracted with EtOAc. The residue obtained on evaporation of the solvent was purified by SGC (HX:EtOAC/90:10) to obtain an yellowish solid. The structural identity of the compound was established by the following analytical data.

IR (KBr, cm"[1]): 3495, 3373, 2918, 2849, 1763, 1689, 1614, 1406.

^{1}HNMR (CDCl$_3$): δ 0.87 (t, 3H); 1.25–1.6 (m, 28H); 3.57 (t, 2H); 6.8 (dd, 1H); 7.04 (d, 1H); 7.6 (d, 1H); 4.3 (s, 2H).

mp: 82–84 °C.

2.1.2.6. 12-(4-Aminophthalimido) dodecane
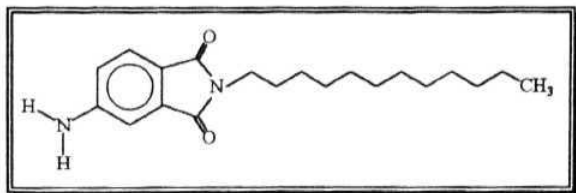
A mixture of AP (0.49 mmol) and dodecylamine (0.49 mmol) in 1 ml of DMF was heated at 110 °C for 6 h. The reaction mixture was added to H_2O and extracted with EtOAc. On evaporation of the solvent the residue was purified by SGC (HX:EtOAc/90:10). A nice yellowish solid was obtained which was characterised by the following analytical data.

IR(KBr, cm^{-1}): 3487, 3379, 2918, 2849, 1763, 1689, 1614, 1494.

^1H NMR (CDCl$_3$): 5 0.85 (t, 3H); 1.25 (m, 18H); 1.63 (t, 2H); 3.61 (t, 2H); 6.8 (dd, 1H); 7.04 (d, 1H); 7.57 (d, 1H); 4.35 (s, 2H).

mp: 72-74 °C.

2.1.2.7. 8-(4-Aminophthalimido)octane
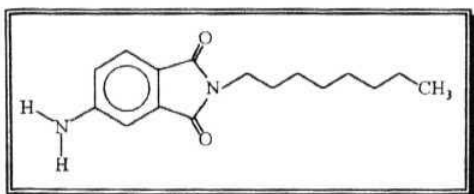
A mixture of AP (0.49 mmol) and octylamine (3 mmol) in 1 ml of DMF was heated at 80 °C for 3 h. The cooled reaction mixture was added to the H_2O and the compound was extracted with EtOAc. The residue thus obtained on evaporation of the solvent was purified by SGC (HX:EtOAc/85:15) to yield an yellowish solid of analytical grade. The product was analysed.

IR (KBr, cm^{-1}): 3476, 3362, 2922, 2851, 1759, 1695, 1630, 1502.

^{1}H NMR (CDCl$_3$): 5 0.85 (t, 3H); 1.25 (m, **10H); 1.6 (t, 2H); 3.65 (t, 2H);** 6.8 (dd, **1H); 7.0 (d, 1H);** 7.55 **(d, 1H);** 4.35 (s, **2H).**

mp: 52-55 °C.

2.1.2.8. 6-(4-Aminophthalimido)hexane
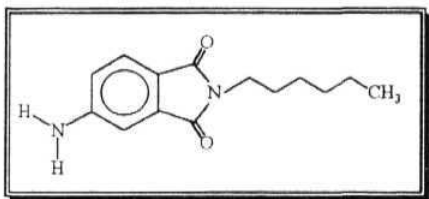
A mixture of AP (0.49 mmol) and hexylamine (7.5 mmol) were heated at 80 °C for 3 h. After the reaction, hexylamine was removed in *vacuum.* The residue was purified by SGC (HX:EtOAc/80:20) to give an yellowish, low melting solid of analytical grade. The product was analysed.

IR(KBr, cm^{-1}): 3440, 3368, 2930, 2858, 1759, 1699, 1616, 1502.

^{1}H NMR (CDCl$_3$): 5 0.9 (t, 3H); 1.31 (m, 6H); 1.65 (t, 2H); 3.65 (t, 2H); 6.75 (dd, 1H); 7.03 (d, 1H); 7.57 (d, 1H); 4.34 (s, 2H).

2.1.2.9. 4-(4-aminophthalimido)butane
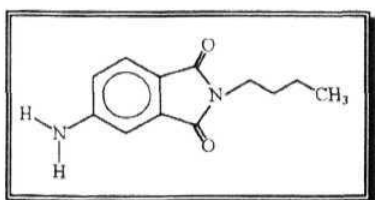
AP (0.62 mmol) and butylamine (0.01 mol) were heated at 80 °C for 4 h. On removal of butylamine in *vacuo,* the residue was purified by SGC (HX:EtOAc/75:25) to obtain an yellowish crystals on evaporation of the solvent.

IR(KBr, cm^{-1}): 3483, 3375, 2753, 1753, 1689, 1626, 1502.

^{1}H NMR (CDCl$_3$): 5 0.94 (t, 3H); 1.4 (m, 2H); 1.65 (t, 2H); 3.66 (t, 2H); 6.84 (dd, 1H); 7.03 (d, 1H); 7.57 (d, 1H); 4.35 (s, 2H).

mp: 118-120 °C.

2.1.2.10. 3-(4-Aminophthalimido)propane
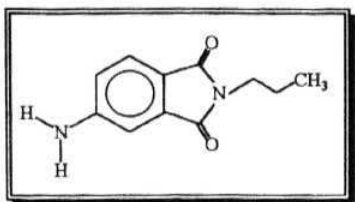
AP (0.49 mmol) and propylamine (0.024 mol) were heated at reflux for 3 h. After removal of propylamine in *vacuo*, the solid was purified SGC (HX:EtOAc/80:20) to give an yellowish solid of analytical grade. It was analysed.

IR(KBr, cm^{-1}): 3479, 3373, 2955, 2872, 1749, 1685, 1630, 1612.

^{1}HNMR (CDCl$_3$): 5 0.97 (t, 3H); 1.66 (m, 2H); 3.63 (t, 2H); 6.82 (dd, 1H); 7.03 (d, 1H); 7.55 (d, 1H); 4.3 (s, 2H).

mp: 52-55 °C.

2.1.2.11. 2-(4-Aminophthalimido)ethane
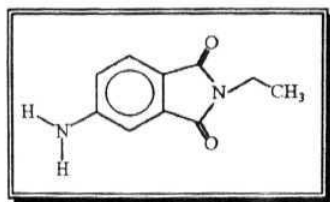
AP (0.17 mmol) and 10 ml of ethylamine solution (70 wt. % in H$_2$O, 0.18 mmol) were stirred for about 8 h at room temperature. H$_2$O was removed from reaction mixture and the residue was purified by SGC (HX:EtOAc/85:15) to yield yellowish crystals of analytical grade. The product was analysed.

IR (KBr, cm^{-1}): 3452, 3356, 2939, 1759, 1689, 1612, 1502.

^{1}H NMR (CDCl$_3$): 5 1.24(t, 3H); 3.69 (t, 2H); 6.82 (dd, 1H); 7.03 (d, 1H); 7.55 (d, 1H); 4.38 (s, 2H).

mp: 159-160 °C.

56

2.1.3. Solution Preparation for Spectral Measurements

Dilute solutions (optical density in the range 0.1 - 0.25 at the longest wavelength absorption maximum which corresponded to the concentration of 2-8 x 10^{-5} M) were used for the measurement of absorption, fluorescence emission and excitation spectra.

For studies in aqueous medium the procedure followed was as follows. Solutions of the compounds were prepared in water either by direct addition of the solid to water or dissolving the compound in organic solvent (like DCM or MeOH), evaporating it and then adding water. The aqueous solutions were sonicated for ~ 15 min. and allowed to stand for about 30 min. This was followed by repeated filtration of the solution so as to avoid any undissolved particles. The solutions were diluted or taken directly depending on the concentration. Usually concentrations of the solutions in *aq* medium were maintained at 2 - 10 x 10^{-5} M. Required amounts of surfactants were added either directly as solid or aliquots of aqueous surfactant solutions to an aqueous solution of the probe for studies in microheterogeneous media and steady-state and time-resolved studies were performed. In some cases where very low concentrations (~ x 10^{-6} M) were needed for measurements. In these cases a few microlitres of methanolic solution of the compound was added to the water to prepare the *aq* solutions.

Quenching experiments were performed at high concentrations of the surfactants such that the probe molecules were almost completely micellised.

These experiments were carried out by adding few microlitres of stock solution of quencher to the probe solution (3 ml in the cuvette) in micelles. A low concentration of probe/micelle was employed during the quenching experiments to ensure that no more than one probe molecule was bound to each micelle. All the physical measurements were done at 25 °C.

2.1.4. Measurement of Fluorescence Quantum yields (ϕ_f)

Quinine Sulfate was used as the reference compound for fluorescence quantum yield measurements of all the samples ($\phi_f = 0.55$ in $1N\ H_2SO_4$).[6] Fluorescence quantum yields were determined by integrating the area under the fluorescence curves and using the expression of Austin and Goutermann.[7]

$$\phi_{sample} = \frac{I_{sample} \times O.D_{standard}}{I_{standard} \times O.D_{sample}} \times \phi_{standard} \qquad \textbf{2.2}$$

where I is the area under the emission curve. O.D is the optical density of the compound at the exciting wavelength. For actual measurements, optically matched solutions of the reference and the sample at the exciting wavelength were used and areas were determined either by the programme available with the spectrofluorimeter or by 'cut and weigh' method. No solution of O.D more than 0.2 at the exciting wavelength was used and no correction for the solvent refractive indices was made.

2.1.5. Measurement of Change in Dipole Moment on Excitation ($\Delta\mu$)

Although a number of expressions have been proposed which correlate the absorption and emission spectral data of the systems with the solvent polarity, the most widely used expression is one based on early experiments of Lippert and Mataga.[8,9] Onsagar reaction field theory provides the basic framework for this equation, which assumes the solute molecule as a point dipole situated in the spherical cavity, known as Onsager cavity, in a homogeneous and continuous dielectric medium.[10] According to this model, the fluorophore-solvent interaction is given by the interaction of the dipole in the cavity with its own reaction field arising from the polarisation of the surrounding dielectric by the dipole. According to Lippert-Mataga equn.[8], the energy difference of the absorption and fluorescence maxima of a compound ($\bar{v}_a - \bar{v}_f$ / cm^{-1}) in a given solvent is related to the solvent polarity function (f – f' or Δf) as shown below

$$\bar{v}_a - \bar{v}_f = \frac{2(\mu_e - \mu_g)^2}{hca^3}\left(f - f'\right) \qquad\qquad \textbf{2.3}$$

where f is (e-1)/(2e+1) and f is $(n^2-1)/(2n^2+1)$, h is the Planck constant, c is the velocity of light, *a* is the Onsager cavity radius and μ_g and μ_e are the ground and excited state dipole moments of the molecule, respectively. ε and n are the bulk solvent properties, dielectric constant and refractive index, respectively. The solution of this equation requires the use of measurable parameters such as

Onsager cavity radius, the absorption and fluorescence energies in solvents of varying polarity. $\Delta\mu$ was estimated from the slope of the plot of $\left(\overline{\nu}_a - \overline{\nu}_f\right)$ vs $\left(f - f'\right)$.

In the original papers on dual fluorescence by Lippert et. al,[11] the excited dipole moments of DMABN (4-dimethylaminobenzonitrile) and DEABN (4-diethylaminobenzonitrile) were determined by solvatochromic measurements, based on the energy difference $\Delta\overline{\nu}$ between the maxima of the locally excited or charge transfer fluorescence band and the absorption maxima, as a function of the solvent polarity and polarizability of the solvent,[8] with the assumption that the charge transfer (CT) state can be populated directly by light absorption. However, Zachariasse et.al [12a,b] have later pointed out that the charge transfer state is not accessible by direct excitation. In such cases, where the emitting state can not be populated directly by excitation, the dipole moment is to be determined by a slightly modified relation between the emission wavenumber $(\overline{\nu}_f^{max}/cm^{-1})$ and the solvent polarity function, $(f - \frac{1}{2}f')$. This relation which is also valid for exciplexes[12c] is shown below

$$\overline{\nu}_f/cm^{-1} = \frac{2\mu_e^2}{hca^3}\left(f - \frac{1}{2}f'\right) \qquad\qquad \textbf{2.4}$$

where μ_e is determined from the slope of the plot of $\overline{\nu}_f$ vs $(f - \frac{1}{2}f')$. We have used equn. 2.4 for determining μ_e in some cases where we thought this expression to be appropriate (sec. 6.2.3).

2.1.6. Calculation of Nonradiative Rate Constants (k_{nr})

The nonradiative rate constants (k_{nr}) were estimated from the measured fluorescence quantum yield (ϕ_f) and the lifetime (τ_f) using

$$k_{nr} = \frac{(1 - \phi_f)}{\tau_f} \qquad\qquad \textbf{2.5}$$

2.1.7. Instrumentation

The IR and ^{1}HNMR spectra were recorded on JASCO FT–IR/5300 and on Bruker ACF-200 at 200 MHz spectrophotometers, respectively. CHN analysis was performed on Perkin-Elmer 2400 CHN analyser. Melting points were determined on Superfit melting point apparatus and were uncorrected. High resolution mass spectra were recorded on Micromass VG/70H instrument at 1ICT, Hyderabad.

The absorption spectra were recorded either on a JASCO Model 7800 or on a Shimadzu Model 160A spectrophotometer. Fluorescence spectra were recorded either on JASCO FP-777 or on a Hitachi-3100 spectrofluorimeter. The fluorescence spectra were not corrected for the instrumental characteristics.

The fluorescence lifetimes were measured on IBH 5000 Single-photon counting spectrofluorimeter.[13] Fig. 2.1 shows the layout of a typical time-correlated single-photon counting fluorimeter.

A hydrogen flash-lamp of pulse-width 1.4 ns and frequency of 40 kHz was employed as the excitation source. A small fraction of the excitation pulse was directed to a photomultiplier tube (1P28) and the photomultiplier signal was fed into a constant-fraction-discriminator (CFD) to discriminate the back-ground noise and generate a precise timing pulse. The output of CFD served as the START purse of the time-to-amplitude converter (TAC). A fluorescence photon recorded by the emission photomultiplier (Hamamastu 3235), as determined by discriminator, generated a pulse which served as the STOP signal for the TAC. The TAC signal produced was proportional to the time taken from the excitation event to the first photon recorded. The signal from TAC was digitised by the analog to digital converter (A/D converter) and sent to the appropriate channel, depending on the digitised value of the TAC voltage, of a multichannel analyser (MCA). The whole process was repeated so that the MCA counts represented the number of photon events as a function of time. After many excitation pulses the MCA memory contents represented a histogram of the emission decay i.e. time profile of the fluorescence intensity. For recording the lamp-profile, a scatterer (dilute solution of MgO in H_2O) was placed in the place of the sample.
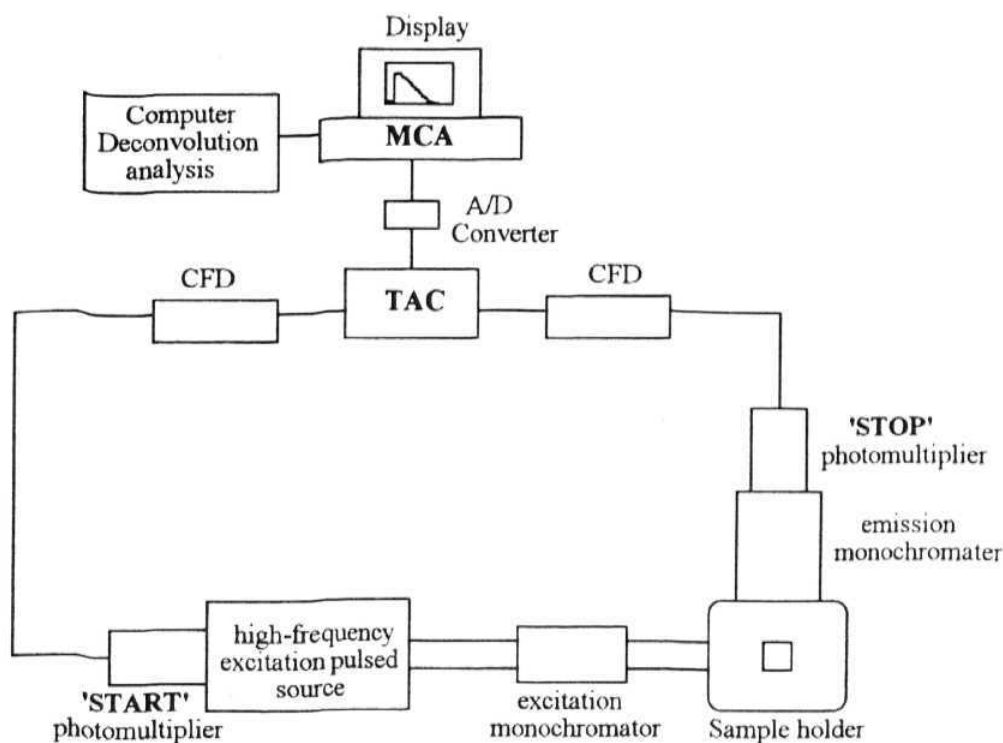
Fig. 2.1. Schematic representation of a single-photon counting apparatus.

Data Analysis

Procedure must be used to extract the decay parameters from the collected data. The programme which we have used is based on reconvolution least-squares method.[14]

When the decay time is long compared to the decay time of the excitation pulse, the excitation may be described as a 5-function. However, when the lifetime is short, distortion of the experimental data occurs by the finite decay time of the lamp pulse and response time of the photomultiplier and

associated electronics. Since the measured decay function is convolution of the true fluorescence decay, it is necessary to analyse the data by deconvolution in order to get the fluorescence lifetime.

The mathematical statement of the problem is given by the following equn.

$$D(t) = \int_0^t P(t') \, G(t-t') \, dt' \qquad\qquad 2.6$$

where D(t) is the fluorescence intensity at any time t. P(t') is the intensity of the exciting light at time t', $G(t-t')$ is the response function of the experimental system. The experimental data D(t) and P(t') from the MCA are fed into a computer (IBM PC clone, 80486, 50 MHz) to determine τ. We have used the IBH programme to analyse the multi-exponential decays.

An excitation pulse profile was recorded and then deconvoluted with the mixing of the excitation pulse and the projected decay to form a new reconvoluted set. The data was compared with the experimental set and the difference between the data points summed, generating χ^2 function for the fit. The deconvolution proceeded through a series of such iterations until an insignificant change of χ^2 occurs between iterations. The quality of the fit is normally assessed by the inspection of reduced χ^2, plot of weighted residuals and autocorrelation function of the residuals. The data points and the fitted curve were finally recorded by a plotter.

64

2.1.8. X-Ray Crystallography

Crystal structure of BIMBP has been determined as described. The crystals of the compound were grown from an acetonitrile solution of the compound. A crystal of dimension 0.22 x 0.15 x 0.10 mm was mounted on a Siemens SMART charge coupled device detector system single crystal diffractometer using graphite monochromated MoKa radiation $(X = 0.71073 \text{ Å})$. Preliminary unit cell constants were determined with a set of 60 narrow frames $(0.3°$ in $\omega)$ scans. A total of 1500 frames of intensity data were collected with a frame width $0.3°$ in ω. The collected frames were integrated using an orientation matrix determined by narrow frame scans. Final cell constants were determined by a global refinement of xyz centroids of 1490 reflections. Absorption correction was not applied to the data. The integration process yielded 5549 reflections of which 1559 were independent reflections. The crystallographic parameters are summarised in Table 2.1. The positional parameters for non-hydrogen atoms along with isotropic thermal parameters, anisotropic thermal parameters, hydrogen coordinates, the bond lengths and bond angles with standard deviations are given in Appendix, Tables A1-A4.

Table 2.1 Crystal Data and Structure Refinement for the Molecule, BIMBP.

Systematic name	N,N'-bis(4-carbomethoxyphenyl)piperazine
Structural Formula	$C_{20}H_{22}N_2O_4$
Formula weight	354.40
Temperature	298 (2) K
Crystal System	Monoclinic
Space group	$P2_1/n$
Unit cell dimensions	a = 9.4015 (4) A alpha = 90°
	b = 8.1435 (4) A beta = 102.978 (2)
	c = 11.8872 (5) A gamma = 90°
Volume, Z	886.85 (7) A^3, 2
Density (calculated)	1.327 Mg/m^3
Absorption coefficient	0.093 mm^{-1}
F (000)	376
Crystal size	0.22 x 0.15 x 0.10 mm
Crystal colour	Dark yellow
θ range for data collection	2.51 to 24.99°
Limiting indices	$-12 \leq h \leq 12, -7 < k < 10, -15 < 1 \leq 13$
Reflections collected	5549
Independent reflections	1559 (R_{int} = 0.0522)
Absorption correction	None

Refinement method	Full-matrix least-squares on F^2
Data / restraints / parameters	1529/0/118
Goodness-of-fit on F^2	**1.053**
Final R indices [I > σ(I)]	R1 =0.0551, wR2 = 0.1208
R indices (all data)	R1 =0.1071, wR2 = 0.1582
Largest diff. peak and hole	0.153 and -0.186 $e\text{Å}^{-3}$

Standard error limits involved in various measurements are:

λmax (abs/fluo)	±1 nm
ϕ_f	±10%
τ(> 1 ns)	±5%
τ (< 1 ns)	±15%

2.2. Theoretical

2.2.1. Semi-empirical Calculations

Quantum chemical calculations can be broadly classified into *ab initio* and semi-empirical methods.[15] The oldest and simplest semi-empirical method of quantum-chemistry, utilising the so-called π - electronic approximation is that of Huckel, usually referred to by the abbreviation HMO (Huckel Molecular Orbital Method). The counterpart of the traditional Huckel method is represented by the so-called Extended Huckel Theory (EHT) proposed in 1963

by R. Hoffman.[16] The methods which follow the Hartee-Fock-Roothan approach can be distinguished as NDDO (Neglect of Diatomic Differential Overlap), CNDO (Complete Neglect of Differential Overlap) and INDO (Intermediate Neglect of Differential Overlap) schemes introduced in 1965 by Pople and his co-workers.[17] The schemes are obtained by various approximations involved in the reduction of the Hartee-Fock-Roothan method. Among INDO type of methods one should consider the semi-empirical approaches due to Dewar et. al and known as MINDO (Modified Intermediate Neglect of Differential Overlap) schemes.[18] Confidence in semi-empirical *procedure is moreover strengthened* by demonstrations of its ability to reproduce experimental results. One of the major assets of MINDO/3 and MNDO was their demonstrated ability to reproduce the ground state properties of molecules of all kinds.[18,19] MNDO is proved to be a good method over MINDO/3 in the case of molecules containing heteroatoms, but at the expense of other weaknesses.[19] To avoid these, a new parametric quantum mechanical molecular model, AM1 (Austin Model 1), based on the NDDO approximation is developed by Dewar et. al.[20] Calculations on several test molecules indicate that AM1 seems to represent a very real improvement over MNDO with no increase in the computational time needed. The main improvements are the ability of the AM1 method to reproduce hydrogen bonds and better estimates of activation energies for reactions. Recent AM1 results on some polar systems show that the method is capable of predicting the excited state properties also

68

fairly well.[21] Recently, Soujanya et. al[22] have demonstrated the ability of this method in predicting the Photophysical features of DMABN which exhibits dual fluorescence.

We have performed our calculations using semi-empirical AM1 method using MOP AC programme (ver. 5) and Hyperchem software. Preliminary optimisation of structures were obtained from MM^+ molecular mechanics programme. Subsequently, more precise geometry optimisation was achieved at semi-empirical level. The influence of the twist angle on the energetics of the ground and excited state was studied by fully optimising the geometry for each dihedral angle (every 10 degrees). Reasonably lower gradient norms (0.01) were chosen. The excited state energies were obtained using configuration interaction with 128 microstates generated by exciting *one electron* from each *of* the eight highest occupied orbitals to the eight lowest unoccupied orb\tals. Calculations were performed on personal computers. Output of each calculation gave the heat of formation, dipole moment, ionization potential, gas phase energy and electron density.

2.2.2. Calculation of Solvation Energies

The solvation of the different electronic states has been taken into account within the basic framework of Onsager's theory.[10] The energy of a dipole μ in a reaction field R is given by

$$E = \vec{\mu} \cdot \vec{R} \qquad \textbf{2.7}$$

When a molecule with a permanent dipole moment $\vec{\mu}$ is surrounded by solvent molecules, the inhomogeneous field of the permanent dipole polarises the environment. The resulting inhomogeneous polarisation of the environment will create a reaction field $\vec{R}$ at the dipole which is given by

$$\vec{R} = \frac{2}{a^3} f \vec{\mu}$$
2.8

$\vec{\mu}$ is the solute dipole causing polarisation of the cavity of radius a. When the solvent is fully equilibrated, f is given by $f(\varepsilon) = (\varepsilon - 1)/(2\varepsilon + 1)$, where 6 is the dielectric constant of the medium. But if the dipole moment of the solute changes so rapidly that the solvent dipoles cannot reorient, although its electrons are polarised, f is given by $f(n) = (n^2 - 1)/(2n^2 + 1)$, where, n is the refractive index of the medium.

The solvation energy of a fully relaxed state of dipole $\vec{\mu}_i$ is given by

$$\Delta E = \frac{2\vec{\mu}_i^2}{a^3} \frac{(\varepsilon - 1)}{(2\varepsilon + 1)}$$
2.9

Since the fluorescence lifetime of most of the molecules are larger than the solvent relaxation time, the emitting states can be assumed fully solvated and the solvation energies were calculated using equn. 2.9. The solvent-modulated

energy of a state have been obtained by adding the solvation energy to the gas phase total energy of a particular state.

2.3. References

1. D. D. Perrin, W. L. F. Armarego, D. R. Perrin, *Purification of Laboratory Chemicals*, II ed., Pergamon Press: New York, **1986,** and references therein.

2. C. Reichardt, *Solvents and Solvent Effects in Organic Chemistry,* VCH: Weinheim, **1988,** Chap. 7, and references therein.

3. K. Dimorth, C. Reichardt, T. Siepmann, F. Bohlmaun, *Liebigs Ann. Chem.,* 661. 1, **1963.**

4. H. K. Hall, R. Zbindens, *J. Am. Chem. Soc.,* 80, 6428, **1958.**

5. J. P. Launay, M. Sowindka, L. Leydier, A. Gourdon, E. Amouyal, M. L. Boillot, F. Heisel, J. A. Miehe, *Chem. Phys. Lett.,* 160, 89, **1989.**

6. W. H. Melhuish, *J. Phys. Chem.,* 65, 229, **1961.**

7. E. Austin, M. Goutermann, *Bioinor. Chem.,* 9, 281, **1978.**

8. a) E. Lippert, Z *Naturforsch,* 10A, 541, 1955; b) N. Mataga, Y. Kaifu, M. Koizumi, *Bull. Chem. Soc. Jpn.,* 29, 465, **1956;** c) N. Mataga, *Bull. Chem. Soc. Jpn.,* 36, 654, **1963.**

9. B. Koutek, *Collect. Czech. Commun.,* 43, 2368, **1978.**

10. C. J. F. Bottcher, *Theory of Electric Polarisation,* 153, **1973.**

11. E. Lippert, W. Liider, H. Nagele, H. Boos, H. Prigge, I. S. Blankenstein, *Angew. Chem.,* 73, 695, **1981.**

12. a) W. Shuddeboom, S. A. Jonker, J. M. Warman, U. Leinhos, W. Kuhnle, K. A. Zachariasse, *J. Phys. Chem.,* 96, 10809, **1992;** b) U. Leinhos, W. Kuhnle, K. A. Zachariasse,./. *Phys. Chem.,* 95, 2013, **1991;** c) A. Weller, Z. *Phys. Chem.,* 133, 93, **1982.**

13. a) D. V. O' Connor, D. Phillips, *Time-Correlated Single Photon Counting,* Academic Press: London, **1984;** b) J. R. Lakowicz, In: *Topics in Fluorescence Spectroscopy,* J. R. Lakowicz, ed., Vol 1, Plenum Press: New York, **1991**.

14. a) P. R. Bevington, *Data Reduction and Error Analysis For The Physical Sciences,* McGraw-Hill: New York, **1964;** b) D. F. Eaton, *Pure. Appl. Chem.,* 62, 1631, **1990.**

15. J. Sadlej, *Semi-Empirical Methods of Quantum Chemistry,* Ellis-Horwood: Poland, **1985** and reference therein.

16. R. Hoffmann, *J. Chem. Phys.,* 39, 1397, **1963;** 40, 2047, 2474, 2480, **1964.**

17. J. A. Pople, D. L. Beveridge, P. A. Dobosh, *J. Chem. Phys.,* 47, 2026, **1967**.

18. M. J. S. Dewar, W. Thiel, *J. Am. Chem. Soc.,* 99, 4899, 4907, 1977.

19. R. C. Bingham, M. J. S. Dewar, D. H. Lo, *J. Am. Chem. Soc,* 97, 1285, 1294, 1302, 1367, **1975.**

20. a) M. J. S. Dewar, E. G. Zoebisah, E. F. Healy, J. J. P. Steiwart, *J. Am. Chem. Soc,* 107, 3072, **1985,** b) M. J. S. Dewar, K. M. Dieter, *J. Am. Chem. Soc,* 108, 8075, **1986.**

21. a) M. M. Awad, P. K. McCarthy, G. S. Blanchard, *J. Phys. Chem.,* 98, 1454, **1994;** b) K. Reihthaler, G. Kohler, *Chem. Phys.,* 189, 94, **1994** c) A. D. Gorse, M. Pesquer, *J. Phys. Chem.,* 99, 4039, **1995.**

22. T. Soujanya, G. Saroja, A. Samanta, *Chem. Phys. left.,* 236, 503, 1995.

**4-AMINOPHTHALIMIDE AND ITS AMPHIPHILE,
11-(4-AMINOPHTHALIMIDO)UNDECANOIC ACID AS
FLUORESCENCE SENSORS OF MICROENVIRONMENTS:
STUDY IN MICELLAR MEDIA**

The present chapter describes the fluorescence response of 4-aminophthalimide (AP, Chart 3.1) and 1 l-(4-aminophthalimido)undecanoic acid (APL, Chart 3.1) in micellar media. While the first section of this chapter is concerned with the study of AP, the second section describes our observation with **APL.**
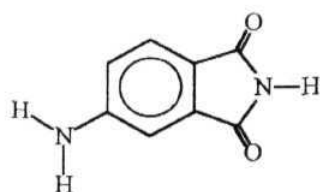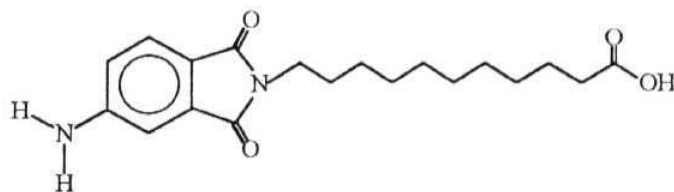
AP   **APL**

CHART 3.1

3.1. AP as Sensor of Microenvironments in Micellar Media

Molecular spectroscopy provides a powerful tool in understanding and description of the photoinduced intramolecular charge transfer (ICT) processes. The use of fluorescent molecules as reporters of the local environment of the microheterogeneous media such as micelles, cyclodextrins, membranes etc. is well-documented in the literature.[1-11] As mentioned previously, fluorescent electron donor-acceptor (EDA) molecules are excellent polarity probes as the fluorescence originating from locally excited ICT state is highly sensitive to the solvent polarity. A number of probes of this kind can be found in the literature.[1-11]

Aminophthalimides are known for their high sensitivity of the fluorescence properties towards minor changes in the structure and dynamics of the environment[12] and have been widely employed as solvation probes for the investigation of solvent relaxation in pure and binary solvents.[12a-e,g,i,j] Picosecond domain experiments have been performed to follow the time-dependent Stokes shift of AP fluorescence in fluid solvents[12g,i,j] revealing strongly solvent dependent relaxation times. Noukakis et al[12e] suggested a large change in dipole moment of APs on electronic excitation that corresponds to the nearly complete charge transfer from the amino nitrogen to the acceptor imide system.

During the studies on EDA molecules Soujanya et al observed that the fluorescence properties of AP were extremely sensitive to the polarity of the

media, in particular, to the hydrogen bonding solvents.[13,14] A detailed study on AP and its N,N-dimethylamino derivative has revealed that the fluorescence of aminophthalimide derivatives originates from a locally excited state with ICT in nature.[14] The change in the dipole moment of the molecule on excitation is found to be approximately 5 D. The specific interaction of AP with hydrogen bonding solvents was also observed by Harju et al who suggested that AP undergoes solvent-mediated proton transfer.[12g,i] Very recently, Das et al[15] also suggested that the unusual Stokes shift of the fluorescence band of AP in alcoholic solvents is due to the solvent-mediated proton transfer, as suggested by Harju et al. However, the fact that N-methyl-AP, which does not contain the imide hydrogen necessary for the proton transfer, shows behaviour similar to AP suggests that the Stokes-shifted fluorescence of AP in alcoholic solvents is simply due to hydrogen bonding interaction. The possible application of AP in determining the water content of a medium is also suggested by Langhals.[16] More recently, Basu et al[17] reported the CT character of triple state of AP by laser flash photolysis studies.

The fluorescence maximum (λ_{max}^{flu}) of AP shifts by more than 100 nm on changing the solvent from 1,4-dioxane to water. 13,14 The fluorescence yield (ϕ_f) and lifetime (τ_f) decrease by a factor of 60-70 and ~ 12, respectively for the same change of solvent.[13,14] Taking advantage of these polarity sensitive fluorescence properties, the guest-host interaction in cyclodextrins using AP as the guest molecule was studied recently.[13] Since micelles are composed of both

hydrophobic and hydrophilic pockets, we thought it appropriate to examine the potential of AP as a neutral polar probe to follow the microheterogeneous environments of the micellar aggregates. AP, because of its solvatochromic fluorescence properties, is expected to provide a precise estimate of the polarity of the microenvironment in which it is solubilised. The microscopic polarity of an organised medium is a fundamental property, a knowledge of which helps understanding its structure and the function. Among the available experimental methods for investigation of the micropolarity, emission technique is particularly a good tool.[5,6] We have chosen three types of commonly used surfactants, cationic (Cetyltrimethylammonium bromide, CTAB), anionic (sodium dodecyl Sulfate, SDS), and neutral (Triton X-100, TX) for our study to find out whether the fluorescence response of the system is dependent on the charge of the micelle.

3.1.1. Absorption Spectra

The change in the absorption spectrum on addition of surfactants (SDS, CTAB, TX) to an *aq* solution of AP is found to be rather small. The representative spectra illustrating the effect of addition of a surfactant on the absorption spectrum of AP are shown in Fig 3.1. The minor changes in the absorption spectra on the addition of the surfactant are in agreement with the fact that the absorption spectrum of AP is not very sensitive to small changes in the polarity of the medium. Because the surfactant induced changes in the
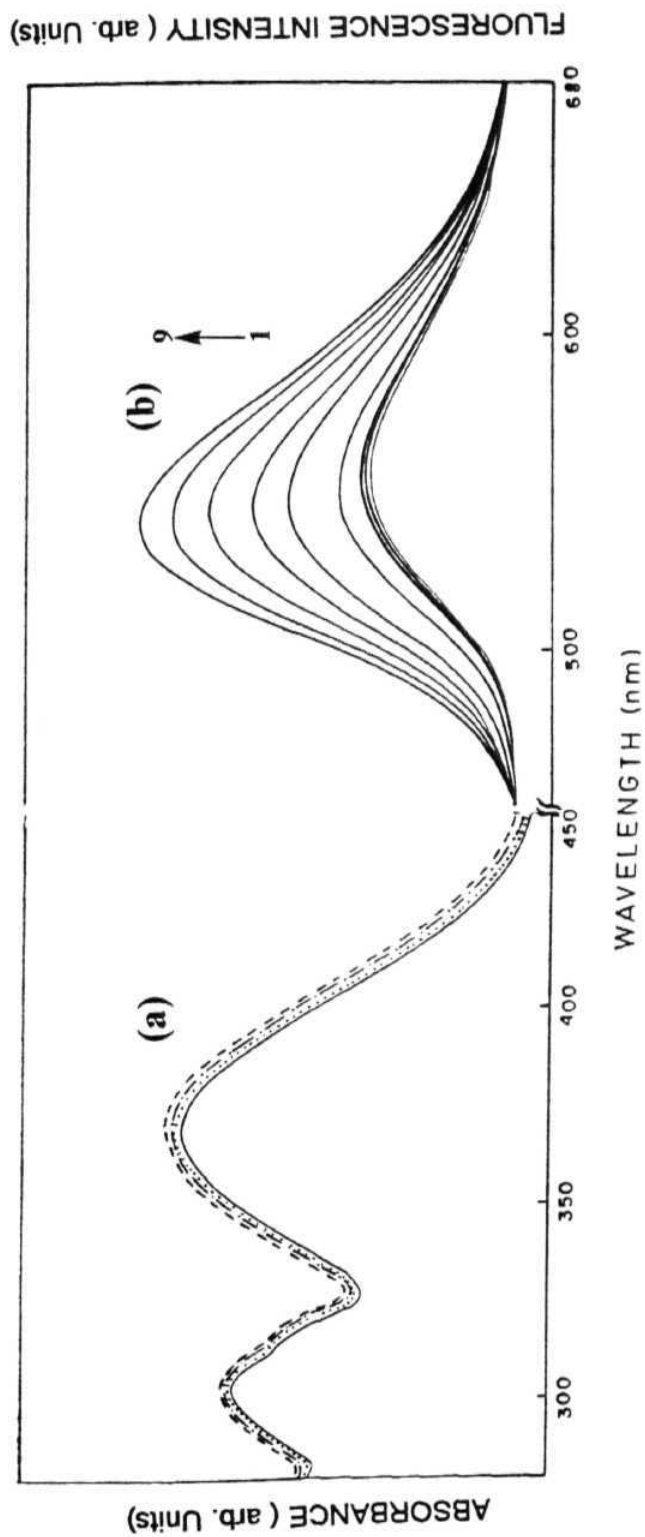
Fig. 3.1. Absorption (a) and fluorescence (b) spectra of AP in aqueous solution with different amount of SDS. The concentrations of SDS (mM) are (a) 0 (——), 6 (····), 35 (– – –), 71 (–·–·). (b) in increasing order of intensity, 0, 2, 6, 10.5, 16.7, 23, 35, 48, and 71, respectively. $\lambda_{exc} = 370$ nm.

78

absorption spectrum of AP is not very significant, no attempt has been made to analyse these spectral data further.

3.1.2. *Fluorescence Spectra*

In contrast to the effect on the absorption spectra, addition of surfactants leads to significant changes of the fluorescence spectrum. Addition of the surfactants is associated with a blue-shift of the spectrum and an enhancement of the fluorescence intensity. The effect of SDS on the emission behaviour of AP is illustrated in Fig. 3.1 However, as seen from the figure, the change in the fluorescence properties is not significant below a certain concentration of the surfactant and above which both the enhancement and the spectral shift are more pronounced. The shift of the spectra and the enhancement of the fluorescence intensity can be rationalised in terms of the binding of the probe molecule to a less polar site in the micelle. As the excited state of AP is more polar than the ground state, [1 4] a lowering of the polarity of the medium destabilises the excited state more than the ground state. As a consequence, the energy gap between the ground and the emitting state is increased and the spectra shift towards the blue region. The fluorescence enhancement is most likely due to a reduction in the internal conversion rate as a consequence of the increased separation between the S_1 and SQ states. The reduction in hydrogen bonding interaction with the solvent may also be partly responsible for the increase in ϕ_f. The fluorescence intensity or the position spectral maximum changes linearly with surfactant concentration beyond the critical micelle concentration (CMC). However, at

higher surfactant concentrations, no farther change in the position of the spectral maximum or the fluorescence intensity could be observed. Obviously, under this condition most of the probe molecules are bound to micelles. The fluorescence behaviour of AP in cationic (CTAB) and neutral (TX) micelles is found to be quite similar to that observed with anionic (SDS) micelle. Although in the case of CTAB, initial addition was associated with a small decrease in the fluorescence intensity, presumably due to heavy atom quenching of the fluorescence by Br^- ions, later addition (beyond CMC) led to expected increase in the fluorescence intensity.

The maximum spectral shift and the fluorescence enhancement data of AP in the three micelles are summarised in Table 3.1. A quantitative analysis of fluorescence enhancement data has been carried out to obtain the CMCs. In Fig. 3.2 is shown a plot of the relative fluorescence intensity (ϕ_f/ϕ_0, ϕ_0 and ϕ_f are the fluorescence yields at zero and at a given surfactant concentration, respectively) against [SDS], The insert in the same figure shows the variation of the relative intensity with surfactant concentration over the entire concentration range used. From the intersection point of the two straight lines shown in the Fig. , the CMC of SDS is estimated to be (7.5 ± 0.5) x 10^{-3} M. In a similar manner, the measured CMC values of CTAB and TX are found to be $(8 \pm 0\ 5)$ x 10^{-4} M and (2.8 ± 0.2) x 10^{-4} M, respectively. Table 3.2 summarises the measured CMC values along with the literature values for comparison.

Table 3.1 Fluorescence Enhancement and Spectral Shift of AP in Aqueous Solution Containing Highest Amount of the Surfactant.

Surfactant	Concentration (mM)	Maximum	
		Enhancement(ϕ_f/ϕ_0)	Shift (nm)
SDS	160	2.74	14.0
CTAB	93	2.61	18.0
Triton X-100	78	2.95	20.5

Table 3.2 Critical Micellar Concentrations of SDS, CTAB and Triton X-100.

Micelle	Measured CMC (10^{-4} M)	Literature CMC[a] (10^{-4} M)
SDS	75.0 ($\pm$5.0)	80.0
CTAB	8.0 ($\pm$0.5)	9.2
Triton X-100	2.8 ($\pm$0.2)	2.6

[a]Collected from Ref. [1]
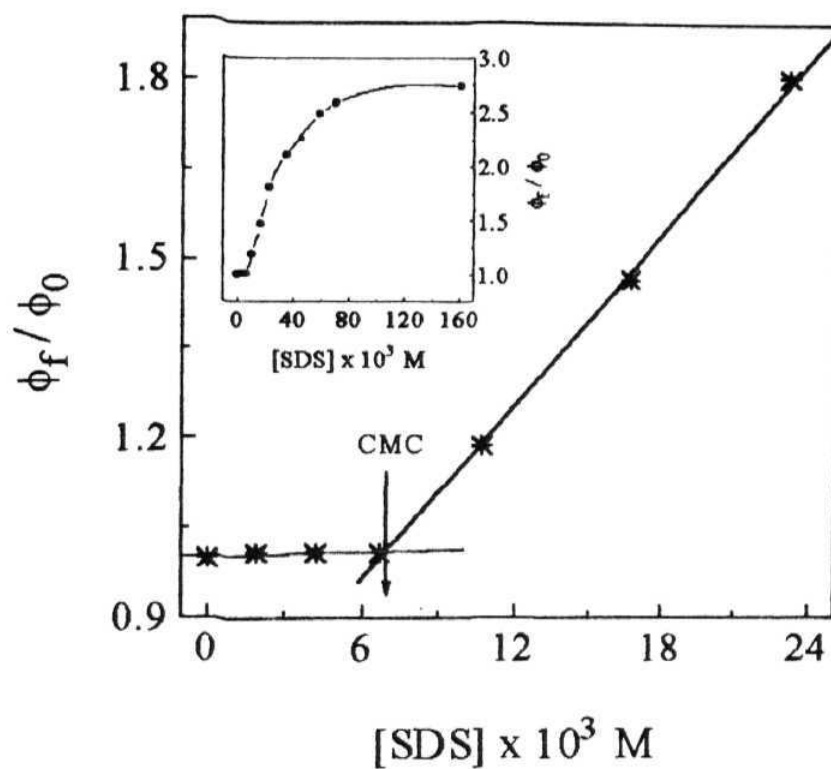
Fig. 3.2.   A plot of the relative fluorescence intensity (ϕ_f/ϕ_0) of AP as a function of SDS concentration in aqueous solution.   The insert shows the variation of the ratio over a larger concentration range.

Micropolarity probes 1,8,18-20 have often been used for the determination of CMC, though some of them have various weak points. 1-Pyrenecarboxaldehyde[18e] appears better among the widely used fluorescence probes for determining CMC. Recently, Miyagishi et al[20] introduced auramine O, a microviscosity fluoroprobe to follow the micellisation and determined CMCs of various ionic, nonionic and zwitterionic surfactants which are in good agreement with those determined by other physical methods such as surface tension . Since auramine O exists as a cation in neutral condition (pH=7) it is not possible to obtain an estimate of CMC of anionic micelle such as SDS. Polar donor-acceptor ionic systems such as ANS[19d] (1-anilinonaphthalene-8-sulfonate) or TNS (6-toluidinonaphthalene-2-sulfonate)[19f,c] are excellent probes. However, they fail to follow the micellisation in some cases involving charged micelles due to the formation of premicellar aggregates. The case for acridine[18h] is similar to those of ANS and TNS. The ability of AP to follow the micellar aggregation *irrespective of its charge* makes this molecule superior to many other probes.

3.1.3. *Time-resolved Fluorescence Study*

The fluorescence decay curves of AP in micellar media were measured under conditions in which it is expected to be completely micellised (corresponding to a high concentration of the surfactants in the plateau region of the plot of (ϕ_f/ϕ_0) vs [surfactant] as shown in the insert of Fig. 3.2). The specific concentrations used for the surfactants along with the measured

83

lifetimes of AP in micellised condition are presented in Table 3.3. These concentrations were chosen such that the addition of surfactants beyond these concentrations failed to bring any further change in the spectral shift, enhancement and lifetime. A typical fluorescence decay curve in micellar media along with the best possible fit is shown in Fig. 3.3. The decay data in the micellar media were fitted to be a biexponential function of the form

$A + B_1 \exp(-t_1/\tau_1) + B_2 \exp(-t_2/\tau_2)$ to obtain the best possible χ^2 and residuals.

Table 3.3 Time-resolved Fluorescence Data of AP in Micellar Media.

Surfactant	Concentration (mM)	Lifetime (ns)		Relative amplitude[a]	
		τ_1	τ_2	R_1	R_2
SDS	160	3.2	0.96	92.0	8.0
CTAB	93	3.1	0.75	92.5	7.5
Triton X-100	78	3.6	0.33	95.9	4.1

[a] Calculated using relative amplitude, $R_j = 100 B_i \tau_i \Big/ \sum_{k=i}^{2} (B_k \tau_k)$.

The fluorescence lifetime data, as presented in Table 3.3 show that the major component of the decay (~ 92-96%) consists of a lifetime between 3.1 and 3.6 ns and the minor component exhibits a lifetime which is lower than the time
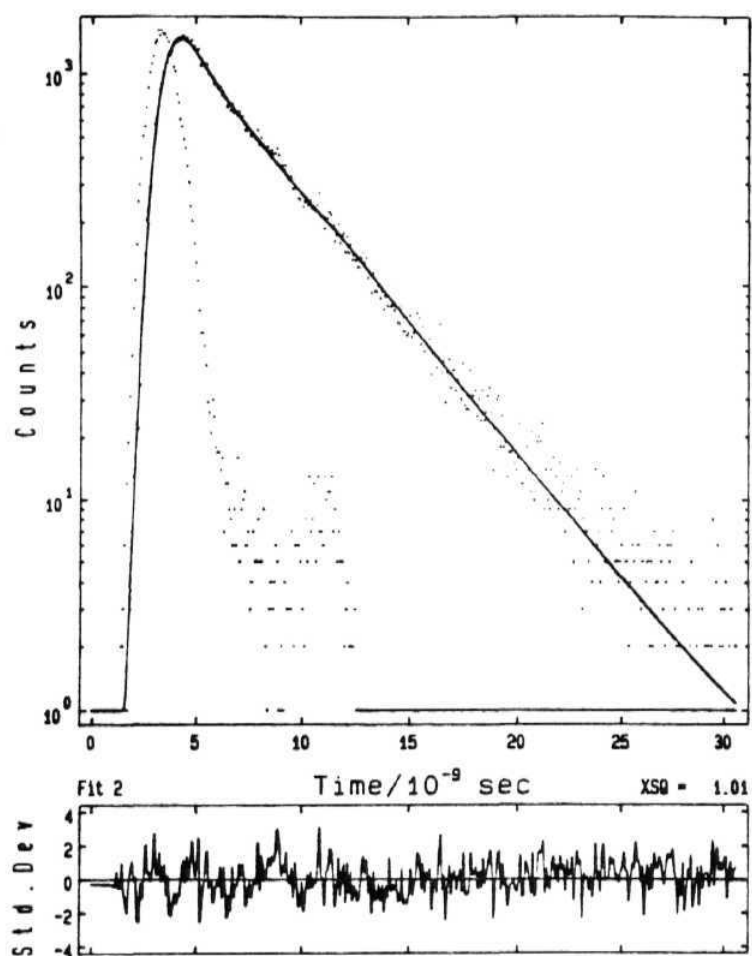
Fig. 3.3. Exciting lamp profile, fluorescence decay curve along with the best fit to the decay curve of AP in aqueous solution in presence of 78 mM CTAB.

85

resolution of our instrument (1.4 ns). We assign the long-lived predominant component to the micellised probe molecule whose lifetime is significantly higher than that of AP in water (1 ns) indicating that the probe is bound to a relatively non-polar site in micelle. The sub-nanosecond component most likely originates from a few molecules in *aq* phase. Although no importance should be attached to the absolute values of the lifetimes of the short-lived components (in view of the resolution of the instrument), the trend in lifetime variation is instructive. The lifetime of the short-lived component in CTAB is less than that in SDS suggesting quenching of the free molecules by Br" ions. However, possible reason for quenching of the same in TX is not clear to us. It can also be seen from the Table that the percentage of the free form in TX (4%) is slightly less than that in other micelles indicating a relatively stronger binding of AP with TX.

3.1.4. *Binding Ability*

Micellar binding of an organic substrate is mainly governed by hydrophobic interactions.[21] The association of a probe molecule with a micelle can be described by the following relationship, for which the binding constant K is given by equn 3.2, where $[S_w]$ and $[S_m]$ denote, respectively, the probe concentration in *aq* and micellar phase. [M] is the concentration of the micelle

$$S_w + M \overset{K}{\Leftrightarrow} S_m \qquad\qquad \textbf{3.1}$$

86

$$K = \frac{[S_m]}{[S_w][M]} \qquad\qquad \textbf{3.2}$$

and is equal to ([surfactant] - CMC)/N, where N is aggregation number of the surfactant. In order to quantitatively estimate the binding of AP with the micelles, we have evaluated the binding constant of the probe by following a method suggested by Almgren et al.[22] This method is possibly best suited for the present system whose ϕ_f in an *aq* and micellar environment are quite different. According to this method,

$$\frac{I_\infty - I_0}{I_t - I_0} = 1 + (K[M])^{-1} \qquad\qquad \textbf{3.3}$$

where I_∞, I_0 and I_t are the relative fluorescence intensities under complete micellisation, in the absence of micellisation and in presence of intermediate amounts of surfactant, respectively. K is the binding constant. A typical plot based on the above in aqueous micelles is shown in Fig. 3.4. The measured K values ($\pm$ 15%) are 3400, 4500 and 5600 M^{-1} in SDS, CTAB and TX, respectively. Since the K values are found to be of the same order of magnitude we can conclude that AP does not show any preference to a particular micelles instead, the binding is independent of the micellar head group. A relatively larger binding constant with the neutral micelle, TX, as measured here is consistent with the lifetime data.
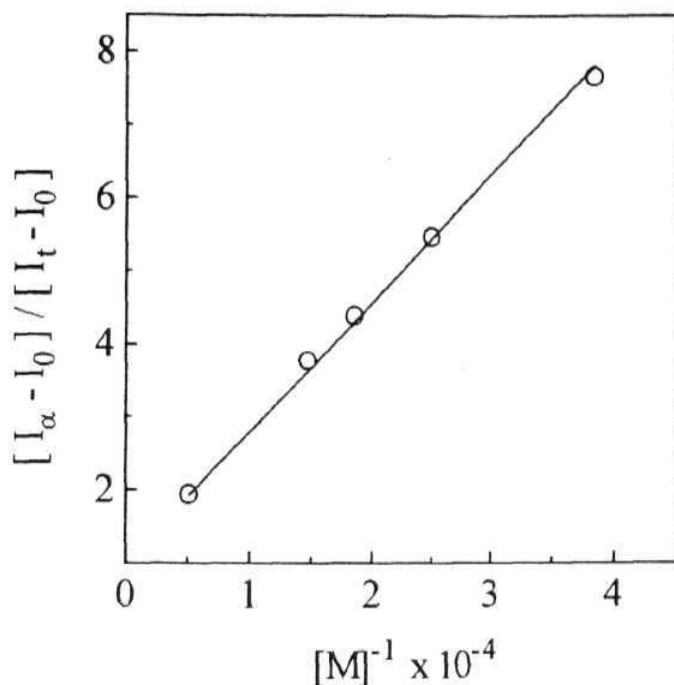
Fig.3.4. Plot of $(I_\infty - I_0)/(I_t - I_0)$ vs $[M]^{-1}$ in the case of Triton X-100. **The** plot is based on equn. 3.3.

3.1.5. *Nature of the Solubilisation Site and Evaluation of Microscopic Polarity*

As mentioned earlier, micelles are characterised by three distinct regions, an inner nonpolar hydrophobic core, a compact Stern layer and a comparatively wider Gouy-Chapman layer. Micelles solubilise a wide variety of hydrophobic and hydrophilic substances,[23] and depending on their structure they can bind either to the nonpolar core or to the surface. It is generally believed however

that aromatic compounds with hydrophilic groups such as aldehydes, ketones and alcohols are solubilised with their hydrophobic moiety in the micellar core and with the hydrophilic groups protruding into or anchored at the micellar surface.[23] The mode of solubilization for PyCHO in micelle is in accordance with this picture.[24]

In the present case, the maximum enhancement under complete micellisation is between 2.6 and 2.9. If AP penetrated into the micellar core then the expected enhancement would have been by a factor of ≈ 70 (since the ϕ_f of AP in nonpolar media is nearly 70 times that in water [14]) when all molecules are micellised. Two to three fold fluorescence enhancement suggests that the microenvironment around the probe is only marginally less polar than water. Since the ϕ_f of AP in methanol is ≈ 10 times that in water one expects an enhancement by a factor of 10 if the molecule sees a methanol-like environment. However, one has to take into consideration that even at highest surfactant concentration a the small percentage of molecules is present in *aq* solution (as indicated by lifetime data) which do not contribute to the enhancement. If we take into account of these molecules, the expected enhancement for a methanol-like environment is ≈ 9. The τ_f of AP in methanol is 5 times that in water. Thus based on the τ_f data one expects ≈ 4.5 fold lifetime enhancement in a methanol-like environment. Therefore, both the intensity and lifetime data indicate that the site in which the micellised probes are located is more polar than methanol. The observed spectral shift lie in the range 15–20 nm. It has been shown earlier[14]

that the emission maximum of AP in methanol is blue-shifted by 22 nm with respect to that in water. Therefore, the spectral shift also that the environment of the binding site is little more polar than methanol. It is therefore concluded that the probe is bound to the interfacial region where the polarity is expected to be that indicated in the measurement. We believe that the polar nature of the probe and strong affinity towards hydrogen bonding solvents are responsible for binding of the probe at the surface separating the micelle from the water molecules.

It is clear from the above discussion that the polarity of the binding site of AP, the interface, is between that of methanol and water. In terms of Reichardt's $E_T(30)$ scale,[25] the polarity lies between 55.4 (MeOH) and 63.1 (H_2O) for all three micelles. We now attempt to pinpoint this polarity using the spectral shift data. Since the lifetime data indicate that under no condition all the molecules are micellised, one needs a small correction to the spectral data presented in Table 3.1, to find out the expected shift under 100% micellised conditions. Assuming the spectral maxima to change linearly as the composition changes, the calculated maximum shifts under completely micellised condition are 15.2, 19.4 and 21.3 nm in SDS, CTAB and TX, respectively. Using these data and a linear relationship[25] between $\bar{v}$ and the solvent polarity parameter, $E_T(30)$, the polarities of the interfaces are calculated to be 57.9, 56.3 and 55.6 for SDS, CTAB and TX, respectively. The results suggest that the variation in

the interface polarity is small and the presence of ionic charges does not to any significant extent influence the interface polarity.

Micropolarities of the micelle-water interface of various micelles are reported in literature which have estimated by employing different kinds of polarity sensitive probes.[1,2,7,26,27] Using fluorescent pH indicators, coumarins as probes, the polarities of the interfacial region of the micelles have been estimated by Fernandez et al.[28] These values are in agreement with those obtained by us. Recently, Durocher et al[29] reported the interface polarities of SDS and CTAB to lie between 50-35 in terms of effective dielectric constant, by using polarity sensitive 3H-indole derivatives as probes.

The polarity values of the solubilization sites of the classical probe pyrene are found to be significantly different in different micelles.[26] However, pyrene, being a hydrophobic probe with no hydrogen bonding tendency, is solubilised in different regions of the micelles depending on the head group and hence the polarities of different regions are reported by pyrene.[1,26] On the contrary, AP being a polar molecule with strong affinity towards hydrogen bonding solvents always prefers to bind to a site where it can still be hydrogen bonded to water molecules. The interface polarities of SDS, CTAB and TX as estimated by pyrenecarboxaldehyde (PCA) as probe are 88, 83 and 66 on Kosowar's Z scale[27] which on conversion to Reichardt's $E_T(30)$ scale using $Z = 1.337 \, Ex(30) + 9.8$[25] become 58.5 54.7 and 42.0, respectively. While the first two values agree fairly well with our values, the surface polarity of TX differs

considerably. We think that PCA, because of the strong hydrophobic character of pyrene, possibly penetrates a little deeper into the core of TX and reports the properties from therein. This conjecture is supported by the fact that when ANS was used as a reporter molecule, the $E_T(30)$ value of the interface of TX was found to be 56.6, a value widely different from that obtained with PCA.[27] This indicates how crucial is the selection of the probe in achieving a specific objective. We can conclude from the above data that if the hydrophobic portion of the probe molecule is large, the molecule may penetrate into the core region of the micelle even though the reporter molecule is polar. Zachariasse et al[30] have estimated the interface polarity of the micelles by employing betaine dye whose absorption spectrum is highly sensitive to the polarity of the medium. The microscopic polarities as estimated by the betaine dye are 57.5, 53.4 and 53.0 for SDS, CTAB and TX, respectively. Again, both the trend as well as the numerical values are in good agreement with our values. The advantage of AP over the betaine dye is that the former allows three parameters to be monitored independently thereby providing a more detailed picture of micellisation than that obtained using the latter where only one parameter, the change in location of the absorption maxima, can be monitored. Also, the micellisation of AP is not expected to be affected by electrostatic interaction with the charged micelles because of the electroneutrality of the probe. This makes this probe superior to other polar ionic probes.[19d,f,31] The hydrogen bonding interaction of the

probe, AP with water molecules is primarily responsible for the location of the molecule at the polar interfacial region.

3.1.6. *AP as Micelle- Water Interface Polarity Probe*

Micelle-aqueous interface incorporates features of electrical double layer, and may be typical of interfacial systems biological interest such as membranes. Most catalytical reactions occur at the interface with water.[3][2] Micelle-water interface polarity is a crucial property in understanding the micellar structure and function. The literature contains conflicting data on the polarity of the micellar interface. While some fluorescence based studies suggest that the interfacial polarity of micelle is dependent on the charge of the micelle and thus varies from micelle to micelle, some other studies point to an almost identical polarity of it.[1] It should be noted that if a probe molecule is bound to different regions in different micelles then one obtains different polarity values (corresponding to the binding sites) even though the interface polarity need not be different. In order to measure the surface polarity of different micellar systems using fluorescence technique one needs to identify a probe which will bind only at the interface irrespective of whether the micelle is charged or not. This can only be achieved if the chosen probe is polar such that there exists a tendency to remain at the surface; it should also contain a small hydrophobic region which will account for binding. It would be an advantage if the probe is prone to hydrogen bonding with the solvent. Thus AP as neutral molecule, with small hydrophobic region and two active centres for hydrogen bonding, is an excellent probe for the

micelle-water interface and the results of **its** fluorescence **behaviour in micellar** media do confirm this.

3.2. Amphiphile, ll-(4-aminophthaIimido)undecanoic Acid as Sensor of Micellar Microenvironment

As AP is found to be bound selectively to the interfacial region, the system cannot be used as a reporter molecule for the hydrophobic core region of the micelle. There have been a growing number of studies on micellar, vesicular and membrane assemblies that have profitably employed specifically synthesised surfactant, lipid molecules that carry a chromophoric unit. One normally obtains information from different depths of an organised medium by using amphiphilic molecules with the fluorophore connected at different positions of the polymethylene chain. Probes covalently bound to different locations of the detergents or lipids are widely employed to analyse different depths of micelles and biological membranes.[2,4,6,33-35] Examples of this kind are surfactant derivatives of indole, coumarin and pyrene-lipid etc.[1,4] NBD-labelled lipids are used as fluorescent analogues of native lipids in biological and model membranes to study a variety of processes.[34] Using pyrene-linked amphiphilic molecules 1 and 2 in various micelles and microemulsions, Zachariasse et al[36] have demonst-

$$Py-(CH_2)_n-COOH \qquad Py-(CH_2)_n-\overset{\oplus}{N}(CH_3)_3Br^{\ominus}$$

1 \qquad n=3-15 \qquad **2**

94
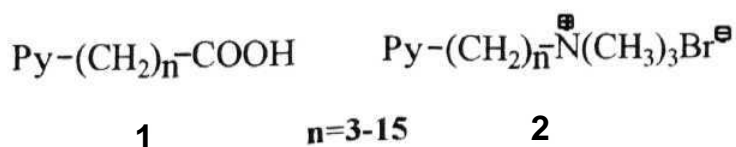
rated that the polarity of the binding site of the probe decreases as n increases. Studies on indole detergents 3 and 4 have been carried out by Turro et al[37] and it was shown that the indole moiety of detergent resides in the interior of the host micelles in contrast to the native fluorophore. Several n-(9-anthroyloxy)fatty acids[38] such as 5 have been extensively employed in micelles. It was found that the fluorophores of the fatty acids reside at graded series of positions in the interior of the micelles depending on the location where the fluorophore is connected with the fatty acid. The fluorophore of the fatty acid was found to be located 15 A from the head group, i.e. near the centre of the micelle when it is attached at 12th position of hydrocarbon chain of the fatty acid (12-(9-anthroyloxy)fatty acid). [38a] Recently, Melo et al have used same probe to monitor the water content inside micelles by incorporation of the fluorescing moiety. [38b]

3   **4**   **5**
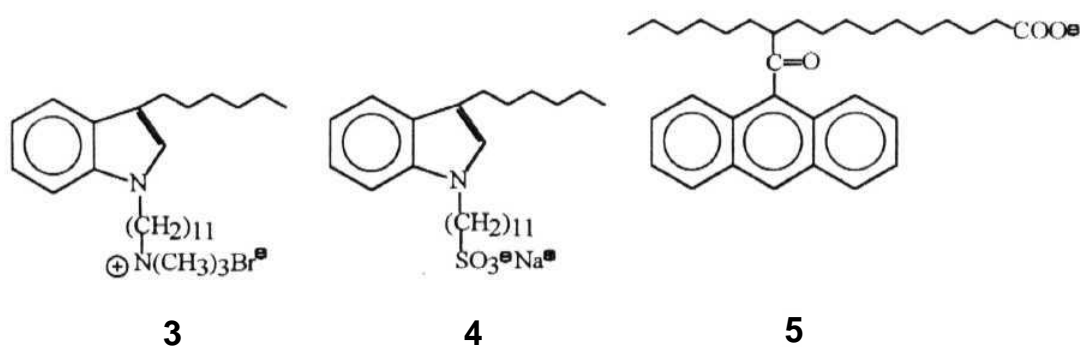
In the light of the above, it was thought that if AP could be covalently attached to the non-polar tail of a surfactant molecule, it might be possible to

incorporate the fluorophore into the hydrophobic core region of the micelles and receive information from therein. With this intention, we have synthesised a new amphiphilic fluorophore, 1 l-(4-aminophthalimido)undecanoic acid (APL). Since it is necessary to have a prior knowledge of the fluorescence behaviour of the probe molecule in homogeneous media for an understanding of the fluorescence response in the microheterogeneous media, we have first studied the Photophysical behaviour of APL in homogeneous media and subsequently studied the same in micellar environments.

3.2.1. APL in Homogeneous Media

The absorption and fluorescence spectra of APL are characterised by broad structureless bands whose locations are mainly determined by the polarity of the media. The representative absorption and emission spectra are shown in Fig. 3.5 and the Photophysical properties are summarised in Table 3.4.
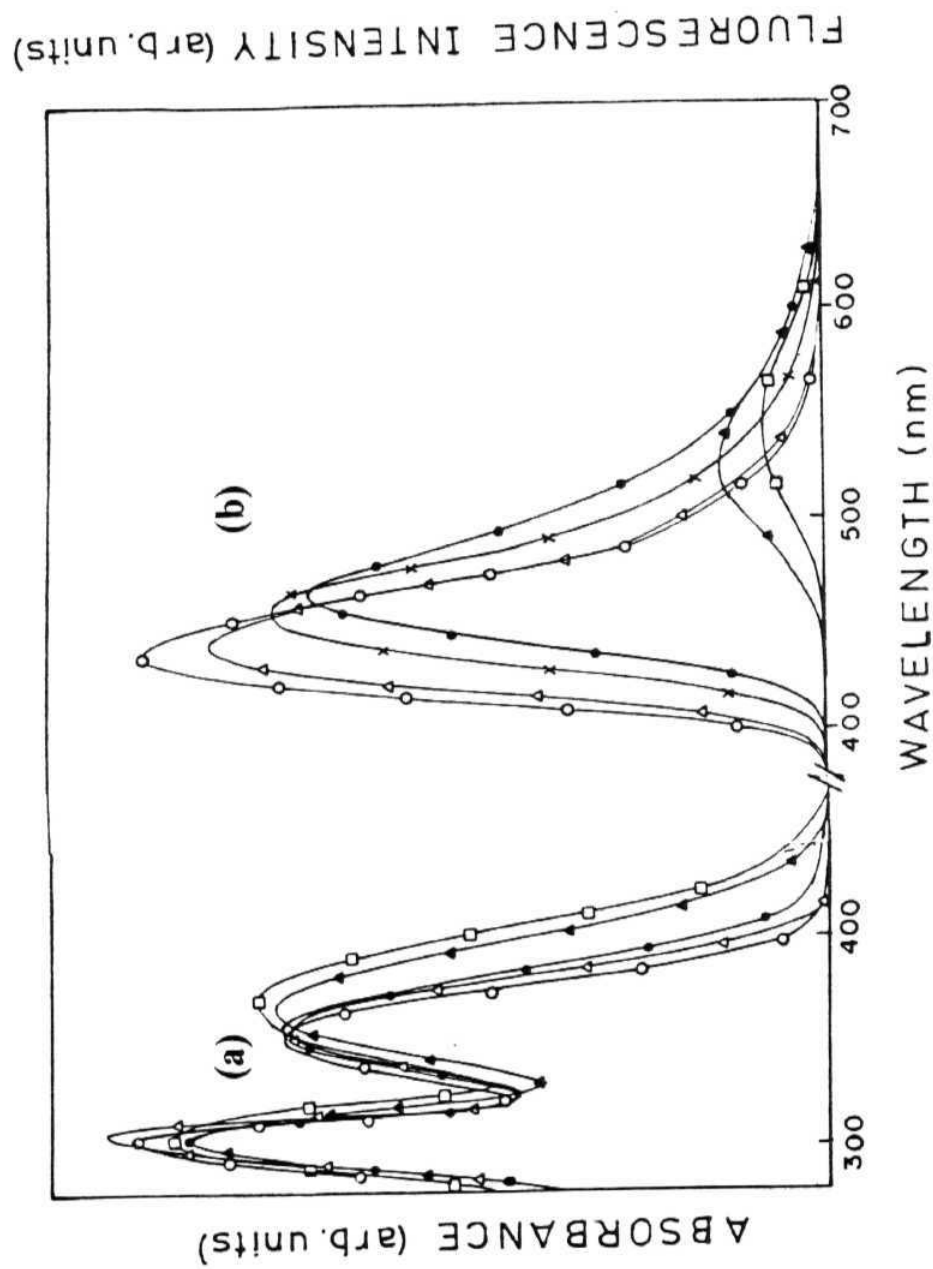
Fig. 3.5. Absorption (a) and fluorescence (b) spectra of APL in 1,4-dioxane (–O–O–); tetrahydrofuran (–Δ–Δ –); acetone (–x–x–); acetonitrile (–●–●–); methanol (–▲–▲–); water (–□–□–). $\lambda_{exc} = 370$ nm.

97

The intramolecular charge-transfer nature of the first absorption band and the fluorescence is evident from the polarity dependence of the band maxima. A greater polarity dependent Stokes shift for fluorescence is indicative of a larger dipole moment of the emitting state. That the fluorescence state of APL is more polar than the ground state and ICT in nature is supported by the fact that the ground and excited state dipole moments of AP are 5.3 and 8.3-8.9 D, respectively.[14] The hydrogen bonding interaction of APL with some solvents is evident from the enhanced Stokes shift of the fluorescence band in methanol and water that cannot be correlated solely to the solvent polarity effect. This is illustrated in Fig. 3.6 with a plot of the $\bar{v}_{flu}^{max}$ vs the microscopic solvent polarity parameter, $E_T(30)$.

Table 3.4 Photophysical Properties of APL in Homogeneous Media.

Solvent	$E_T(30)^a$	λ_{abs}^{max}/nm	λ_{flu}^{max}/nm^b	ϕ_f	τ_f/ns	$k_{nr}/10^7 s^{-1}$
1,4-Dioxane	35.8	354.5	438.5	0.50	16.4	3.1
Tetrahydrofuran	37.4	357.7	442.5	0.46	13.6	4.0
Acetone	42.4	359.3	459.5	0.45	14.6	3.8
Acetonitrile	45.8	358.5	466.0	0.45	16.4	3.4
Methanol	55.3	368.5	526.5	0.11	6.9	12.9
Water	63.1	368.5	554.0	0.01	1.1(86.4%) 7.7(13.6%)	90.0

a Measured using betaine dye (sec. 2.1.1). b Excited at 370 nm.
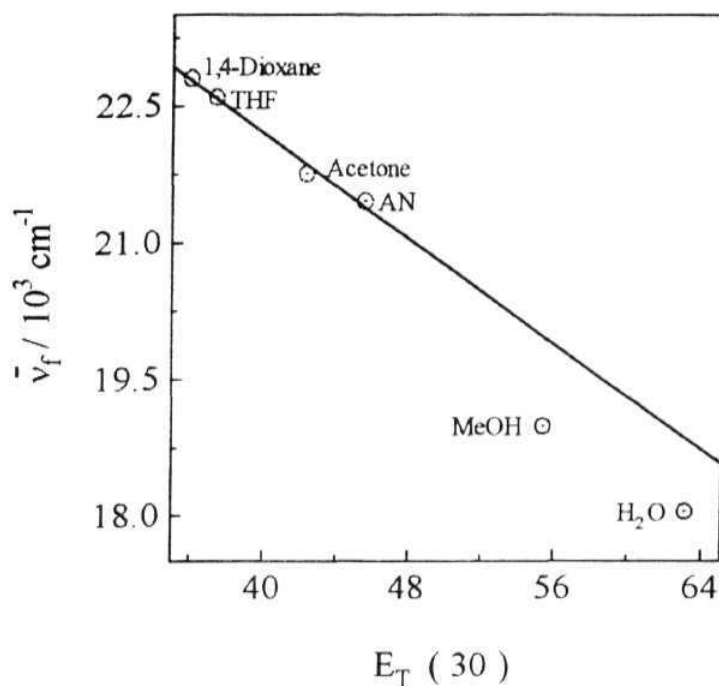
Fig. 3.6. Plot of the energy of the fluorescence maximum (in cm^{-1}) vs microscopic solvent polarity parameter, $E_T(30)$. The data points in aprotic solvents are fitted to the line shown. THF- tetrahydrofuran, AN - acetonitrile.

The fluorescence decay of APL in all solvents except in water was found to be single exponential. The decay in water was found to be biexponential with the lifetime of 1.1 ns for the major component (86%) and ~ 7 ns for the minor component. Because of the larger contribution and similarity with the lifetime of AP in *aq* medium (1 ns), the former is taken as the lifetime of APL in *aq* medium for subsequent measurements. Preliminary experiments aimed at finding out the

origin of the long-lived component were not very conclusive. However, further investigations have been undertaken on a series of AP-derivatives (discussed in chapter 4) to find out whether aggregation or self-coiling is responsible for the biexponential decay of APL or related molecules. The ϕ_f and τ_f do not show any significant solvent dependence as long as aprotic solvents are used. However, in protic solvents, a drastic reduction in ϕ_f and τ_f is observed due to the hydrogen bonding interactions between the probe and the solvent molecules. This results in an enhancement of the nonradiative decay rate by an order of magnitude (Table 3.4).

3.2.2. APL in Micellar Media

The three kind of micelles chosen for this study are cationic (CTAB), anionic (SDS) and neutral (TX), same as those employed earlier for studies involving AP.

3.2.2.1. Absorption Behaviour

The effect of the addition of the surfactants on the absorption spectrum of APL is not very significant. This is illustrated in Fig. 3.7. In view of the fact that the surfactant-induced spectral changes are small, no further analysis of the absorption spectra has been carried out.
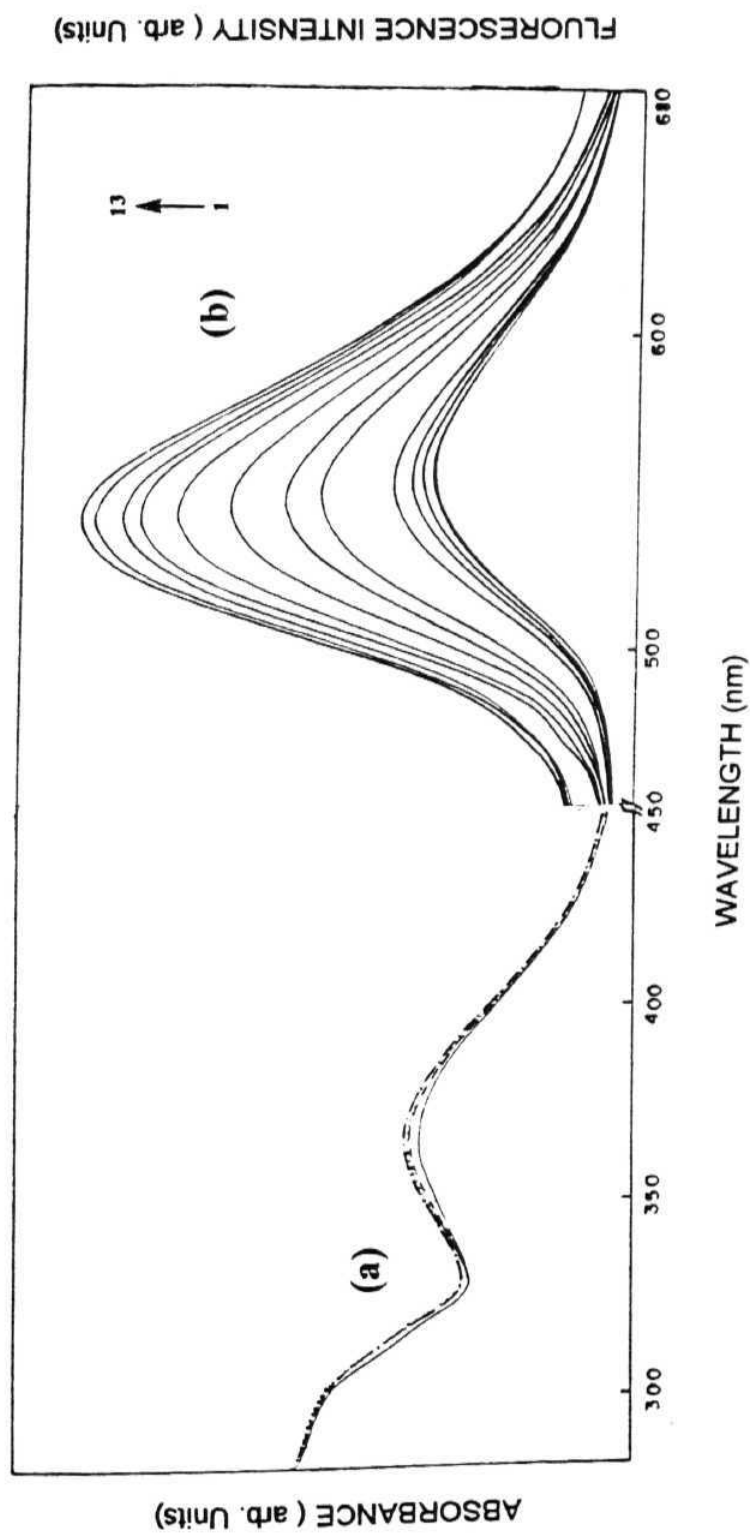
Fig. 3.7. Absorption (a) and fluorescence (b) spectra of APL in aqueous solution with different amounts of SDS. The concentrations of SDS (mM) are (a) 0 (——), 7.4 (····), 77 (———), 150 (–·–·–). (b) in increasing order of intensity, 0, 2.4, 4.7, 7.4, 8.7, 14.3, 18.4, 24.5, 35.8, 48, 77, 131, 150. $\lambda_{exc} = 370$ nm.

3.2.2.2. *Fluorescence Behaviour*

Addition of surfactants to an *aq* solution of APL causes a blue-shift of the spectrum and an enhancement of the fluorescence yield indicating the passage of the fluorophore from the polar *aq* medium to a relatively nonpolar site in the micellar environment. The spectral shift and enhancement were noticeable only beyond a certain concentration of the surfactant. The change in the fluorescence spectra of APL with the surfactant concentration is shown in Fig. 3.7. A typical plot of (ϕ_f/ϕ_0) vs [surfactant] is shown in Fig. 3.8 from which the CMCs are evaluated. The insert in the plot shows the variation of *fa/00* over the entire range of the surfactant concentration. It can be seen from the Table 3.5, except for TX, the estimated CMC values agree rather well with the literature values. A summary of the fluorescence enhancement and the spectral shift data are presented in Table 3.6. The data clearly show the ability of APL to follow the aggregation behaviour of the surfactant molecules.
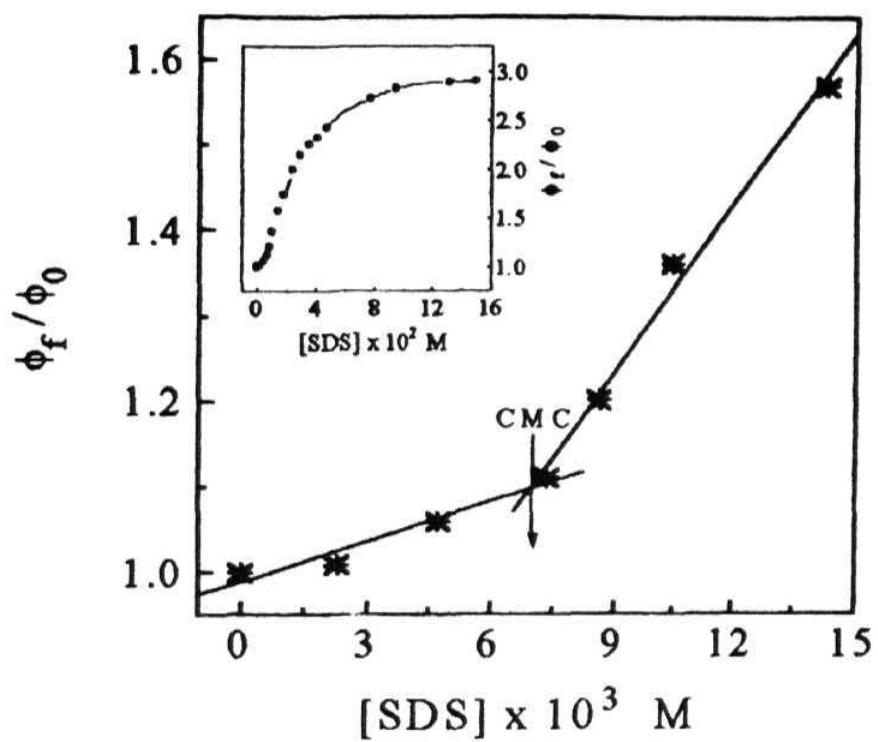
Fig. 3.8. A plot of the relative fluorescence intensity, (ϕ_f/ϕ_0) of APL as a function of SDS concentration in aqueous solution. The insert shows the variation of the ratio over a larger concentration range.

Table 3.5 Critical Micellar Concentrations of SDS, CTAB, Triton X-100.

Micelle	Measured CMC $(10^{-4}$ M)	Literature CMC[a] $(10^{-4}$M)
SDS	70.5 (±5.0)	80
CTAB	9.6 (±0.5)	9.2
Triton X-100	6.0 ($\pm$ 1.0)	2.6

[a] Collected from Ref. **[1],**

Table 3.6 Fluorescence Spectral Shift and Enhancement of Intensity and Lifetime in Micellar Environment.

Surfactant	Concentration $(10^{-2}$ M)	(I_f / I_0)	Shift (nm)	τ_1/ns (R_1)[a]	τ_2 / **ns**
SDS	15.0	2.9	15	3.3 (99.5)	0.04
CTAB	11.7	2.8	21	3.5 (93.7)	0.33
Triton X-100	9.4	3.0	23	3.9 (97.2)	0.95

[a] Calculated using relative amplitude, $R_i = 100 B_i \tau_i \Big/ \sum_{k=i}^{2} (B_k \tau_k)$.

3.2.2.3. Flu florescence Decay Measurements

The fluorescence lifetimes of APL in micelles under completely micellised conditions were measured at high concentration of the surfactants (indicated in Table 3.6). The fluorescence decay curves were fitted to biexponential decay functions yielding lifetimes (Table 3.6) between 3.3-3.9 ns (93.7-99.5%) and < 1 ns (6.3-0.5%). We assign the long-lived component to micellised-APL, while the short-lived one to unbound-APL in the aqueous medium. This assignment is based on the fact that in a given micellar environment, the lifetimes remain constant with only the relative amplitudes of the two components vary when the surfactant concentration is changed. The quenching of APL present in the *aq* phase in surfactant-added solutions is presumably due to the counterions present in the media. This is substantiated by the fact that in TX where no counter ion is present, the short-lived component has a lifetime (0.95 ns) very close to that of APL in *aq* medium. A typical plot of fluorescence decay of APL in micelle along with the fitted curve is shown in Fig. 3.9.
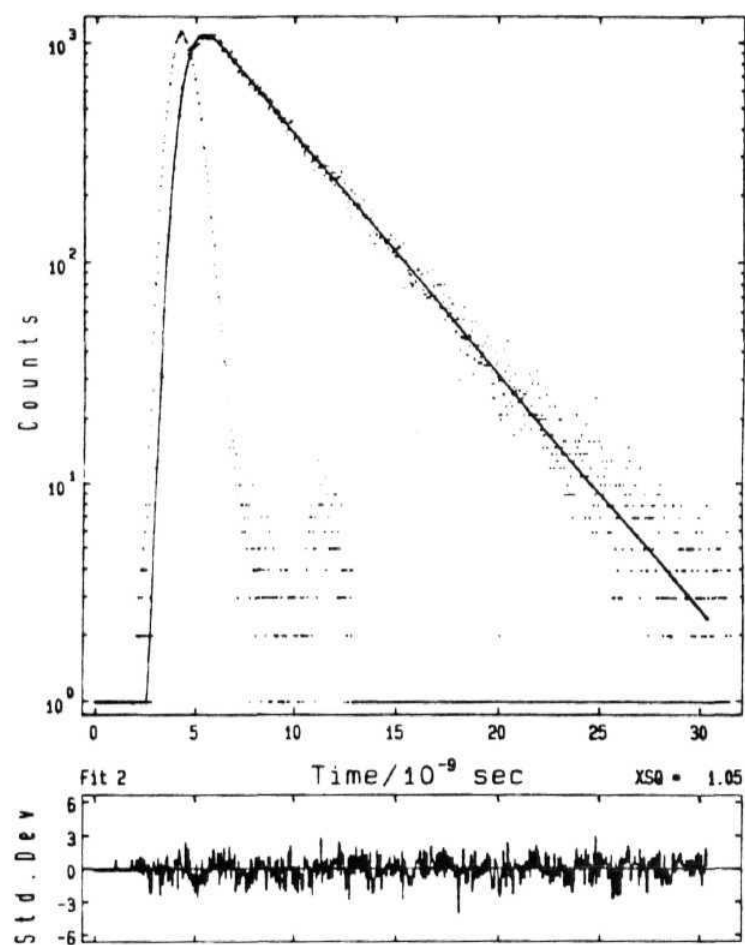
Fig. 3.9. Exciting lamp profile, fluorescence decay curve along with the best fit to the decay curve of APL in aqueous solution in presence of 94 mM Triton X- 100.

3.2.2.4. Binding Ability

The binding constants of APL with the micelles are estimated from the fluorescence data using the equn 3.3. A typical plot based on equn 3.3 is shown in Fig 3.10. The measured K values (± 15%) with SDS, CTAB and TX are 4200, 8000 and 8500 M^{-1}, respectively. A comparison of the K values of APL with those of AP shows that the attachment of the fatty acid chain helps in better binding of the probe molecule.
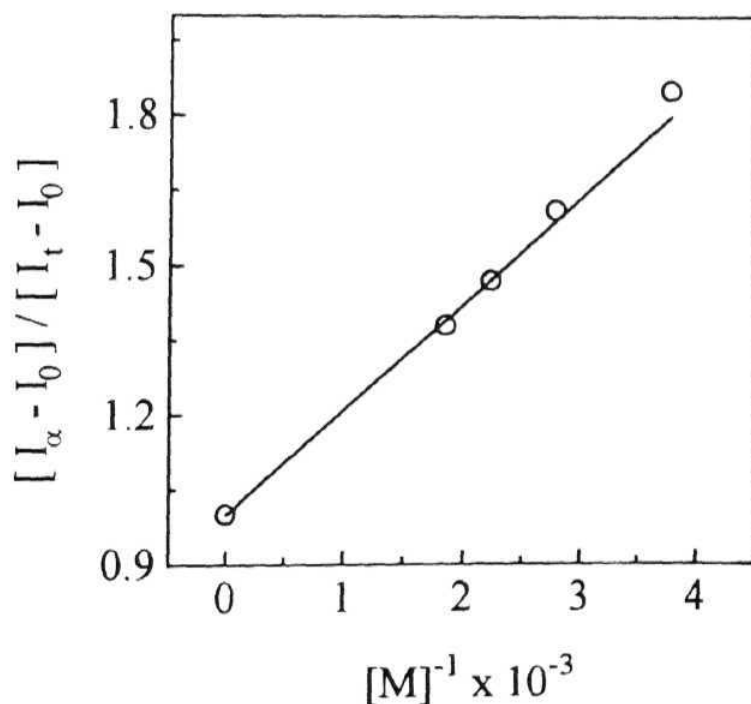
Fig. 3.10. Plot of $(I_\infty - I_0)/(I_t - I_0)$ against $[M]^{-1}$ in the case of SDS. The plot is based on equn. 3.3.

3.2.2.5.   Quenching in Micellar Solutions

As quenching studies are often useful in determining the location of the fluorophores and their accessibilities,[4,39] we examined the fluorescence quenching behaviour of micellised AP and APL (at high surfactant concentration so that the molecules are almost completely micellised) towards *aq* quenchers, I" and Cu $^{+2}$ which are capable of quenching fluorescence of molecules located in the water-accessible interfacial region or in *aq* medium.   The quenching behaviour of both the compounds was also examined in *aq* medium for comparison.   Depending on the micellar charge, we have used either one or both the quenchers.   The linearity of the quenching plots, based on Stern-Volmer equation, shown in Fig 3.11, is indicative of a single class of fluorophores, all equally accessible to the quenchers.   Further, absence of any non-linearity in the plots suggests relatively small contribution of quenching by a static mechanism. The quenching data are collected in Table 3.7.
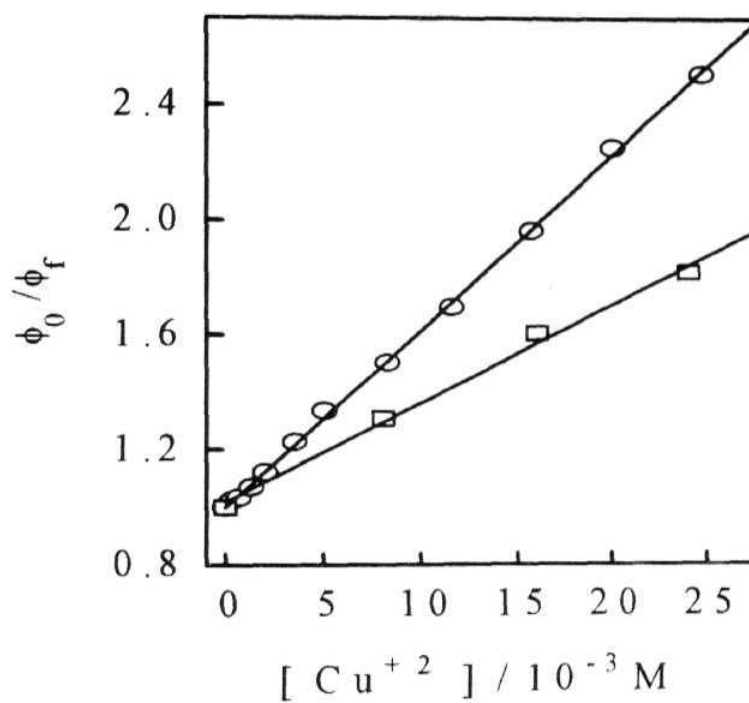
Fig **3.11.** A plot of relative fluorescence intensity in SDS micelle, for AP (□, 70 mM SDS) and for APL (○, 150 mM SDS).

Table 3.7   Quenching Constants of AP and APL in Aqueous and Micellar Media.

Probe	Quencher	$k_q \big/ 10^9 \, M^{-1} s^{-1}$			
		Aqueous	CTAB	SDS	Triton X-100
AP	I$^-$	10.6	25.9	-	2.4
	Cu^{+2}	6.8	-	33.0	0.3
APL	I$^-$	9.8	41.6	-	2.7
	Cu^{+2}	4.7	-	18.8	0.2

3.2.2.6. Location of APL in Micelles

Surfactant-induced changes in the fluorescence properties of APL are clear indications of the fluorophore occupying a less polar site in the micellar environment. However, as stated earlier, the micelles are characterised by different regions of polarity and it is necessary to find out the exact location of the AP moiety (in APL) by a quantitative analysis of the fluorescence data. On the basis of its covalent attachment with the non-polar tail, if the fluorophore is assumed to occupy a site in the non-polar core region, the expected enhancement in intensity and lifetime based on the data presented in Table 3.4 would have been 50 and 15, respectively, in fully micellised condition. A

111

fluorescence spectral shift of more than 100 nm is expected. However, the experimentally observed values (Table 3.6) are far less than the expected values indicating that the microenvironment around the fluorophore is slightly less polar than water. Since the changes in fluorescence properties of APL are very similar to those of free AP, it appears that the location of the fluorophore is very similar in both cases. Based on the interface polarities (as estimated from with AP, sec. 3.1) and assuming a linear variation of the $\bar{\nu}_{flu}^{max}$ with $E_T(30)$, the calculated shifts of the fluorescence maximum on complete transfer of the fluorophore from *aq* to the micellar interface works out to be 18.6, 24.3 and 26.7 nm, respectively, in three micelles. The shift data presented in Table 3.4 is fairly close to these values. Further, when the small percentage of the molecules present in the *aq* phase even at high surfactant concentration are taken into consideration from the lifetime data, the calculated shifts (17.2, 22.4 and 25.8 nm in SDS, CTAB and TX, respectively) are even closer to the experimental values. Therefore, we are led to conclude that the fluorophore in APL is also located at the micelle-water interface.

It can be seen from the quenching data that both I" and Cu^{+2} ions are good quenchers of AP and APL in *aq* medium. In a cationic micellar environment (CTAB), the quenching of AP with I" is enhanced presumably due to high local concentration of these ions near the interface because of electrostatic interaction. The quenching behaviour of AP with Cu^{+2} ion in anionic micelle is also very similar for the same reason. In TX, where

112

electrostatic forces are not operative, the quenching rate constant is lower than that in the *aq* medium indicating a lesser accessibility of the probe molecules towards the quenchers. A comparison of the quenching data of AP with that of APL shows that the quenching trend is very similar in both cases. If the AP moiety in APL penetrates into the deeper hydrophobic region, then a drop in k_q value in the micellar environment would have been observed for APL. The similarity of k_q values of APL with that of AP (which is known to locate at the interface in all three micelles) suggests that covalent linking of the chromophore to the non-polar end of the fatty-acid chain did not help incorporation of the fluorophore into the micellar core.

Based on above observation, the binding of APL with the micelles can be best represented by a folding of the hydrocarbon chain which brings the fluorophore at the interface. This is schematically represented in Fig. 3.12. The driving force behind such an arrangement is most likely the strong hydrogen bonding interaction of the fluorophore with the water molecules. Thus, although derivatisation of a system is expected to give some indication of the probe location in a host[34,35,37,38,40-44] the results show that the actual location of the probe could be quite different. Similar folding of the polymethylene chain in micellar environments or in membranes is reported in some cases.[34,45-47]
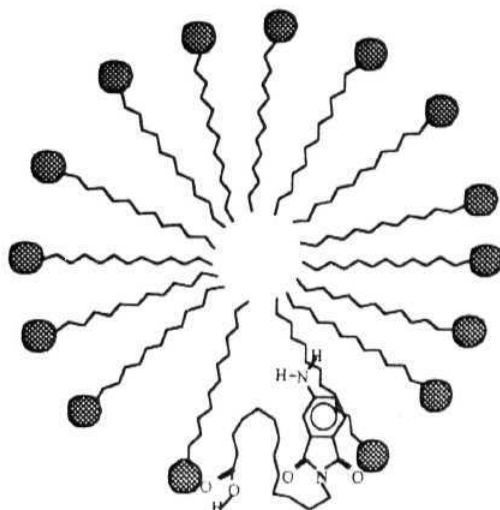
Fig.3.12. Schematic representation of binding of APL with the micelle.

3.3. References

1. K. Kalyanasundaram, *Photochemistry in Microheterogeneous Systems,* Academic Press: New York, 1987.

2. K. Kalyanasundaram In: *Photochemistry in Organised and Constrained Media,* V. Ramamurthy, ed., VCH: New York, **1991,** Ch. 2.

3. K. Bhattacharyya, M. Chowdhury, *Chem. Rev.,* 93, 507, 1993.

4. K. Lakowicz, *Principles of Fluorescence Spectroscopy,* Plenum Press: New York, **1983.**

5. J. K. Thomas, *Acc. Chem. Res.,* JQ, 133, 1977; *Chem. Rev.,* 80, 283, **1980.**

6. N J . Turro, M. Gratzel, A. M. Braun, *Angew. Chem. Int. Ed. Engl.*, 19, 675, **1980**.

7. F. Griesser, C. J. Drummond, *J. Phys. Chem.*, 92, 5580, **1988** and references therein.

8. G. von Bunau, T. Wolff, *Adv. Photochem.*, 14, 273, **1988** and reference cited therein.

9. *Micellisation, Solubilisation and Microemulsions*, K. L. Mittal, ed., Vol 1, 2, Plenum Press: New York, **1991**.

10. R. G. Weiss, V. Ramamurthy, G. S. Hammond, *Acc. Chem. Res.*, 26, 530, **1993**.

11. *Organic Phototransformations in Microheterogeneous Systems*, M. A. Fox, ed., Academic Press: Washington DC, **1982.**

12. a) W. R. Ware, S. K. Lee, G. J. Brant, P. P. Chow, *J. Chem. Phys.*, 54, 4729, **1971;** b) V. Nagarajan, A. M. Brearley, T. J. Kang, P. F. Barbara, *J. Chem. Phys.*, 86, 3183, **1987;** c) T. Hagan, D. Pilloud, P. Suppan, *Chem. Phys. Lett.*, 139, 499, **1987;** d) N. Ghoneim, P. Suppan, *J. Lumin.*, 44, 83, **1989;** e) N. Noukakis, P. Suppan, *./. Lumin.*, 47, 285, **1991;** f) N. A. Nemkovich, V. Boumann, H. Reis, N. Detzer, *J. Photochem. Photobiol.*,A: *Chem.*, 89, 127, **1995;** g) E. Laitinen, K. Salonen, T. Harju, *J. Chem. Phys.*, 104, 6138, **1996;** h) B. A. Pryor, P. M. Palmer, P. M. Andrews, M. B. Berger, T. Troxler, M. R. Topp, *Chem. Phys. lett.*, 271, 19, **1997;** i) T. O.

Harju, A. H. Huizer, C. A. G. O. Varma, *Chem. Phys.,* 200, 215, **1995;** j) C. Chapman, M. Maroncelli, *J. Phys. Chem.,* 95, 9095, **1991.**

13. T. Soujanya, T. S. R. Krishna, A. Samanta, *J. Photochem. Photobiol., A: Chem.,* 66, 185, **1992;** J. *Phys. Chem.,* 96, 8544, **1992.**

14. T. Soujanya, R. W. Fessenden, A. Samanta, *J. Phys. Chem.,* 100, 3507, **1996.**

15. S. Das, A. Datta, K. Bhattacharyya, *J. Phys. Chem.,* 101, 3299, **1997.**

16. H. Langhals, *Anal. Lett.,* 23, 2243, **1991.**

17. S. Aich, C. Raha, S. Basu, *J. Chem. Soc, Faraday Trans.,* 93, 2991, **1997.**

18. a) N. Kawashima, N. Fujimoto, K. Meguro,./. *Colloid Interface Sci.,* 103, 459, **1985;** b) R. C. Dorrance, T. F. Hunter, *J. Chem. Soc, Faraday Trans.,* 68, 1312, **1972;** c) M. Gonzalez, J. Vera, E. B. Abuin, E. A. Lissi, *J. Colloid Interface Sci.,* 98, 152, **1984;** d) P. Horowitz, *J. Colloid Interface Sci.,* 61, 197, 1977; e) K. P. Ananthapadmanabhan, E. D. Goddard, N. J Turro, P. L. Kuo, *Langmuir,* 1, 352, 1985; f) K. Y. Law, *Photochem. Photobio.,* 33, 799, **1981;** g) R. M. E Shishtawy, K. Fukunishi, *Bull Chem. Soc. Jpn.,* **68,** 929, **1995;** h) T. Wolff, *J. Colloid Interface Sci.,* 83, 658, **1981;** i) K. Muthuramu, V. Ramamurthy, *J. Photochem.,* 26, 57, **1984.**

19 a) H. -C. Chiang, A. Lucton, *J. Phys. Chem.,* 79, 1935, 1975. b) K. S. Birdi, *J. Phys. Chem.,* 81, 934. 1977; c) H. -C. Chiang, A. Lucton, *J. Phys. Chem.,* 81, 935, 1977;d) R. C. Mast, L. U. Haynes, *J. Colliod Interface Sci.,* 53, 35, **1975;** e) K. S. Birdi, T. Krag, J. Klausen, *J. Colloid Interface.*

116

Sci., 62, 562, 1977; f) A. Nag, K. Bhattacharyya, *J. Photochem. Photobiol., A: Chem.,* 47, 97, **1989.**

20. a) S. Miyagishi, H. Kurimoto, Y. Ishihara, T. Asakawa, *Bull. Chem. Soc. Jpn.,* 67, 2398, **1994;** b) S. Miyagishi, H. Kurimoto, T. Asakawa, *Bull. Chem. Soc. Jpn.,* 68, 135, **1995.**

21. L. Sepulveda, E. Lissi, F. Quina, *Add. Colloid Interface Sci.,* 25, 1, 1986.

22. M. Almgren, F. Griesser, J. K. Thomas, *J. Am. Chem. Soc,* 101, 279, 1979.

23. J. H. Fendler, E. J. Fendler, *Catalysis in Micellar and Macromolecular Systems,* Academic Press: New York, **1975.**

24. M. Gratzel, K. Kalyanasundaram, J. K. Thomas, *J. Am. Chem. Soc,* 96, 7869, **1974.**

25. C. Reichardt, *Solvents and Solvent Effects in Organic Solvents,* VCH: Weinheim, **1988.**

26. K. Kalyanasundaram, J. K. Thomas, *J. Am. Chem. Soc,* 99, 2039, 1977.

27. K. Kalyanasundaram, J. K. Thomas, *J. Phys. Chem.,* 81, 2176, 1977.

28. M. S. Fernandez, P. Fromherz, *J. Phys. Chem.,* 81, 1755, 1977.

29. a) R. S. Sarpal, M. Belletete, G. Durocher, *J. Phys. Chem.,* 97, 5007, **1993;** b) S. Nigam, M. Belletete, R. S. Sarpal, G. Durocher, *J. Chem. Soc, Faraday Trans.,* 91, 2135, **1995.**

30. K. A. Zachariasse, N. V. Phue, B. Kozankiewicz, *J. Phys. Chem.,* 85, 2676, **1981.**

31 R **R.** Hautala, N. E. Schore, N. **J.** Turro, *J. Am. Chem. Soc,* 95, 5508, **1973.**

32. a) *Surfactants in Solution,* K. L. Mittal, ed., Plenum Press: New York, **1984;** b) C. A. Bunton, G. Savelli, *Adv. Phys. Org. Chem.,* 22, 213, **1986**.

33. C. D. Stubbs, B. W. Williams, In: *Topics in Fluorescence Spectroscopy,* J. R. Lakowicz ed., Vol 3, Plenum Press: New York, **1991** , 331p.

34. a) A. Chattopadhyay, E. London, *Biochemistry,* 26, 39, **1987.** b) A. Chattopadhyay, *Chem. Phys. Lipids,* 53, **1, 1990.**

35. F. S. Abrams, A. Chattopadhyay, E. London, *Biochemistry,* 31, 5322, **1992.**

36. K. A. Zhachariasse, B. Kozankiewicz, W. Kuhnle In: *Surfactants in Solution,* K. L. Mittal, B. Lindmann, eds., Vol 1, Plenum Press: New York, **1984,** 584p.

37. a) N. E. Schore, N. J. Turro, *J. Am. Chem. Soc.,* 96, 306, **1974;** *J. Am. Chem. Soc,* 97, 2488, **1975;** b) N. **J.** Turro, Y. Tanimoto, G. Gabor, *Photochem. Photobiol,* 31, 527, **1980.**

38. a) E. Blatt, K. Ghiggino, W. H. Sawyer, *J. Chem. Soc, Faraday Trans.,* I, 77, 255, **1981;** *J. Phys. Chem.,* 86, 4461, **1982,** *Chem. Phys. Lett.,* 114, 47,1985; b) E. C. C. Melo, S. M. B. Costa, A. L. Macanite, H. Santos. *J Colloid Interface Sci.,* J H, 439, **1991.**

39. M. H. Gehlen and F. C. DeSchryver, *Chem. Rev.,* 93, 199, **1993.**

40. a) T. C. Werner, R. M. Hoffman, *J. Phys. Chem.,* 77, 1611, **1973;** b) F. Podo, **J.** K. Blasie, *Proc. Nath Acad. Sci., USA,* 74, 1032, **1977.**

41. K. R. Thulborn, W. H. Sawyer, *Biochim. Biophys. Acta.*, 511, 125, **1978.**

42. E. **D.** Matayoshi, A. M. Kleinfeld, *Biophys. J.*, 35, 215, **1983.**

43. D. B. Chalpin, A. M. Kleinfeld, *Biochim. Biophys. Acta*, 731, 465, **1983.**

44. **J.** Eisinger, J. Flores, *Biophys. J.,* 37, 6, 1982; *ibid* 41, 367, **1983.**

45. **P. R.** Worsham, D. W. Eaker, D. G. Whitten, *J. Am. Chem. Soc.*, 100, 7091, **1978.**

46. M. V. Bockstacle, J. Gelan, H. Martens, J. Put, F. C. DeSchryver, J. C. Dederen, *Chem. Phys. Lett.*, 70, 605, 1980.

47. T. Handa, K. Matsuzaki, M. Nakagaki, *J. Colloid Interface Sci.,* 116, 50, **1987.**

PHOTOPHYSICAL BEHAVIOUR OF
n-(4-AMINOPHTHALIMIDO)ALKANES IN POLAR MEDIA AND
ITS IMPLICATIONS

In this chapter the Photophysical behaviour of some N-alkyl-4-aminophthalimide derivatives with varying alkyl chain length is described. This study is undertaken with a view to find out whether any perturbation of the microenvironment around the fluorophore can be induced by the hydrocarbon chain in polar media.

4.1. Introduction

Hydrophobic interactions play a pivotal role in many chemical phenomena such as the formation of surface films, micelles, lipid bilayers, protein-amphiphile complexes, folding of globular proteins, biological membranes and are the basic forces for host-guest interactions.[1] It has been well-established that in hydrophilic or aggregating media such as aqueous or aqueous-organic binary solvents, hydrophobic interactions force molecules with long hydrocarbon chains to form aggregates even at very low concentrations and self-coil.[2] Aggregation and self-coiling may be one of the simplest ways in

which hydrophobic forces manifest. These considerations may be taken as a first good reason to investigate thoroughly the phenomena of aggregation and self-coiling.

Aggregation can be defined as a cluster of neutral organic species in equilibrium with its monomeric form as well as with clusters of differing aggregate numbers. Besides *aq* medium, most aggregating media studied are aqui-organo binary systems.3 The properties of these aggregates, including aggregation number, microscopic polarity and microscopic viscosity within the aggregate have been the primary objects of examination.[4]

Menger first proposed the concept of intermolecular aggregation in order to explain the rate of retardation of hydrolysis of certain long-hydrocarbon chain esters.[5]   Knowles then suggested that self-coiling of long-chain molecules can also be the cause of such rate retardation.[6] Breslow and co-workers have used the hydrophobic effect to accelerate reactions between lipophilic compounds by placing them in water, thereby intentionally bringing the reactants in close proximity[7]   It has been reported that the self-coiling can be used to expedite the formation of macrocyclic entities from molecules of flexible chains.[8]

A number of fluorescence studies have been reported in the systems of long-chain hydrocarbon aggregates in order to examine the molecular mobility, local polarity and viscosity inside   aggregates.[8-10]   That the conformation of the polymer chain can be affected by hydrophobic interactions has been demonstrated by the observation of excimer emission in pyrene appended

121

systems.[10] **Jiang** et al[11] **have** demonstrated the hydrophobicity-enforced chain folding and aggregation phenomena by monitoring excimer formation of naphthyl appended systems such as 1 and 2. Very recently, using fluorescence techniques Tung et al[8c-f] have illustrated the important role of the hydrophobic interactions by studying several long-chain hydro and fluoro carbon compounds linked by naphthyl chromophore. Zhen et al [12] reported the formation of

$$Np-CH_2CH_2O(CH_2)_{10}OCH_2CH_2-Np \qquad Np-CH_2CH_2O-C_{12}H_{25}$$

1   **2**
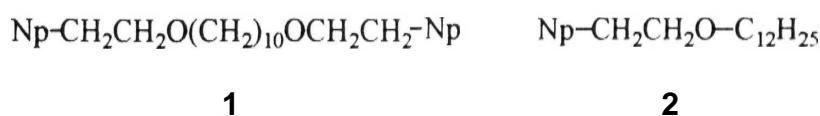
aggregates of 3 by monitoring excimer formation in aqui-organo mixtures. It was found that the microscopic polarity within the aggregate was small enough not to allow TICT formation. However, the excimer formation could be obser-

3
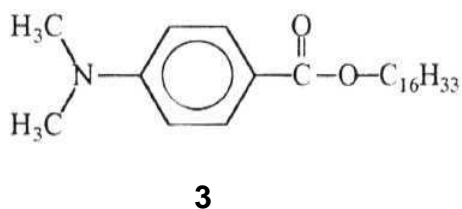
ved at this polarity. Demas et al [13] concluded intramolecular fold back of the alkyl chain in a series of surfactant-active complexes of the form $[(bpy)Re(CO)_3NC-(CH_2)_nCH_3]^{\oplus}$ (bpy=2,2'-bipyridine, n=0-17). This conclusion was based on the observation of the dependence of the lifetime of the charge transfer band on **the** length of the alkyl group in solvents such as acetonitrile, methanol and toluene.

In the course of our study on **AP-labelled** amphiphilic molecule, 11-(4-aminophthalimido)undecanoic acid, (APL) it was observed that the fluorescence decay of APL in *aq* medium was biexponential with lifetimes of ~ 1 ns for the major component and ~ 8 ns for the minor component. Interestingly, in the absence of the fatty acid chain the decay was clearly single exponential ($\tau_f \approx$ 1 ns). APL being an amphiphilic molecule, it is quite possible that the long-lived component arises due to inter or intramolecular interactions in hydrophilic media with the hydrophobic interaction as the driving force. In order to have an insight into this problem, we have prepared and examined the fluorescence behaviour of a series of n-(4-aminophthalimido)alkanes (APn, Chart 4.1) derivatives in which the environment sensitive fluorophore, AP is linked with alkyl chain of varying length. Since aggregation or self-coiling is
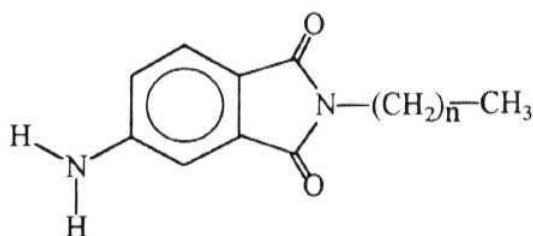
APn   n=1,2,3,5,7,11,15

CHART 4.1

expected mostly in polar media, the studies on these systems have been carried out in pure MeOH, H_2O and binary mixtures of DMSO-H2O.

4.2. Spectral Features of APn

4.2.1. Absorption Spectra

Absorption spectra of all the AP-derivatives $(AP1\text{-}AP15)$ consist of a structureless charge transfer band as the lowest energy transition both in MeOH and in *aq* medium.   Some representative spectra in MeOH and H_2O are shown in Figs. 4.1 and 4.2, respectively.   The spectral data of the systems are compiled in Table 4.1.   In MeOH, there is no noticeable change in the position of the spectral maxima or bandwidth as n varies from 1 to 15 indicating a similar environment around the fluorophore for all the systems.   In *aq* medium, even though no significant difference in the spectral behaviour of the compounds, $AP1$ to AP7 could be observed, minor broadening along with ~ 2-5 nm red shift of the absorption band is observed in the case of higher homologues, $AP11$ and AP15.
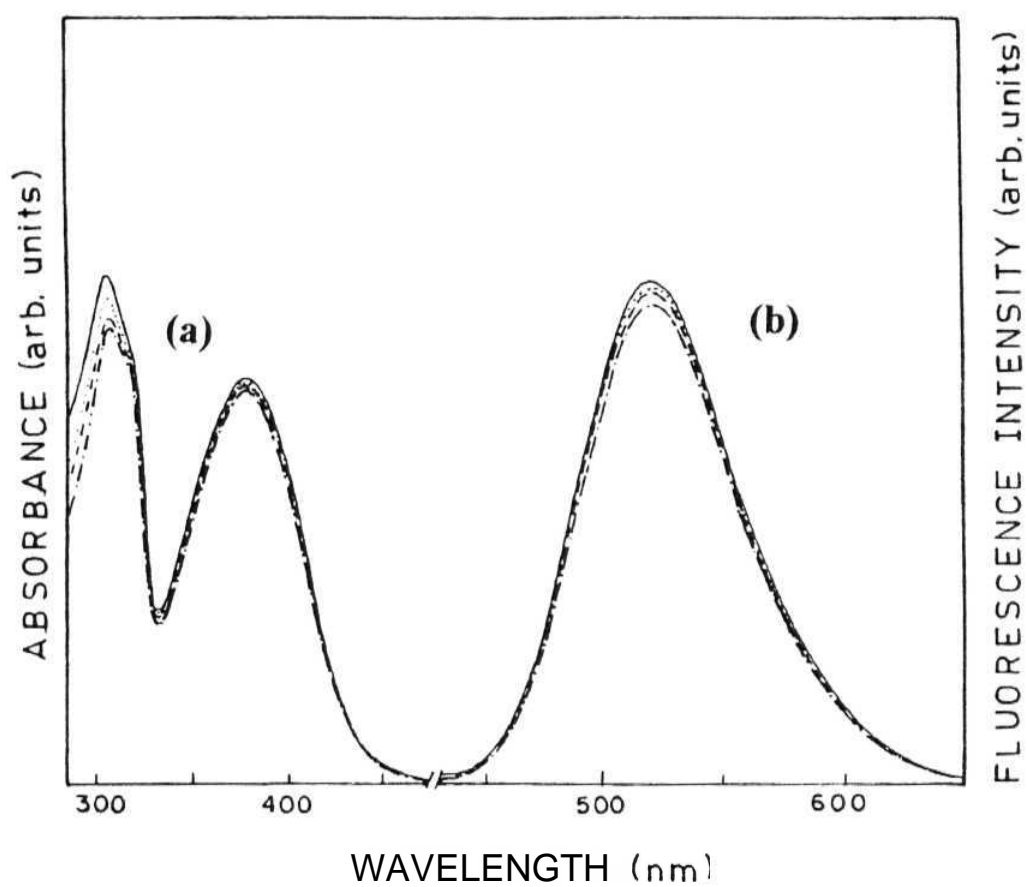
Fig. 4.1. Absorption (a) and fluorescence (b) spectra of N-alkyl-AP derivatives in MeOH at room temperature : (——) AP3; (••••) AP7; (——) AP11; (·—·—·) AP15. $\lambda_{exc} = 370$ nm.
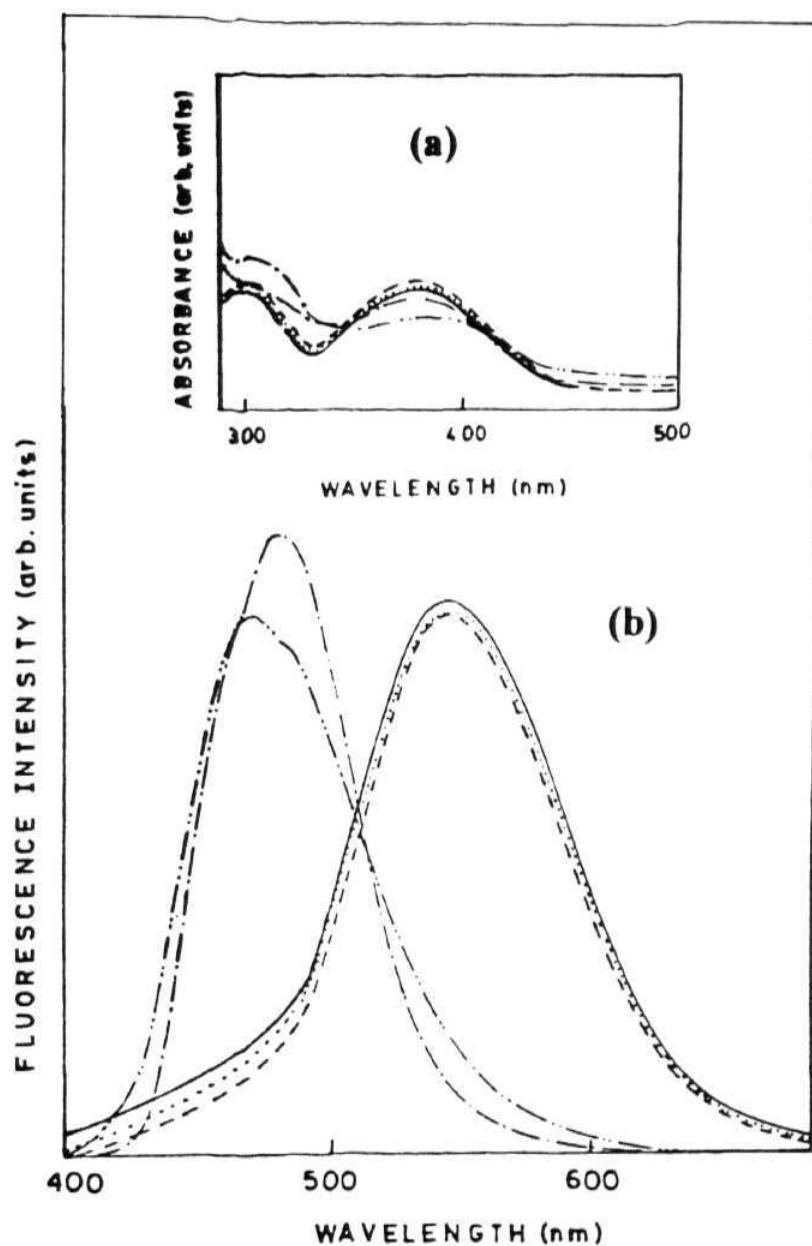
Fig 4.2. Absorption (a) and fluorescence (b) spectra of N-alkyl-AP derivatives in aqeous medium at room temperature (—) AP2, (⋯) AP3; (——) AP7, (—•-•) AP11; (··–··–··) AP15. λ_{exc} = 370 nm.

126

Table 4.1 Spectral Data of APn in MeOH and H$_2$O at Room Temperature.

System	MeOH		H$_2$O		
	λ_{abs}^{max} (nm)	λ_{flu}^{max} (nm) [a]	λ_{abs}^{max} (nm)	λ_{exc}^{max} (nm) [b]	λ_{flu}^{max} (nm) [a]
AP1	378	520	377	372	544
AP2	378	520	377	374	545
AP3	378	521	377	374	545
AP5	378	520	377	374	543
AP7	378	521	378	376	543
AP11	378	522	380	412	480
AP15	379	522	385	397	470

[a] Excited at 370 nm. [b] Monitored at the fluorescence maxima indicated in the last column.

4.2.2. Fluorescence and Excitation Spectra

The room temperature fluorescence spectra of APn are broad unstructured bands whose location is determined by the polarity of the medium. This is in agreement with the Photophysical behaviour of AP.[14] The fluorescence spectra of the systems in MeOH and H_2O have been shown in Figs. 4.1 and 4.2, respectively and the spectral data can be seen in Table 4.1. The location of the emission maxima and the bandwidths (fwhm 3000 cm^{-1}) remain about the same as n varies from 1 to 15 in MeOH, indicating that neither intra nor intermolecular interactions are dominant in this medium. In water, for systems AP1 to AP7, there is no noticeable change either in the location of the emission maxima or bandwidth (fwhm ~ 3000 cm^{-1}). This again suggests that the alkyl chain does not influence the photophysics of AP moiety. Interestingly, in the case of AP 11 and AP 15, the emission spectra were found to be considerably different (Fig. 4.2) in the same concentration range (~ 1 x 10^{-5} M) as that for the lower chain systems. Similar behaviour was observed for these systems even at lower concentrations (~ 1x 10^{-6} M) tried for. This peculiar behaviour can arise in principle due to intra or intermolecular interactions (or both) by hydrophobic forces induced by the long alkyl chains. Since the concentration range at which the unusual blue-shifted fluorescence spectra is observed is rather low it may appear that intramolecular interaction (presumably self-coiling) is responsible for the observed effect rather than inter molecular aggregation. However, Guthrie[15] and Menger et al[5a] have reported from a

study of hydrolysis of aryl alkanoates in *aq* medium that the critical aggregation concentration of the substrates of alkyl chain length of 12 carbons or above can be as low as 10^{-7} M. This implies that aggregation of neutral molecules with long alkyl chain can take place at a very low concentration. And hence, the observed spectral behaviour of the higher homologues, AP 11 and AP 15 can be due to aggregation as well. In order to find out whether aggregation or self-coiling is responsible for the blue-shifted fluorescence maxima we have performed experiment with the lowest possible concentration of the probe ($\sim$ 1 x 10^{-6} M). Practical restrictions did not allow us to perform experiments at too low concentrations. The reason being the low molar extinction coefficients of these systems (ε_3 $_{80}$ $\sim$ 3700 $M^{-1}cm^{-1}$) and low fluorescence yield in *aq* medium. Within these limitations, the spectral data observed at lowest permissible concentrations were found to be identical with those at relatively higher concentrations.

In order to understand the origin of the blue-shifted fluorescence band of AP1 1 and AP 15 in water we have measured the fluorescence excitation spectra of all the systems monitoring the fluorescence bands. The spectral data are collected in Table 4.1 and the representative excitation spectra are shown in the Fig. 4.3. As can be seen, while there is hardly any variation in the position of the spectral maxima of derivatives AP1-AP7, for AP 11 and AP 15, the excitation maxima are drastically red-shifted.

It may be noted in this context that the absorption spectrum of AP is rather insensitive to the polarity of the medium A small red shift with increase in the polarity of the medium could be observed.[14] In the case of a change in the local environment of the fluorophore due to fold-back of the hydrocarbon chain or self-coiling (intramolecular effect induced by hydrophobic forces), the microenvironment of the fluorophore was expected to be less polar and hence a small blue-shift of the absorption or excitation spectrum was expected. Obviously, a large red-shift of the maximum of the fluorescence excitation spectrum can not be understood in terms of self-coiling of the hydrocarbon chain around the fluorophore. This clearly indicates that the blue-shifted fluorescence of AP 11 and AP 15 originates from intermolecular aggregation that takes place even at a very low concentration. The excitation spectral data shows that the aggregates which emit at ~ 480 and 470 nm absorb at 412 and 397 nm, in the case of AP11 and AP 15, respectively.
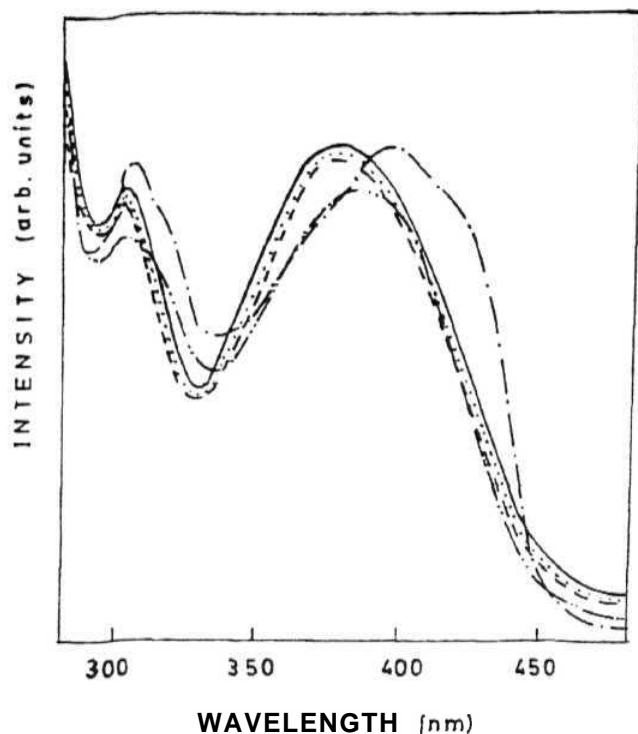
Fig. 4.3. Fluorescence excitation spectra of N-alkyl-AP derivatives in aqueous medium (——) AP2; (••••) AP3; (——) AP7; (—-) AP11; (··—··—··) AP15.

4.2.3. Fluorescence Spectra in Water-Organic Binary Mixtures

Having understood the origin of apparently unusual fluorescence of AP11 and AP15 in *aq* solutions we have carried out further experiments to substantiate our conclusion. Fig. 4.4. shows the fluorescence spectra of dilute solutions of AP11 (~5 x 10^{-5} M) in DMSO-H2O mixtures. It can be seen that with increase in the volume fraction of water ((p) in the solution, a blue-shift of the spectrum is observable from Fig. 4.4. At $\varphi \sim 0.6$, it appears that most of the molecules are in monomeric form as the emission corresponds closely to that of the fluorophore in pure organic medium. The blue shift of the spectrum with

131

increase in the amount of water in the solvent can only be explained in terms of the formation of the molecular clusters or aggregates as a result of hydrophobic interactions. This observation suggests that the association of the molecules readily takes place with increase in hydrophilicity of the medium as a result of hydrophobic interactions. The difference in the fluorescence excitation spectra of the compounds in pure water and water-DMSO mixture shown in Fig. 4.5, also support that aggregation is responsible for the anomalous fluorescence behaviour of AP11 and AP 15 in aqueous solutions.
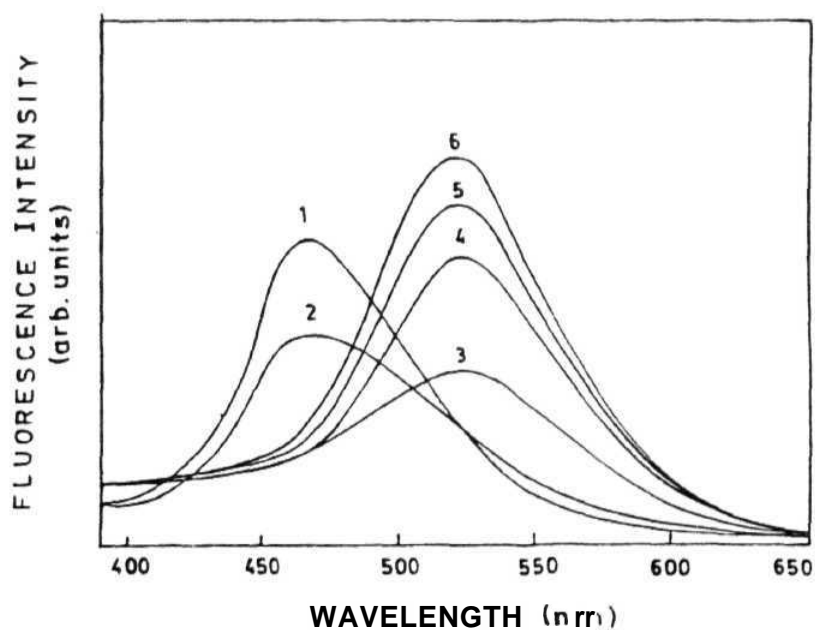
Fig. 4.4. Fluorescence spectra of AP 11 in DMSO-water mixtures. The φ values for the spectra labelled 1 to 6 are 1, 0.80, 0.60, 0.50, 0.45, 0.40 respectively.
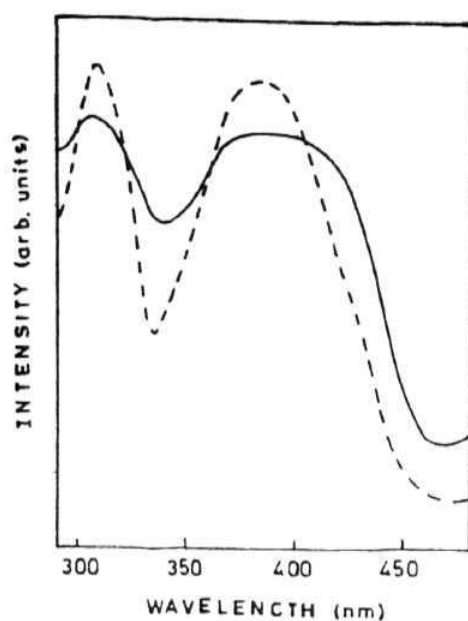
Fig. 4.5. Fluorescence excitation spectra of AP1 1 in DMSO-water mixtures. The φ values are (—) 1; (——) 0.4.
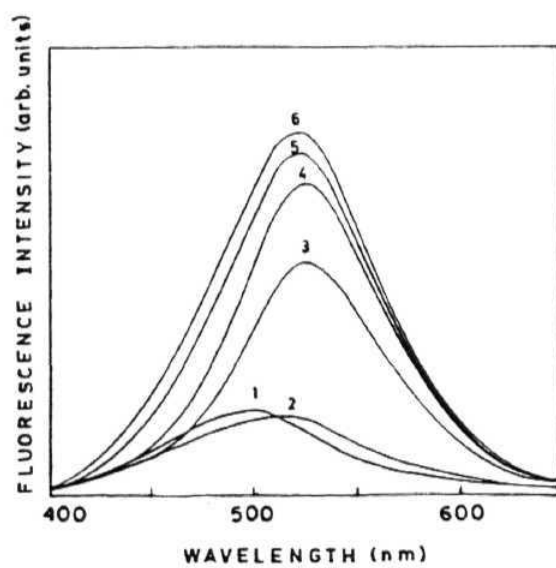
Fig. 4.6. Fluorescence spectra of **AP** 11 in aqueous solution containing various amount of SDS. The SDS concentrations (mM) for the spectra labelled 1 - 6 are 0, 5, 11, 37, 98, 158, respectively.

4.2.4. Effect of Surfactant on the Fluorescence Behaviour of APn with Long Alkyl Chain

To confirm the formation of the aggregates, **we** have studied the effect of the surfactant on the fluorescence behaviour systems with long alkyl chain ($n \geq 11$) in hydrophilic medium. It is known that hydrophobic-lipophilic forces are mainly responsible for the formation of micelles in hydrophilic media and their binding

with organic hydrophobic probes.[16] Fig 4.6 shows the effect of sodium dodecyl Sulfate (SDS) on the fluorescence spectra of AP11 ($\sim 2 \times 10^{-6}$ M). It should be noted that the addition of SDS to an *aq* solution of AP (monomeric) leads to a blue-shift of the fluorescence maximum (sec. 3.1.2) which can be attributed to binding of the fluorophore at the micelle-water interface. However, addition of SDS to the *aq* solution of AP11 leads to a red shift of the emission band even when the surfactant concentration is below critical micellar concentrations (CMC) of the micelle. A further shift towards red associated with an increase in the intensity of the fluorescence is observed at higher concentrations of SDS. After a certain concentration of the surfactant, only enhancement in the intensity with no change in the position of the emission maximum (Fig. 4.6) could be noticed. This observation can only be rationalised in terms of deaggregation of the clusters of the host molecules by the surfactant molecules. With increase in the amount of SDS, more and more AP11 molecules are deaggregated. Since emission from monomeric AP 11 is expected at a wavelength longer than that

134

observed for the aggregated system, the spectrum shifts towards red. At higher concentration of SDS, since the deaggregation is more or less complete, no further shift of the spectral maximum could be observed with increase in the concentration of the surfactant. The fluorescence enhancement at high concentration of SDS is due to the micellisation of the monomeric AP 11 molecules. It is interesting to note that the location of the fluorescence maximum of AP 11 at highest concentration of SDS is almost identical with that observed with AP in micellar environment.

4.2.5. *Time-resolved Fluorescence Study*

As stated earlier, the above study was undertaken with a view to find out the origin of the unusual long-lived second component in the fluorescence decay of APL and DAPL. Since this component could only be observed for systems with polymethylene chain, it was apparent that hydrophobic interaction induced by the long hydrocarbon chain is responsible for the appearance of the second component. However, it was not clear immediately whether intermolecular interaction (leading to aggregation) or intramolecular interaction (leading to self-coiling) gives rise to the long-lived component. The above experiments clearly show that the long-lived component has to be assigned to aggregate of the probe molecules. The lifetime measurements have been performed on all the systems in *aq* solution. The fluorescence decay curves of all the systems have been analysed using a bi-exponential decay function to obtain the best possible fits. It can seen from the Table 4.2, **all the** systems contain a second component with a

135

relatively long lifetime even though the weightage of this component to the total decay is relatively small for AP2-AP7. However, as expected, the second component is present in appreciable amount for even fairly dilute solution of AP11 and AP15. However, we are unable comment on why the τ_2 values are different for different systems.

Table 4.2   Time-resolved Fluorescence Data of N-Alkyl-AP Systems in Aqueous Medium at Room Temperature.

Probe	Concentration (M)	τ_1 (ns)	τ_2 (ns)	$B_1{}^a$
AP15	4.4×10^{-6}	0.61	4.1	0.72^b
AP11	2.2×10^{-6}	0.63	3.7	0.61^b
AP7	$4.3 \times JO^{"5}$	1.2	9.8	0.96
AP5	11×10^{-5}	1.2	8.4	0.91
AP3	1.8×10^{-6}	0.98	3.1	0.90
AP2	13×10^{-5}	1.2	4.4	0.97

[a] The fluorescence decay curves were analysed using $I(t) = B_1 e^{-t/\tau_1} + B_2 e^{-t/\tau_2}$.

[b] For AP 15 and AP 12 a third component could be observed with lifetimes of 11 ns (5.3%) and 9.9 ns (1.0%), respectively when fitted to a tri-exponential decay function.

4.3. References

1. **a)** C. Tanford, *The Hydrophobic Effects*, Wiley: New York, 1980. b) W. Blokzijl, J. B. F. N. Engberts, *Angew. Chem. Int. Edn. Engl,* 32, 1545, **1993**.

2. a) X. -K. Jiang, *Acc. Chem. Res.,* 21, 362, **1988;** b) C. -H. Tung, C. -B. Xu, In: *Photochemistry and Photophysics,* J. F. Rabek, ed., Vol 4, CRC Press: Boca Raton, **1991,** Chap. 3.

3. X. -K. Jiang, Y. Li, B. -Z. Haung, *Proc. Ind. Acad. Sci., (Chem. Sci.),* 98, 409, **1987.**

4. a) C. -B. Xu, C. -H. Tung, *Acta. Chim. Sin. Engl. Ed,* 72, **1989;** b) C. -B. Xu, Y. -Y. Liu, H. -S. Shou, C. -H. Tung, *Acta. Chim. Sin. Engl. Ed.,* 141, **1988**.

5. a) F. M. Menger, C. E. Portony, *J. Am. chem. Soc.,* 90, 1875, **1968;** b) F. M Menger, V. V. Venkataram, *J. Am. Chem. Soc,* 108, 2980. **1986**.

6. C. A. Blyth, J. R. Knowles, *J. Am. Chem. Soc,* 93, 3021, **1971.**

7. **R.** Breslow, *Acc. Chem. Res.,* 24, 159, **1991.**

8. a) X. -K. Jiang, W. -Q. Fan, Y. -Z. Hui, *J. Am. Chem. Soc,* 10i, 3839, **1984;** b) X. -K. Jiang, , Y. -Z. Hui, Z. -X. Fei, *J. Am. Chem. Soc,* 689, **1988;** c) C. -H. Tung, Y. -H. Wang, *J. Am. Chem. Soc,* 112, 6322, **1990;** d) C. **-H.** Tung, Y. Li, Z. **-Q.** Yang, *J. Chem. Soc, Faraday Trans.,* 90, 947, **1994;** e) C. -H. Tung, H. -F. Ji, *J. Chem. Soc, Faraday Trans.,* 91.,

2761, **1991; f) C. -H. Tung, L. -Z. Wu,** *J. Chem. Soc, Faraday Trans.,* 92, 1381, **1996**.

9. C. -H. Tung, Y. -Y. Liu, C. -B. Xu, *Acta. Chem. Sin. Engl. Ed.,* 1, 52, **1988**.

10. a) F. M. Winnik, M. A. Winnik, S. Tazuke, *J. Phys. Chem.,* £1, 594, **1984;** b) F. M. Winnik, M. A. Winnik, S. Tazuke, C. K. Ober, *Macromolecules,* 20, 38, **1987.**

11. X -K. Jiang, Y. -Z. Hui, X -Z Fei, *J. Am. Chem. Soc,* 109, 5862, **1987.**

12. Z. Zhen, C. -H Tung, *Chem. Phys. Lett.,* 180, 211, **1991**.

13. a) G. A. Reitz, W. J. Dressiek, J N Demas, *J. Am. Chem. Soc,* 108, 5344, **1986;** b) G. A. Reitz, J. N. Demas, B. A. DeGraff, M. Eileen, M. Stephen, *J. Am. Chem. Soc,* HO, 5051, 1988.

14. T. Soujanya, R. W. Fessenden, A. Samanta, *J. Phys. Chem.,* 100, 3507, **1996**.

15. J. P. Guthurie, *Can. J. Chem.,* 51, 3494, **1973.**

16. K. Kalyanasundaram, *Photochemistry in Microheterogeneous Systems,* Academic Press: New York, **1987.**

4N,N-D1METHYLAMINOPHTHALIMIDE AND ITS FATTY ACID DERIVATIVE AS SENSORS IN MICELLAR MEDIA.

The fluorescence behaviour of 4-N,N-dimethylaminophthalimide (DAP, Chart 5.1) and its fatty acid derivative, 11-(4-N,N-dimethylaminophthalimido)undecanoic acid (DAPL, Chart 5.1) in micellar media is described in this chapter. The aim of this investigation is to find out the potential of these compounds as fluorescence probes for characterising the organised environments.

DAP   DAPL
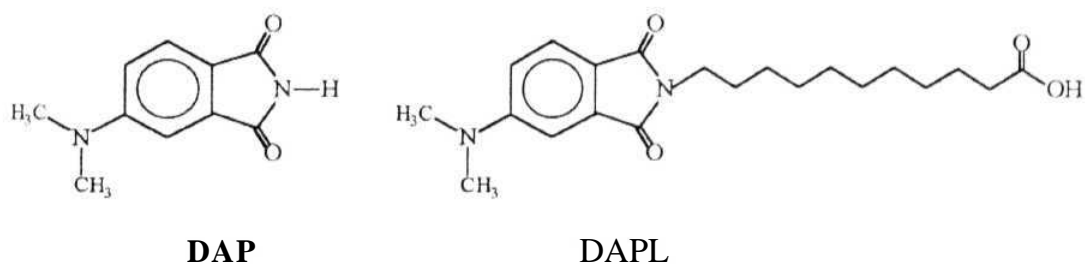
CHART 5.1

5.1. Introduction

The elegant usage of the fluorescent EDA molecules in probing the microstructures of various organised media, is well documented.[1-11] In the

previous chapter, such usage is illustrated with EDA molecules, AP and its derivative, APL. A new class of fluorescence probes, which show remarkably higher sensitivity toward solvent polarity are systems, where the electron donor and the acceptor moieties are formally linked by a single bond. On excitation, this class of systems often display an additional charge transfer emission band which is believed to originate from a state (called TICT state) in which the donor and acceptor moieties are perpendicular to each other.[3] The fluorescence originating from such a state is much more sensitive to the solvent polarity due to the large dipolar character of the TICT state resulting from complete decoupling of the donor and acceptor orbitals with one unit of charge transfer. In some EDA systems, the TICT state is well-above the locally excited ICT state or the barrier to ICT→TICT process is sufficiently large so that the TICT does not influence the Photophysical behaviour of the systems. AP can be considered as one such systems. In many systems, TICT can be nonfluorescent. The presence of a *low-lying* TICT state, whether emitting or not, enhances the sensitivity of the fluorescent properties of the locally excited ICT state because of the polarity dependence of the nonradiative ICT→TICT process.[12] The best known examples of such systems are coumarin dyes.[1,3] The highly sensitive fluorescence properties of the coumarins have been explained due to the presence of low-lying nonfluorescent TICT state and this has been exploited extensively[13] to probe the micropolarity of the organised systems and to study the solvent relaxation processes.

Recently, a comparative study of the Photophysical behaviour AP and DAP has revealed that the fluorescence properties of DAP are much more sensitive to the solvent polarity compared to AP.[14] This observation is attributed to the presence of a nonfluorescent TICT state below the locally excited emitting state of DAP and also due to the enhanced dipole moment of its fluorescent state.[14] Therefore, one expects, that the fluorophores based on DAP to be superior to those based on AP. In addition, the dimethyl substitution of the amino hydrogens of AP is expected to enhance the hydrophobicity of the fluorophore which might help its deeper penetration into the core region of the micelle. With this view in mind we have explored the potential of DAP and DAPL as fluorescence probes in micellar media.

DAP exhibits a shift of ~120 nm on changing the solvent from 1,4-dioxane to water.[14] The fluorescence quantum yield (ϕ_f) decreases by a factor of ~ 620 for the same change of solvent. In aprotic media, when the solvent changes from 1,4-dioxane to acetonitrile, the ϕ_f decreases by a factor of ~ 5 and the nonradiative rate constant (k_{nr}) increases by a factor of ~ 10.[14] On the other hand, the fluorescence yield, lifetime and k_{nr} values remain more or less same in these solvents for AP. This disparity in the fluorescence behaviour of DAP when compared to that for AP, is attributed to the presence of a nonradiative decay channel (nonfluorescent TICT state) even though the emission in both cases originates from the ICT state. Clearly, the change in the fluorescence yields with variation of solvents, which is an indicator of the

141

effectiveness of a probe, is much higher for DAP than that of AP. [14] All these observations suggest that DAP can act as a more efficient probe than AP. We have therefore undertaken the following investigation employing DAP and its derivatives in three types of surfactants, cationic (CTAB), anionic (SDS), and neutral (TX). [15]

5.2. **DAP** as a Sensor for Micellar Media

5.2.1. Absorption Spectra

Fig. 5.1 shows the absorption spectra of DAP in the presence of CTAB surfactant. The changes in the spectra on addition of the surfactant are rather small. A very similar behaviour is observed with SDS and TX. This observation is in accordance with the results obtained with AP and APL.

5.2.2. Fluorescence Spectra

Addition of surfactants to an *aq* solution of DAP has marked effect on its fluorescence behaviour. Fig. 5.1 displays the fluorescence spectra of DAP as a function of CTAB concentration. A blue-shift of the spectral maximum and an enhancement of the fluorescence intensity are the two noticeable observations that can be made on addition of CTAB to an *aq* solution of DAP. The change in the fluorescence properties is significant only beyond a certain concentration of the surfactant. The blue-shift of the spectra and increase in the fluorescence yield are clearly due to as the binding of the probe to a less polar site of the micellar environment than the bulk *aq* phase once the micelles are formed. The
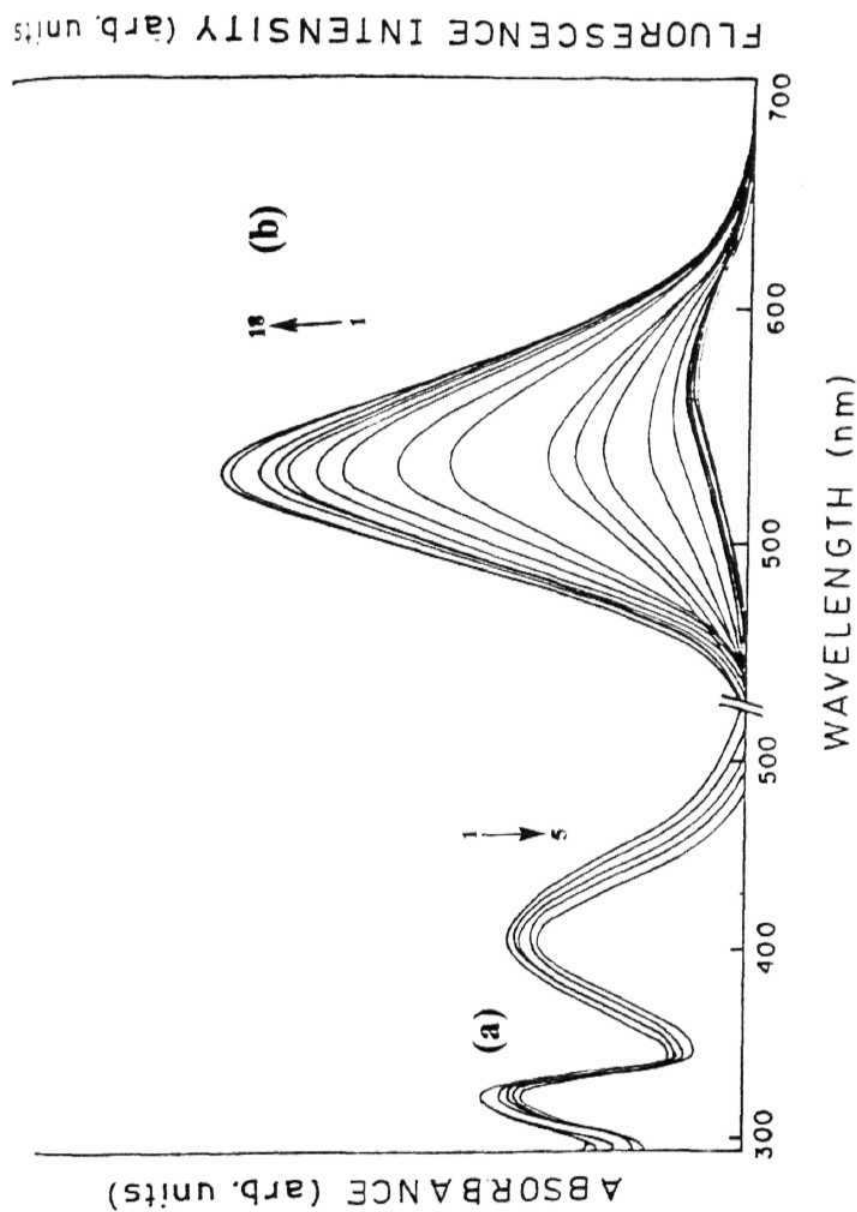
Fig. 5.1. Absorption (a) and fluorescence (b) spectra of DAP in aqueous solution with different amounts of CTAB. The concentrations of CTAB (mM) (a) for the spectra labelled 1- 5 are 0, 6, 12, 30, and 71 respectively; (b) in increasing order of intensity, 0, 0.2, 0.4, 0.6, 0.8, 1.0, 1.5, 2, 2.5, 6.3, 10, 15, 21, 28, 33, 39, 62, 71, respectively. $\lambda_{exc} = 410$ nm.

143

decrease in the polarity of the microenvironment of the probe leads to greater destabilisation of the emitting state compared to the ground state (as the excited state dipole moment of DAP is higher than the ground state moment).   This results in an increased separation between the SQ and S_1 states which lowers the nonradiative transition rate from S_1 leading to an increase in the fluorescence yield. The reduction in hydrogen bonding interaction with the solvent could also be responsible for an increase in the fluorescence yield on micellisation.   The behaviour of DAP in cationic (SDS) and neutral (TX) micelles is found to be quite similar.

The maximum spectral shift and the fluorescence enhancement data in three micelles are gathered in Table 5.1.   A quantitative analysis of the fluorescence enhancement data gave the CMC values of the surfactants employed (Fig. 5.2).   The insert in Fig. 5.2 shows the variation of the *fc/fo* with the surfactant concentration over the entire range used. From the inflection point of the two straight lines in the Fig. 5.2, the CMC of the CTAB is estimated to be (0.6 ± 0.03) x 10^{-3} M. Similarly, the estimated CMC values of SDS and TX are found to be (7.8 ± 0.4) x 10^{-3} M and (0.26 ± 0.02) x 10^{-3} M, respectively.   A fairly good agreement of the measured CMC values with the literature can be found from Table 5.1. The important point that is to be noted here is that the change in the relative fluorescence intensity and shift in the emission maximum (Table 5.1) for DAP are considerably higher in micellar

144

media when compared to those for AP. This makes DAP clearly more efficient than AP in monitoring even subtle changes in the surrounding environment.
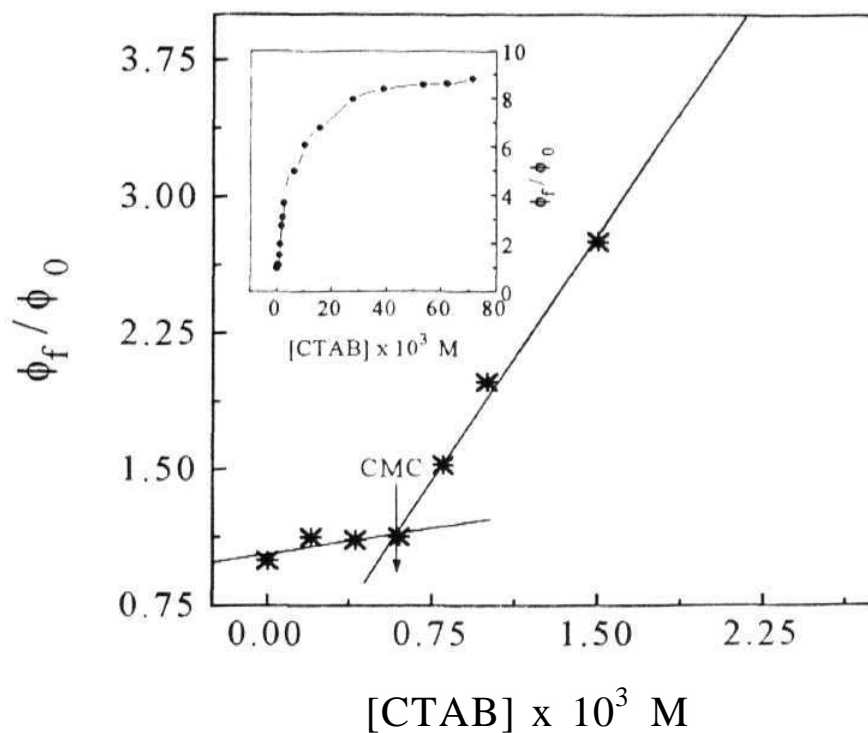
Fig. 5.2. A plot of the relative fluorescence intensity (ϕ_f/ϕ_0) of DAP as a function of CTAB concentration in aqueous solution. The insert shows the variation of the ratio over a larger concentration range.

Table 5.1 Fluorescence Enhancement, Spectral Shift and Lifetime of DAP in Micellar Media along with the Binding Constants.

Surfactant	Concentration (mM)	Maximum		CMC (mM)		K (M^{-1})	τ_1 (ns) (R$_1$)b
		ϕ_f/ϕ_0	Shift (nm)	Literature	Measured		
SDS	75	7.1	30	8.00	7.80	11600	0.52 (98.7)
CTAB	72	8.8	41	0.92	0.60	11850	0.34 (98.8)
Triton X-100	139	20.7	53	0.26	0.24	21400	0.81 (96.7)

a From ref. [1]. b Calculated using relative amplitude, $R_i = 100 B_i \tau_i \Big/ \sum_{k=i}^{2} \left(B_k \tau_k \right)$.

5.2.3. Time-resolved Measurements

The fluorescence lifetimes of **DAP** have been measured by selecting the surfactant concentrations such that most of the probe molecules are micellised. The lifetime data in micellar media are shown in Table 5.1 which has been obtained from a biexponential fit of the fluorescence decay curves in the respective media. The lifetime of the major species (97-99%) ranges between 0.3-0.8 ns which is considered as the lifetime of the micellised probe. This lifetime is 2-5 folds higher than that of DAP in *aq* medium (~ 0 18 ns). Though the enhancement of lifetime of DAP on micellisation is very clear from the data, it is not possible to quantify the lifetime enhancement data because the time-resolution of our instrument (1.4 ns) is considerably lower than the lifetimes measured both in *aq* and micellar media.

5.2.4. Binding Strength of DAP with Micelles

Binding constants (K) of DAP with the micelles have been determined by following the method described earlier (equn. 3 3). The plot based on this equn. is shown in Fig. 5.3 from which the K values ($\pm$ 10%) are evaluated as 11600, 11850 and 21400 M^{-1} in SDS, CTAB and TX, respectively. The measured K values are consistent with the spectral shift data. Compared to the binding of **AP** with the micelles, **DAP** binds relatively strongly (K values are higher by a factor of 3.4 - 3.8) which could be most likely due to the hydrophobic influence of the methyl groups.
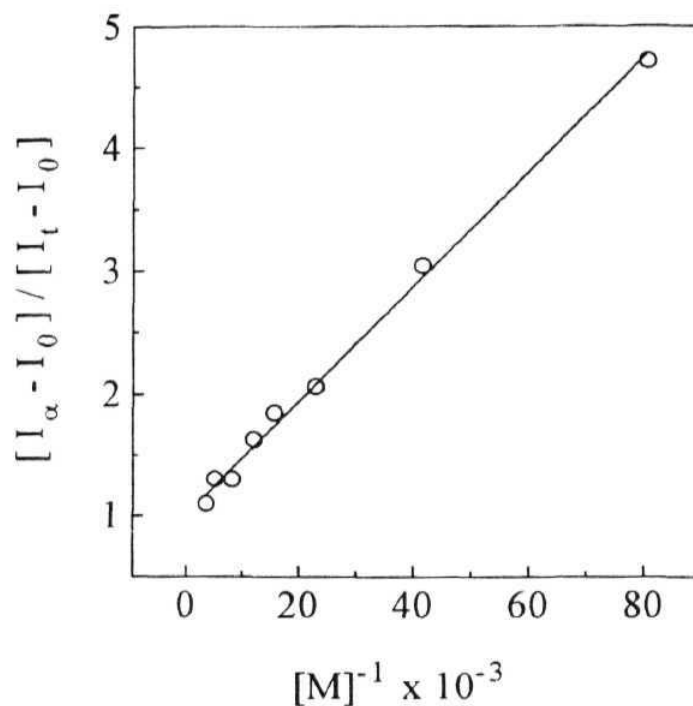
Fig. 5.3. Plot of $(I_\infty - I_0)/(I_t - I_0)$ vs $[M]^{-1}$ in Triton X-100 for DAP. The plot is based on equn. 3.3.

5.2.5. *Location of DA P in Micelles*

With DAP, the observed enhancement of fluorescence intensity in micellar environment is 7-21 fold, whereas the expected enhancement for a 1,4-dioxane like environment is nearly 600 fold. Quite obviously, DAP experiences an environment that is considerably polar. However, the polarity experienced by DAP is less polar than water. One arrives at a similar conclusion on

148

consideration of the spectral shift data. The microscopic polarities (in $E_T(30)$[16] scale) for the solubilization sites of DAP, by following the method described in the previous chapter, are 57.3, 55.1 and 52.8 in SDS, CTAB and TX, respectively. The interface polarities as estimated by DAP are not very different from those estimated by AP. The slightly lower polarity estimates obtained with DAP are presumably due to a slightly deeper penetration of this probe towards the core region compared to AP.

One of the findings that is common in both cases is that the interface in SDS micelle is relatively more polar than in CTAB and TX. This is in accordance with the observation of Menger and co-workers who proposed the SDS micellar aggregates to have a large wet Stern region, and a rough surface.[17] There were also supportive reports for the more porous nature and 'wet' micelles of SDS from small angle neutron scattering (SANS) studies.[18] On the other hand, SANS data on CTAB micelles excluded the possibility of wet and rough surfaces.[18a,19] Recently, Sarpal et al[20] have also provided the evidence for surface roughness of SDS micelles by employing 3H-indole derivatives as fluorophores. The irregularities caused by the surface roughness are probably filled by the water molecules. The more porous nature or high surface roughness of SDS micelles is probably the reason for higher polarity sensed by DAP and AP in SDS micelles, when compared with that in CTAB and TX micelles. This observation further highlights the efficiencies of these systems as reporter molecules.

5.3. 11-(4-N,N-Dimethylaminophthalimido)undecanoic Acid as an Amphiphilic Fluorophore

As the residence of DAP is found to be near the surface, we thought of examining its fatty acid derivative, DAPL where the fluorophore, DAP is attached to its nonpolar end of the fatty acid chain, with the idea that such covalent linkage might help pushing the fluorescing moiety towards the micellar core. Even though such an attempt was unsuccessful in the case of APL, we thought that enhanced hydrophobicity introduced in the fluorophore by methylating the amino group, might be of some help in achieving the objective. The fluorescence spectrum of DAPL in *aq* solution was reported to be unusually broad to suggest the presence of multiple components in the spectrum.[15] We thought that this could be due to various microenvironments experienced by DAPL. Self-coiling and/or aggregation were considered to be responsible for this behaviour. However, a detailed investigation led us to conclude that aggregation was responsible for this. In our investigations, we have carried out experiments with $\sim 1 \times 10^{-6}$ M concentrations of the probe molecule such that aggregation did not affect the spectral results.

5.3.1. Spectral Characteristics of DAPL in Homogeneous Media

The spectral data of DAPL in homogeneous media are presented in Table 5.2 and some representative absorption and fluorescence spectra are
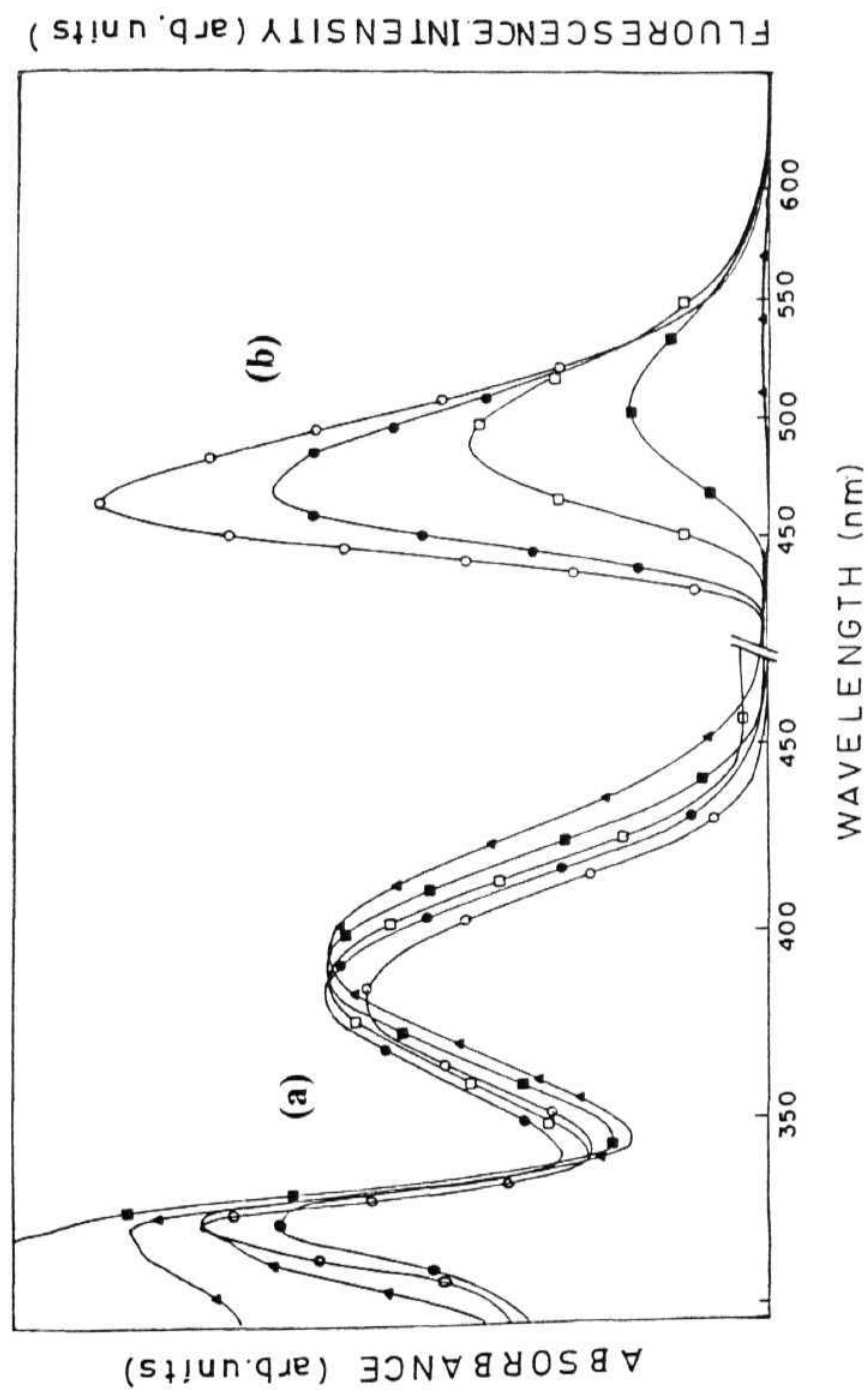
Fig. 5.4. Absorption (a) and fluorescence (b) spectra of DAPL in various solvents : (–O–O–) 1,4-dioxane; (–●–●–) tetrahydrofuran; (–□–□–) acetone; (–■–■–) acetonitrile; (–▲–▲–) methanol. $\lambda_{exc} = 410$ nm.

151

shown in Fig. 5.4. The spectral features are found to be quite similar to those of DAP showing more pronounced solvatochromic shifts of the fluorescence maxima than those for absorption, indicating an emitting state that is more polar than the ground state. In hydroxylated solvents, the Stokes shift of the fluorescence maximum is considerably larger than that expected based on the polarity of the medium alone. This behaviour is due to the hydrogen bonding interaction between the probe and the solvents. A plot of the Stokes shift $(\Delta\bar{\nu},cm^{-1})$ vs solvent polarity function (Δf) according to Lippert-Mataga equn. (sec. 2.1.5) is shown in Fig. 5.5 to depict the polarity and hydrogen bonding interaction effects of the solvents on the emission energy of DAPL. As can be seen from the Figure the hydrogen bonding interaction of DAPL is evident from the enhanced Stokes shift in protic solvents that can not be correlated to the polarity alone. In any given solvent, both the absorption and fluorescence maxima of DAPL are Stokes-shifted with respect to those for APL (Table 3.4). This is presumably due to higher ground and excited state dipole moments of the DAP moiety.
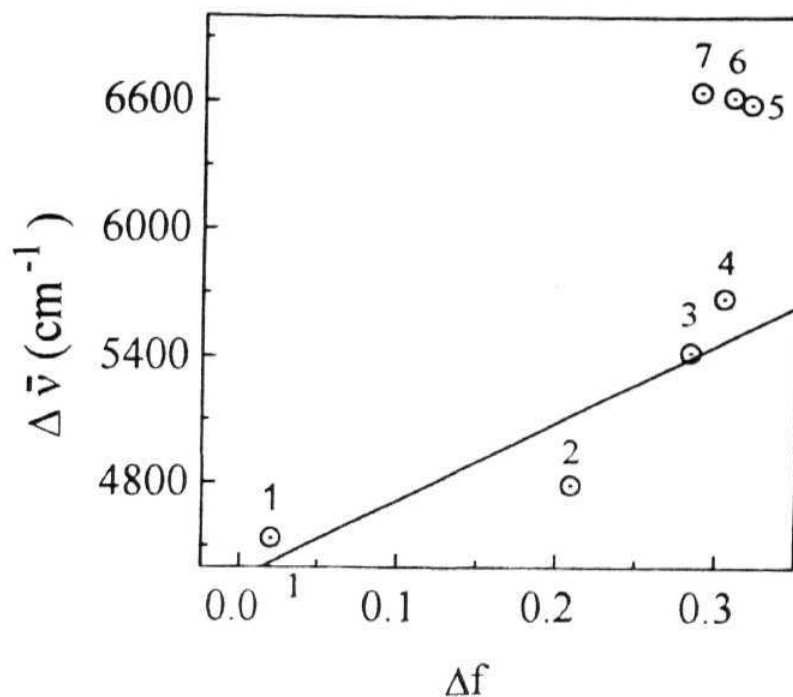
Fig. 5.5. Dependence of the Stokes shift ($\Delta\bar{\nu}$) of DAPL on the solvent polarity function Δf (sec. 2.1.5) according to the Lippert-Mataga equn. (equn. 2.3). The solvents are 1. 1,4-dioxane; 2. tetrahydrofuran; 3. acetone; 4. acetonitrile; 5. ethanol; 6. methanol; 7. water. The straight line represents the best fit to the data collected only in the aprotic solvents.

The fluorescence yield (ϕ_f) and lifetime (τ_f) of DAPL as a function of the polarity of the solvent are shown in Table 5.2 along with the calculated rate constants for the nonradiative decay process (k_{nr}). It is observed that while ϕ_f,

Tf and k_{nr} values of APL (Table 3.4) remain more or less constant in aprotic solvents, for DAPL, there is a reduction in ϕ_f and τ_f and enhancement of the nonradiative rates on increase of the polarity of the media. This behaviour is consistent with the difference in the behaviour of AP and DAP Which has been interpreted due to the existence of a nonemissive TICT state (that acts as a nonradiative decay channel) below the emitting locally excited state of DAP. This additional polarity dependent property makes DAPL a probe superior to APL. In hydrogen bonding solvents, a drastic decrease in ϕ_f and τ_f is observed for both the compounds.

Table 5.2 Photophysical Properties of DAPL in Homogeneous Media.

Solvent	$E_T(30)^a$	λ_{abs}^{max} (nm)	$\lambda_{flu}^{max,b}$ (nm)	ϕ_f	τ_f (ns)	k_{nr} $(10^7 \ s^{-1})$
1,4-dioxane	35.9	384	465	0.66	18.30	0.79
THF^c	37.2	383	469	0.59	15.80	2.58
Acetone	42.5	386	488	0.340	11.70	5.62
AN^d	46.5	392	504	0.213	7.40	10.60
BuOH	49.9	395	527	0.037	2.50	38.90
PrOH	50.6	396	530	0.025	2.10	47.10
EtOH	51.9	393	532	0.013	1.12	88.20
MeOH	55.1	395	535	0.006	0.89	111.00
H$_2$O	63.1	417	575	0.001	0.16 (73.6%)^e 7.2 (26.4%)	640.00

^{a} Measured using betaine dye. ^{b} Excited at 410 nm. ^{c} Tetrahydrofuran. ^{d} Acetonitrile. ^{e} Calculated using relative

amplitude, $R_i = 100 B_i \tau_i \Big/ \sum_{k=1}^{2} \left(B_k \tau_k \right)$.

5.3.2. DAPL as Sensor for Microenvironments of Micelles

5.3.2.1. *Spectral Features*

Studies have been carried with SDS, CTAB and TX surfactants. No noticeable change could be observed in the absorption spectrum of DAPL on addition of the surfactants to an *aq* solution of DAPL. A representative absorption spectrum in micellar medium is shown in Fig. 5.6.

Fig. 5.6 displays the fluorescence spectra of DAPL as a function of TX concentration. A blue-shift of fluorescence maxima with an enhancement of the fluorescence yield can be noticed from Fig. 5.6, as has been observed with other AP derivatives. The binding of the fluorophore to a less polar site in the micelle is indicated by these data. The spectral shift and enhancement are observable only beyond a certain concentration of the surfactant and also, at sufficiently higher concentration of the surfactant, there is no change either in the location of the spectral maximum or in the fluorescence intensity indicating that most of the molecules are in bound condition.
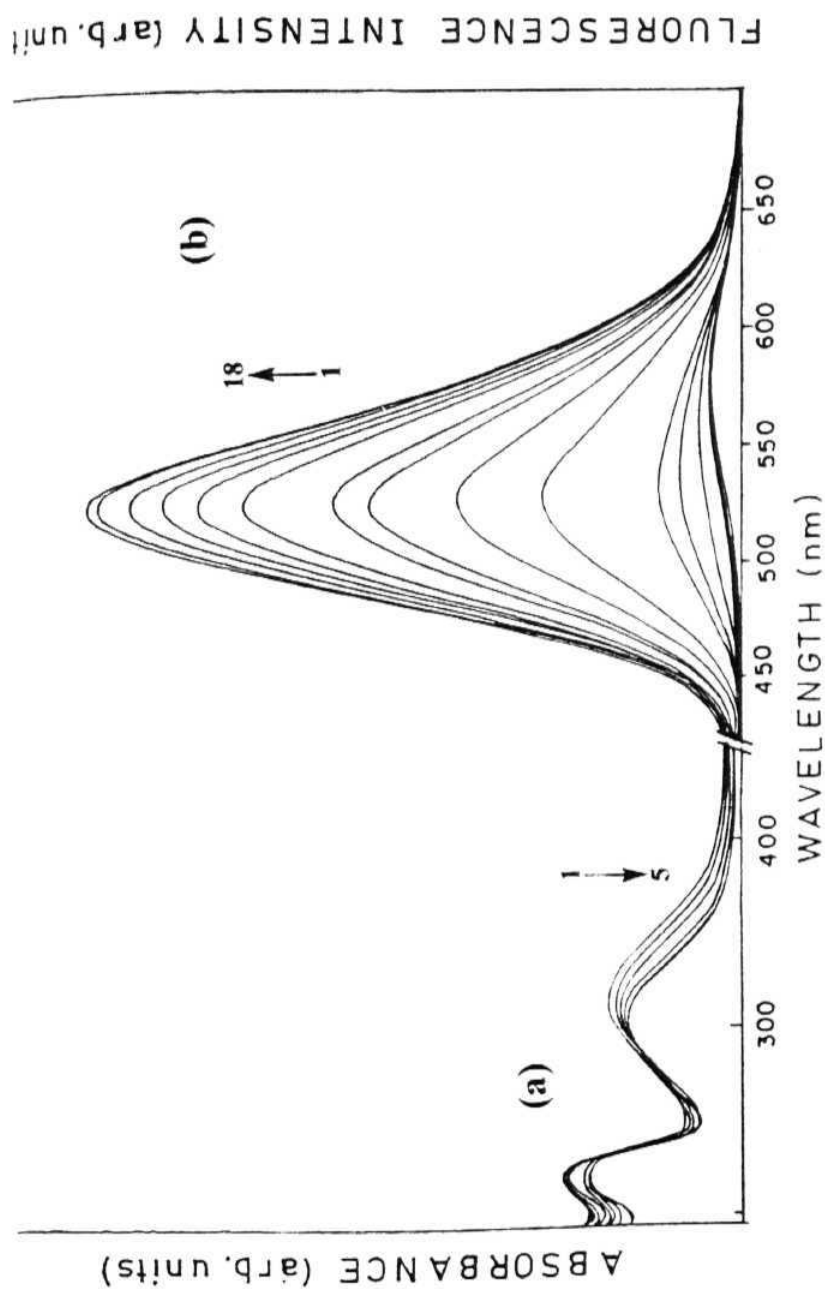
Fig. 5.6. Absorption (a) and fluorescence (b) spectra of DAPL in aqueous solution with different amounts of Triton X - 100. The concentrations of Triton X - 100 (mM) (a) for the spectra labelled 1 - 5 are 0, 0.2, 12, 45, and 128 respectively; (b) in increasing order of intensity, 0, 0.06, 0.13, 0.2, 0.27, 0.4, 0.7, 0.9, 3.7, 6.5, 9.2, 12, 23, 34, 45, 62, 111, 128, respectively. $\lambda_{exc} = 410$ nm.

157

A representative plot of ϕ_f/ϕ_0 of DAPL against the surfactant concentration from which the CMC values of the surfactants have been evaluated is shown in Fig. 5.7. The estimated CMC values are tabulated in Table 5.3. Again, a good agreement with the literature values can be noticed. A summary of the maximum spectral shift and fluorescence enhancement data is also given in the Table 5.3. The τ_f values of DAPL under completely micellised condition are shown in Table 5.3.
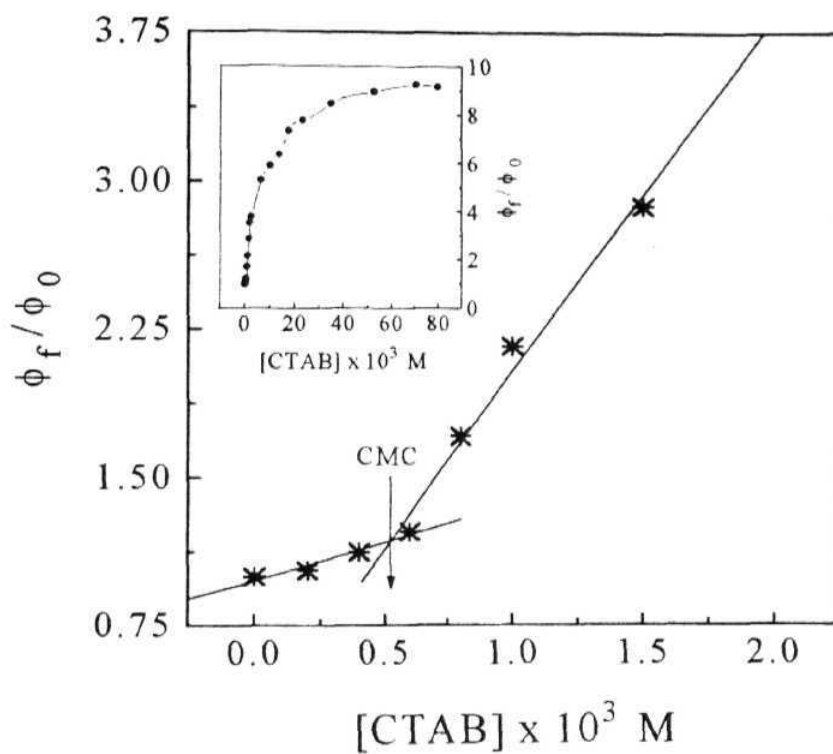
Fig. 5.7. A plot of relative fluorescence intensity of DAPL (ϕ_f/ϕ_0) as a function of CTAB concentration in aqueous solution. The insert shows the variation of the ratio over a larger concentration range.

Table 5.3 Fluorescence Data of DAPL in Micellar Media.

Surfactant	Concentration (mM)	Maximum		CMC (mM)		K^c (M^{-1})	τ_1 (ns) $(R_1)^b$
		ϕ_f / ϕ_0	Shift (nm)	Literature^a	Measured		
SDS	75	7.2	31.0	8.00	7.4	17400	0.56 (97.2)
CTAB	80	9.2	44.5	0.92	0.6	18100	0.34 (98.7)
Triton X-100	128	22.4	54.0	0.26	0.27	24100	0.81 (96.8)

a From ref. [1]. b Calculated using relative amplitude, $R_i = 100 B_i \tau_i \left/ \sum_{k=i}^{2} \left(B_k \tau_k \right) \right.$. c $\pm 10\%$.

5.3.2.2. *Binding Ability*

The binding constants, evaluated from the fluorescence intensity data using equn. 3.3, are given in Table 5.3. A typical plot for this probe based on this equation is shown in Fig. 5.8. Considerably higher K values of DAPL when compared to the native probe, DAP with the respective micelles, suggest that the attachment of the fatty-acid chain help better binding of the probe molecule. A similar observation was also noted for APL. 2-4 folds increase in the binding ability of DAPL over that of APL with the micelles show that former is a better probe than the latter.
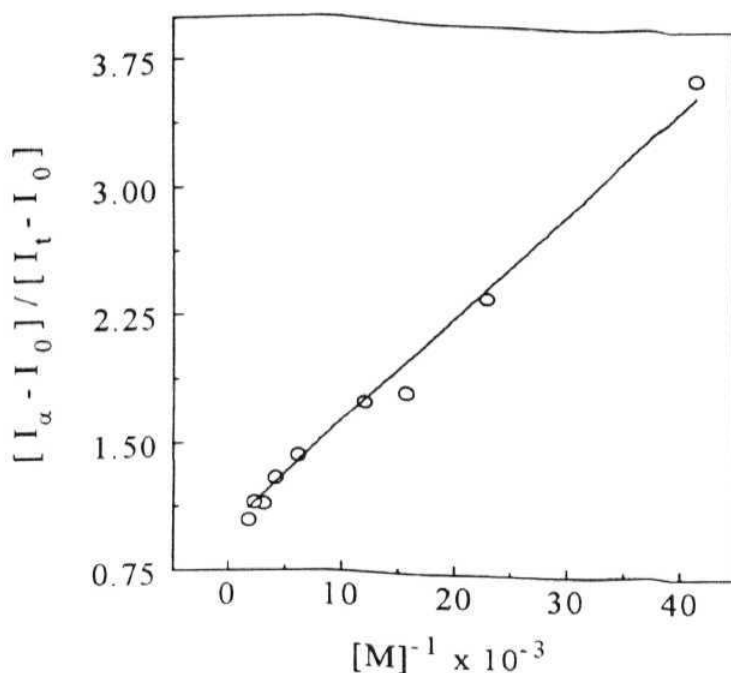
Fig. 5.8. Plot of $(I_\infty - I_0)/(I_t - I_0)$ against $[M]^{-1}$ in Triton X-100 for DAPL. The plot is based on equn. 3.3.

5.3.2.3. Quenching Studies

Quenching studies have been performed in both *aq* and micellar media using aqueous quenchers I^- and Cu^{+2} as they are helpful in determining the location of the probe. The plots of the relative fluorescence intensity against the quencher concentrations were found to be linear, indicating the absence of any

significant static quenching over the quencher concentration range used. The quenching data are tabulated in Table 5.4.

Table 5.4 Quenching Data of DAP and DAPL in Aqueous and Micellar Media.

Probe	Quencher	$k_q{}^a / 10^9 \, M^{-1} \, s^{-1}$			
		H_2O	SDS	CTAB	Triton X-100
DAP	Cu^{+2}	16.2	66	-	2.33
	I-	11.9		118	-
DAPL	Cu^{+2}	18.3	64	-	2.62
	I-	8.1		81.6	-

[a] The uncertainties in k_q values are fairly high as τ_0 values were low and could not be measured accurately with the experimental set-up in this study.

5.3.2.4. Location of DAPL in Micelles

The observed maximum shift and enhancement in micellar media lie between 31-54 nm and 7.2-22.4, respectively. The values are very similar to those obtained for DAP. Therefore, it appears that the DAP moiety of DAPL resides at a site very similar to that resided by the native probe, DAP. The micropolarities estimated for the Solubilisation site of the probe are 56.9, 54.4 and 52.7 (in $E_T(30)$ scale) for SDS, CTAB, and TX, respectively. These values are again very close to the micropolarities sensed by DAP in respective micellar microenvironments.

It can be seen from the quenching data presented in Table 5.4 that both I" and Cu^{+2} are good quenchers of DAP and DAPL fluorescence in *aq* medium. Secondly, the quenching rates of DAP and DAPL with Cu^{+2} and I~ in anionic (SDS) and cationic (CTAB) micelles, respectively, are considerably higher due to high local concentration of the quencher ions near the surface because of electrostatic attraction. In neutral micelles, TX where electrostatic forces are absent, the quenching rate constant is quite lower than that in *aq* medium, suggesting lesser accessibility of probe molecules towards the quenchers. Finally, the similarity of the quenching data of DAPL and DAP clearly suggests that the location of fluorescing moiety in the former is very similar to the later in micelles. Therefore, it is concluded that the binding of DAPL with the micelles is very similar to that of APL (as depicted in Fig. 3.12) i.e. folding of the hydrocarbon chain brings the terminal fluorescing moiety near the surface.

DAPL is proved to be a potential indicator to follow the micellisation process irrespective of the charge of the micelle. In terms of sensitivity, as was expected, dimethylamino derivatives are superior to their amino counterparts. Chain folding appears to be a general phenomenon for AP or DAP fluorophore labelled fatty acids.

5.4. References

1. K. Kalyanasundaram, *Photochemistry in Microheterogeneous Systems*, Academic Press: New York, **1987.**

2. K. Kalyanasundaram In: *Photochemistry in Organised and Constrained Media*, V. Ramamurthy, ed., VCH: New York, **1991,** Chap. 2.

3. K. Bhattacharyya, M. Chowdhury, *Chem. Rev.,* 93, 507, **1993.**

4. K. Lakowicz In: *Principles of Fluorescence Spectroscopy,* Plenum Press: New York, **1983.**

5. J. K. Thomas, *Acc. Chem. Res.,* 10, 133, **1977;** *Chem. Rev.,* **80,** 283, **1980.**

6. N. J. Turro, M. Gratzel, A. M. Braun, *Angew. Chem. Int. Ed. Engl.,* 19, 675, **1980.**

7. F. Griesser, C. J. Drummond, *J. Phys. Chem.,* 92, 5580, **1988.**

8. G. von Bunau, T. Wolff; *Adv. Photochem.,* 14, 273, **1988** and references cited therein.

9. *Micellisation, Solubilisation and Microemulsions,* K. L. Mittal, ed., Vol 1, 2, Plenum Press: New York, **1991.**

10. **R.** G. Weiss, V. Ramamurthy, G. S. Hammond, *Acc. Chem. Res.,* 26, 530, **1993.**

11. *Organic Phototransformations in Microheterogeneous Systems,* M.A. Fox, ed., Academic Press: Washington DC, **1982.**

12 a) J. M. Hicks, M. T. Vandersall, Z. Babarogic, K. B. Eisenthal, *Chem. Phys. Lett.,* 116, 18, **1985;** b) J. M. Hicks, M. T. Vandersall, E. V. Sitzmann, K. B. Eisenthal, *Chem. Phys. Lett.,* 115, 413, **1987.**

13 a) **M.** Maroncelli, G. R. Fleming, *J. Chem. Phys.,* 86, 6221, **1987;** b) W. R. Bergmark, A. Davis, C. York, A. Macintosh, G. Jones II, *J. Phys. Chem.,*

94, 5020, **1990;** c) A. Nag, K. Bhattacharyya, *Chem. Phys. Lett.*, **169,** 12, **1990;** d) M. L. Horng, J. A. Gardecki, A. Papazyan, M. Maroncelli, *J. Phys. Chem., **99,** 17311,* **1995.**

14. T. Soujanya, R. W. Fessenden, A. Samanta, *J. Phys. Chem.,* **100**, 3507, **1996.**

15. A preliminary report on DAPL appeared in : B. Ramachandram, *M. Phil. Dissertation,* University of Hyderabad, **1995.**

16. C. Reichardt, *Solvents and Solvents Effects in Organic Chemistry,* VCH: Weinheim, **1988.**

17. a) F. M. Menger, D. W. Doll, *J. Am. Chem. Soc.*, **106,** 1109, **1984; b)** F. **M.** Menger, *Angew. Chem. Int. Ed. Engl.*, **30,** 1086, **1991.**

18. a) **J.** B. Hayter, J. Penfold, *Colloid Polym. Sci.,* **261**, 1022, **1983;** b) R. Trilo, E. Caponetti, V. Graziano, *J. Phys. Chem.,* **89**, 5743, **1985.**

19 S. S. Berr, E Caponetti, J. S. Johnson, R. M. Jones, L. J. Magid, *J. Phys. Chem.,* **90**, 5766, **1987.**

20 R. S. Sarpal, M. Belletete, G. Durocher, *Chem. Phys. Lett.,* **221,** 1, **1994.**

PHOTOPHYSICAL STUDIES ON TWO CARBOSTYRIL DYES AND N,N'-BIS(4-CARBOMETHOXYPHENYL)PIPERAZINE

The present chapter is divided into two sections. The first section is devoted primarily to the study of the possible role of the rotary decay process on the fluorescence properties of two Carbostyril dyes, C124 and C165. The potential of these systems as fluorescence probes for micellar media is also explored. The following section describes the fluorescence characteristics of a symmetrical molecule, N,N'-bis(4-carbomethoxyphenyl)piperazine as a function of the polarity of the media.

6.1. Photophysical Behaviour of Carbostyrils, C124 and C165

A number of coumarin derivatives which are extensively used as laser dyes, non-linear optical chromophores and fluorescence probes are known to possess a low-lying nonfluorescent twisted intramolecular charge transfer (TICT) state which affects the fluorescence properties of the dyes.[1-3] Since Carbostyrils, C124 and C165 (Chart 6.1), used as laser dyes,[4] are structurally and electronically very similar to the coumarin dyes, Cl and C120 (Chart 6.1), **a** study of the Carbostyrils should reveal whether substitution of the ring **O** atom

by an NH group can have any influence on the Photophysical properties. As an identification of a nonradiative pathway (such as transition to a TICT state) helps the design of more efficient dye systems, we examined whether a rotary decay mechanism plays any role in determining the fluorescence characteristics of structurally similar Carbostyrils. Another point of interest is that both C124 and C165 can exist in tautomeric forms; enol or lactim and keto or lactam form (as shown in Chart 6.1). As 2-hydroxyquinoline is known to exist in two tautomeric forms[5] it is also relevant to study any possible effect of the keto-enol tautomerisation on the Photophysical behaviour of the Carbostyrils.
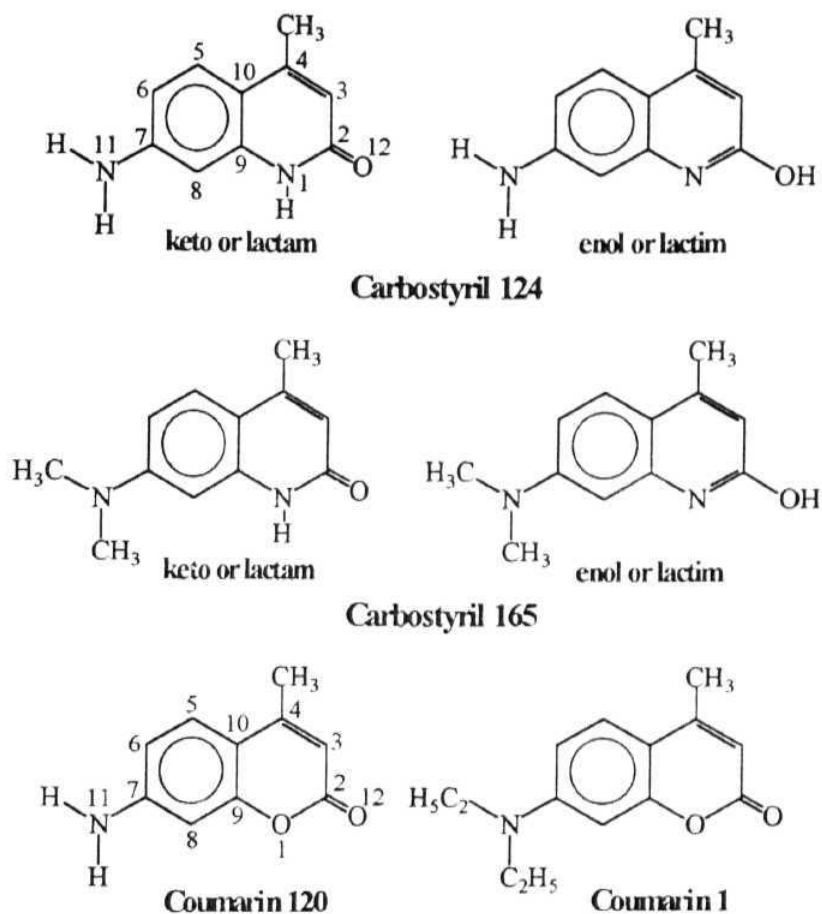
CHART 6.1

6.1.1. Spectral Characteristics

A summary of the absorption and fluorescence spectral data of two compounds is given in Table 6.1. The representative absorption and fluorescence spectra of the two compounds are shown in Figs. 6.1 and 6.2. A loss of the vibrational structure in the spectra along with a red shift of the spectral maxima has been observed with an increase in the polarity of the solvent. As the shift is more pronounced for fluorescence, the emitting state of

169

the Carbostyrils is more polar than the ground state. A comparison of the location of the emission maxima of the two compounds reveals that C165 is more polar than C124, which is understandable in terms of a larger inductive effect of the dimethylamino group. The similarity of the spectral behaviour of the Carbostyrils and the coumarins[1a,c] is a reflection of the structural similarity of the two sets of compounds.
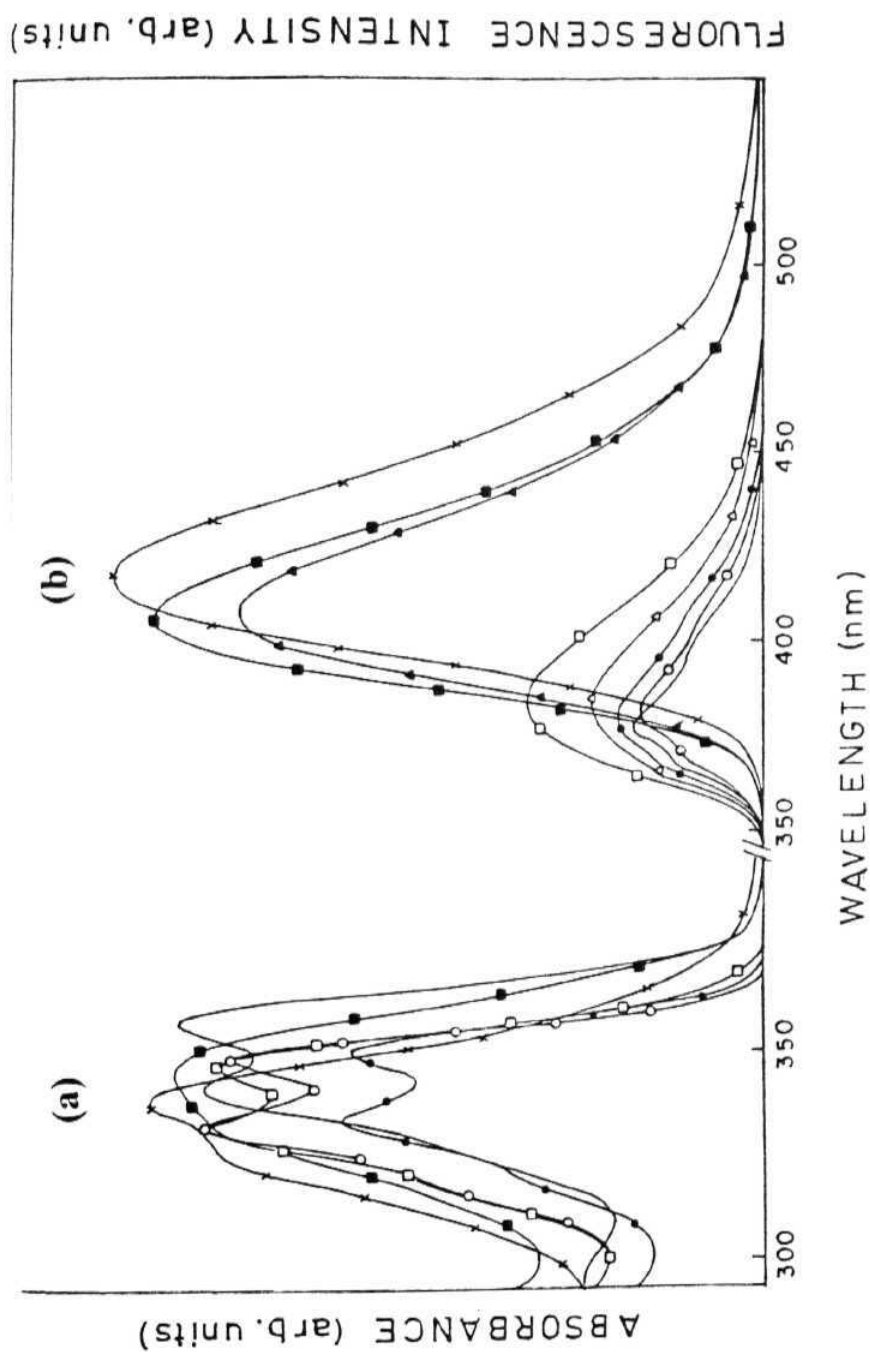
Fig. 6.1. Absorption (a) and fluorescence (b) spectra of C124 in different solvents at room temperature : (——) 1,4-dioxane; (–O–O–) tetrahydrofuran; (–●–●–) ethyl acetate; (–Δ–Δ–) acetone; (–□–□–) acetonitrile; (–▲–▲–) ethanol; (–■–■–) methanol; (–x–x–) water. $\lambda_{exc} = 335$ nm.

171
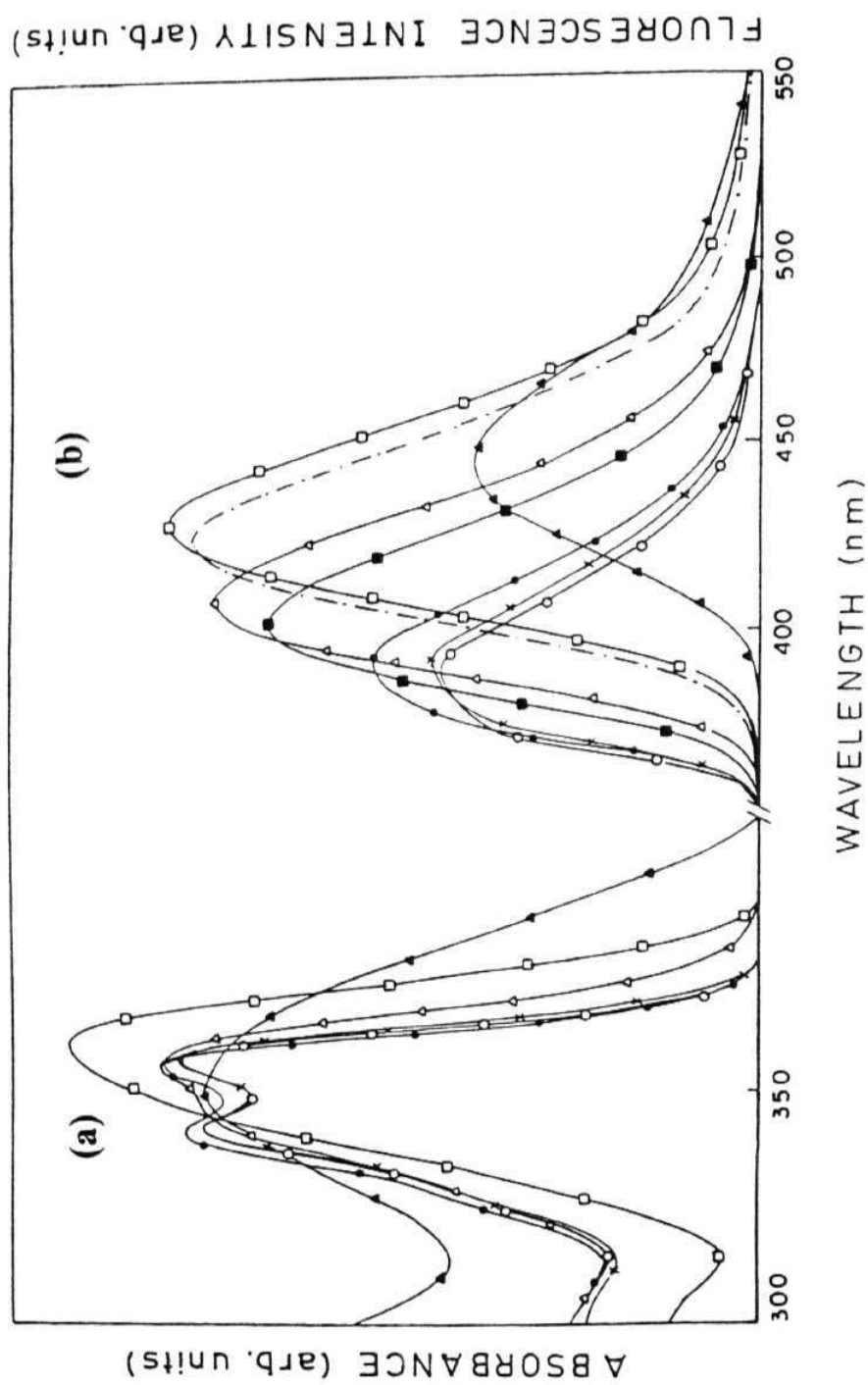
Fig. 6.2. Absorption (a) and fluorescence (b) spectra of C165 in different solvents at room temperature :

(–O–O–) 1,4-dioxane; (–×–×–) tetrahydrofuran; (–●–●–) ethyl acetate; (–■–■–) acetone; (–Δ–Δ–) acetonitrile;

(–•–•–) ethanol; (–□–□–) methanol; (–▲–▲–) water. λ_{exc} = 345 nm.

172

Table 6.1 Absorption and Fluorescence Data of C124 and C165 at Room Temperature in Different Solvents.

Solvent	ε^a	n^a	Δf^b	C124			C165		
				$\bar{\nu}_{abs}^{max}\,(cm^{-1})$	$\bar{\nu}_{flu}^{max}\,(cm^{-1})$	$\Delta\bar{\nu}\,(cm^{-1})$	$\bar{\nu}_{abs}^{max}\,(cm^{-1})$	$\bar{\nu}_{flu}^{max}\,(cm^{-1})$	$\Delta\bar{\nu}\,(cm^{-1})$
1,4-dioxane	2.21	1.4224	0.0205	28604	26455	2149	27972	25706	2266
Ether	4.20	1.3524	0.0285	28571	26455	2116	28011	25873	2138
Chloroform	4.81	1.4459	0.1483	28735	26315	2419	27548	24844	2704
Ethyl acetate	6.02	1.3724	0.1996	28637	26385	2251	28011	25575	2436
Tetrahydrofuran	7.58	1.4072	0.2096	28425	26246	2178	27894	25542	2352
Acetone	20.56	1.3587	0.2841	28571	26075	2495	27933	24937	2995
Ethanol	24.55	1.3614	0.2887	28735	24570	4165	27731	23696	4038
Methanol	32.66	1.3284	0.3086	28985	24539	4445	27700	23474	4226
Acetonitrile	35.94	1.3441	0.3046	28752	26041	2710	27894	24691	3203
Water	78.34	1.3330	0.3199	29377	23952	5425	28490	22573	5917

a From ref. [18]. b As defined in eqn. 2.3. c Excited at 335 nm. d Excited at 345 nm.

6.1.2. Dipole Moment Change on Excitation ($\Delta\mu$)

In order to quantity the polar nature of the excited states of the Carbostyrils we have analysed the solvatochromic data of the two systems in terms of the solvent polarity functions using Lippert-Mataga equn. (sec. 2.1.5). The Lippert-Mataga plots ($\Delta\bar{\nu}$ vs Δf) for the two dyes are shown in Figs. 6.3 and 6.4. The Onsager cavity radius which is needed for the calculation of $\Delta\mu$, is estimated from the AM1 optimised distance between the amino nitrogen (N-11) and the carbonyl oxygen (0-12), which corresponds to the maximum distance across which charge separation occurs. This choice is based on a recent publication[6] in which it is shown that the length of the alkyl group attached to the amino group is unimportant in determining the dipole moment. The estimated radii are 3.565 and 3.575 A for C124 and C165, respectively. As can be seen from the plots that although the data points in aprotic solvents are correlated to the polarity function, in hydroxylic solvents Stokes shifts are much larger than that predicted by the Lippert-Mataga equn. This is indicative of a specific solute-solvent interactions. It has been recently reported that the hydrogen bonding interaction is primarily responsible for the enhanced Stokes shift in alcoholic solvents and water.[7] In view of this, the $\Delta\mu$ values have been estimated from the data collected in aprotic solvents. The dipole moment data of the Carbostyrils and the coumarins are collected in Table 6.2 for both the ground and excited states

174
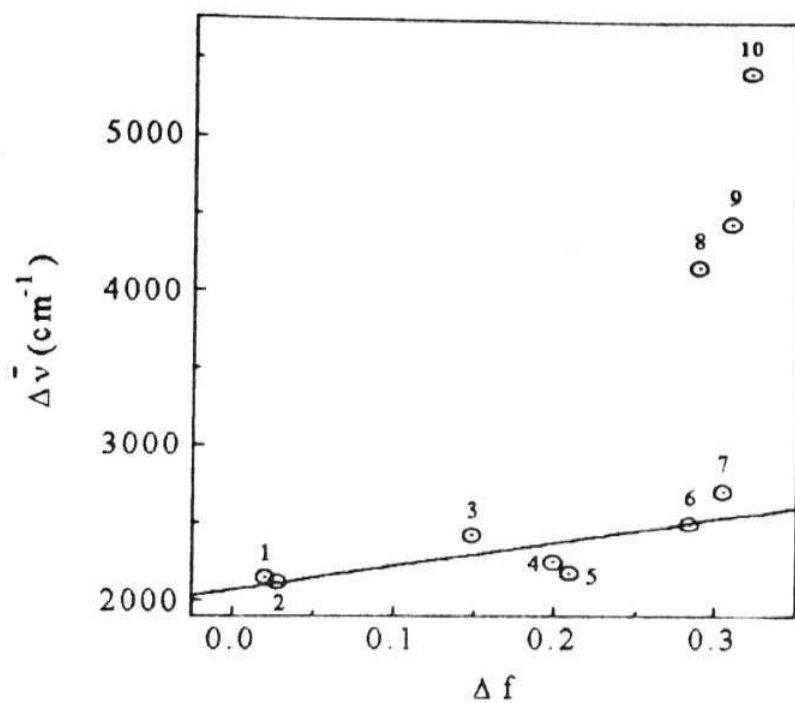
Fig. 6.3. Dependence of the Stokes shift ($\Delta\bar{\nu}$) of C124 on the solvent polarity function Δf (sec. 2.1.5) according to the Lippert-Mataga equn. (equn. 2.3). The solvents are 1. 1,4-dioxane; 2. diethyl ether; 2. chloroform; 4. ethyl acetate; 5. tetrahydrofuran; 6. acetone; 7. acetonitrile; 8. ethanol; 9. methanol and 10. water. The straight line represents the best fit to the data collected only in the aprotic solvents.

175
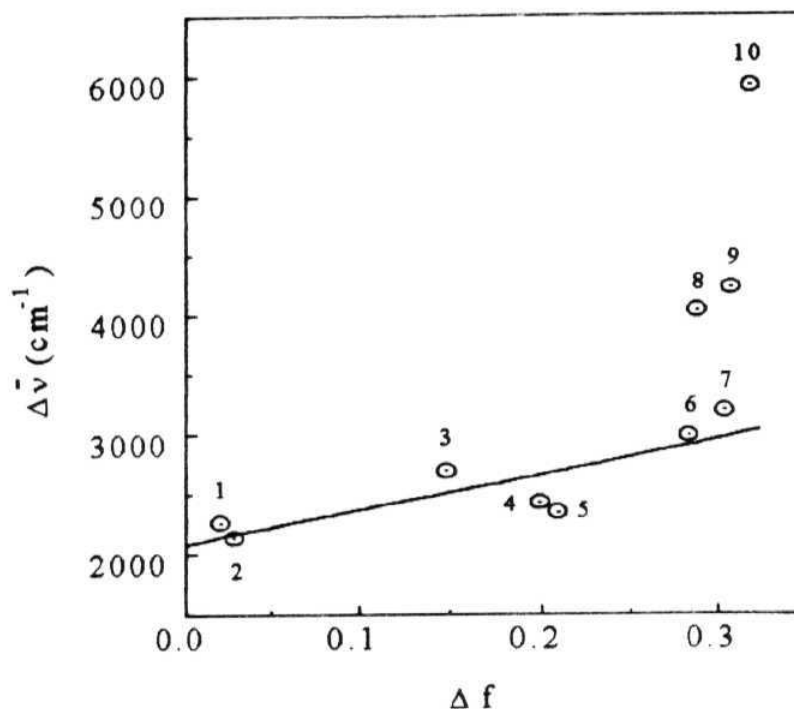
Fig. 6.4. Dependence of the Stokes shift ($\Delta\bar{\nu}$) of C165 on the solvent polarity function Af (sec. 2.1.5) according to the Lippert-Mataga equn. (equn. 2.3). The solvents are 1. 1,4-dioxane; 2. diethyl ether; 3. chloroform; 4. ethyl acetate; 5. tetrahydrofuran; 6. acetone; 7. acetonitrile; 8. ethanol; 9. methanol and 10. water. The straight line represents the best fit to the data obtained in the aprotic solvents.

176

The changes in the dipole moments, 2.63 D for C124 and 3.69 D for C165 are similar to the reported $\Delta\mu$ values of coumarins; 2.61,[1c] 2.16 D[8] for the amino derivative and 3.72[1c], 3.46 D[8] for the dimethylamino derivative. A close similarity of the $\Delta\mu$ values of the coumarins and Carbostyrils indicates that neither the ring oxygen of the coumarins nor the NH group of the Carbostyrils are involved in the charge separation process. This conclusion is further substantiated by the theoretical calculations of the charge densities at different atoms of the two systems (sec. 6.1.5).

Table 6.2 Dipole Moments of the Carbostyrils in the Ground and Excited States.

Compound	Dipole moment or Dipole moment changes		
	μ_g (AM1)(D)	$\Delta\mu$ (expt.) (D)	μ_e (D)
C124	5.78	2.63	8.41[a]
C165	5.99	3.69	9.68[a]
C120	6.03	—	8.19[b]
C1	6.35	—	9.81[b,c]

[a] Values obtained from AM1 calculated μ_g and experimental $\Delta\mu$. [b] Theoretical values taken from ref. [8]. [c] Values reported are for 4-methyl-7-N,N-dimethylaminocoumarin (instead of the ethyl group as in the case of C165).

6.1.3. Role of Keto-Enol Tautomerism

As stated earlier, unlike the coumarins the Carbostyrils can exist in two tautomeric forms. Mason et al examined the keto-enol tautomerism of several hydroxyquinoline derivatives and concluded that the enol form contributes to the absorption spectra.[9] Recently, the absorption and fluorescence of both the forms of 2-hydroxyquinoline have been detected in a supersonic jet expansion experiment.[5] While exploring the lasing potential of the Carbostyrils, the keto form was assumed to be predominant by Hammond et al.[10] However, no rationale of such a proposition was forwarded. Although a close similarity of the fluorescence behaviour of the Carbostyrils and coumarins possibly indicates an insignificant contribution of the enol form in the excited state, it is not clear whether the enol form contributes to the absorption. One point to be noted is that despite the presence of the enol form in the ground state, the keto form could be the only excited state species in view of an enhancement of the acidity of the -OH group and the basicity of the ring nitrogen in the excited state.[11] In order to find out any possible contribution of the enol form in the ground state we carefully examined the absorption spectra of the Carbostyrils in a large number of solvents of different polarity. Assuming the keto-enol equilibrium to be solvent dependent, it was expected that a change in the polarity of the solvent would lead to a variation of the relative intensity distribution of the peaks. However, apart from a general loss of the spectral resolution with increase in the polarity (which could be due to an enhancement of the charge transfer character

of the state), we did not observe any noticeable variation in the spectral pattern that might suggest the presence of more than one form in the ground state. We also studied the temperature dependence of the absorption spectra in the temperature range 268-323 K. However, no variation in the intensity distribution could be observed as function of the temperature. The predominance of the keto form in the ground state is also supported by the results of theoretical calculations based on AM1 method (sec 6.1.5).

6.1.4. *Fluorescence Quantum yields (fa) and Lifetimes* (τ_f)

The *fa* and τ_f values of the dyes in various solvents have been collected in Table 6.3. It is seen that C165 is more fluorescent than C124 and the *fa* values of both the compounds increase with increasing polarity. The measured τ_f values also show a similar trend. The fluorescence lifetime of C124 is almost half of that for C165 in non-polar media.

Table 6.3 Fluorescence Quantum yield and Lifetime of the Carbostyrils.

Solvent	ϕ_f		τ_f (ns)	
	C124	C165	C124	C165
1,4-dioxane	0.13	0.36	0.5	1.3
Ether	0.15	0.35	—	—
Chloroform	0.13	0.27	—	—
Ethyl acetate	0.16	0.45	—	—
Tetrahydrofuran	0.13	0.37	0.6	1.4
Acetone	0.20	0.66	—	—
Acetonitrile	0.30	0.79	1.4	3.2
Ethanol	0.54	0.85	—	—
Methanol	0.68	0.90	3.8	4.4

Although the spectral data of the coumarins and Carbostyrils are very similar, the variation in ϕ_f and τ_f of the Carbostyrils is in contrast to that for the corresponding coumarins. It has been observed that ϕ_f of Cl falls off significantly with increasing polarity.[1a] The ϕ_f of Cl (which resembles C165) drops from 0.99 in ethyl acetate to 0.055 in H_2O indicating a drastic enhancement of the nonradiative rate in polar media. This has been interpreted in terms of a polarity dependent change in the rate of the nonradiative transition to a non-emissive TICT state.[1a] The enhancement of fc and τ_f of both C124

and C165 with increasing solvent polarity suggests the absence of a rotary decay pathway in these systems. The alkylation of the amino group is known to stabilise the TICT state relative to the locally excited state and lower the barrier involved in the twisting process.[12] Therefore, one should have expected the rotary decay of the emitting state in C165, more so, because of its structural similarity with C1.

6.1.5. Theoretical Study

6.1.5.1. Keto-Enol Tautomerism

In order to account for the contrasting behaviour of two sets of compounds and obtain supportive data on the charge distribution and a dominant lactam form of the Carbostyrils, AM1 calculations have been performed. The ground state calculations have been performed for fully optimised keto and enol forms of C124 and C165 and the corresponding derivatives without the amino or the dimethylamino group (4-methyl-2-hydroxyquinoline and 4-methyl-2-quinolone) and the results are presented in Table 6.4. It can be seen from the Table that substitution at the 7-position by an amino or a dimethylamino group stabilises the keto form relative to the enol form. In carbostyrils, keto forms are more stable than the enol forms by $\approx$ 6.3 kcal/mol. Since this stabilisation is found to be more than that in 7-unsubstituted compounds by nearly 1 kcal/mol, the contribution of the enol form in carbostyrils can be said to be insignificant.

Table 6.4 AM1 Calculated Heats of Formation (in kcal/mol) of Some Carbostyril Derivatives.

Compound	Keto form	Enol form	ΔH_0 of Tautomerisation
7-unsubstituted compound	-4.125	1.180	5.305
C124	-6.107	0.213	6.320
C165	4.207	10.461	6.254

6.1.5.2. Ground State Charge Distribution

The ground state charge distributions of the coumarins and Carbostyrils have also been calculated and shown in Fig. 6.5. It can be seen the substitution of the ring oxygen of the coumarin by an NH group does not significantly affect the electron densities at other centres. It is particularly interesting to note that the charge densities of the two centres primarily responsible for charge separation in these compounds, N-11 and O-12 (Chart 6.1), are changed only by 0.006 e and 0.066 e, respectively, on substitution. This further validates our conclusion that the charge distribution of the two sets of compounds are very similar.

Coumarin 120   **Carbostyril 124**
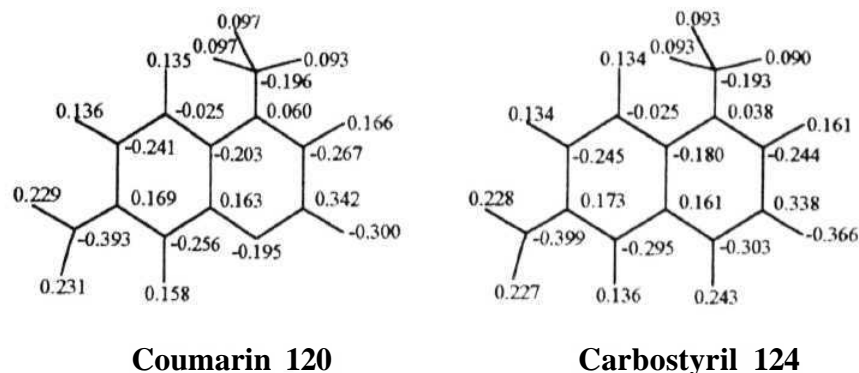
Fig. 6.5. Calculated atomic charges (in decimal fractions of an electronic charge) for C120 and C124 in the ground state.

6.1.5.3. *Ground and Excited State Properties*

In order to rationalise the difference in behaviour of the coumarins and Carbostyrils with respect to the twisting of the amino or the dimethylamino group, AM1 calculations of the ground and excited states of Carbostyrils have been carried out as a function of the twist angles. The suitability of this method in predicting the ground and excited state properties of large polar systems is well-documented.[8] Recently, it has been shown[13,14] that AM1 calculated properties of DMABN, a molecule extensively studied for the TICT phenomenon, are in excellent agreement with the experimental results. The ground and excited state properties, namely, the heats of formation (AHf), and the dipole moment values (D), obtained from complete optimisation of each molecule at various twist angles, are summarised in Tables 6.5 and 6.6, for C124 and C165, respectively. The variation of the ground and excited state energy as

a function of the twist angle of the amino or dimethylamino group is depicted in Figs. 6.6 and 6.7, respectively.

Table 6.5 The Ground and First Excited Singlet State Properties of C124 as a Function of the Twist Angle.

Twist angle	Ground state		Excited state	
ΔH_f (Deg)	ΔH_f (kcal mol$^-$	μ_g (D)	ΔH_f (kcal mol$^-$	μ_e (D)
0	-5.817	5.78	74.11	6.19
10	-5.551	5.74	74.34	6.13
20	-4.784	5.63	75.01	6.01
30	-3.606	5.48	76.04	5.79
40	-2.156	5.28	77.29	5.54
50	-0.610	5.06	78.66	5.26
60	-0.843	4.84	80.00	4.94
70	2.029	4.67	81.21	4.54
80	2.801	4.55	82.09	4.13
90	3.069	4.51	82.43	3.93

Table 6.6 The Ground and First Excited Singlet State Properties of C165 as a Function of Twist Angle.

Twist angle	Ground state		Excited state	
	ΔH_f	μ_g	ΔH_f	μ_e
(Deg)	(kcal mol$^-$	(D)	(kcal mol$^-$	(D)
0	4.580	5.99	84.05	6.84
10	4.631	5.93	84.06	6.79
20	4.897	5.77	84.19	6.66
30	5.531	5.53	84.66	6.46
40	6.531	5.23	85.42	6.25
50	7.725	4.93	86.37	6.14
60	8.935	4.69	87.35	6.12
70	10.008	4.49	88.53	5.89
80	10.786	4.35	89.81	4.85
90	11.264	4.57	90.64	3.93
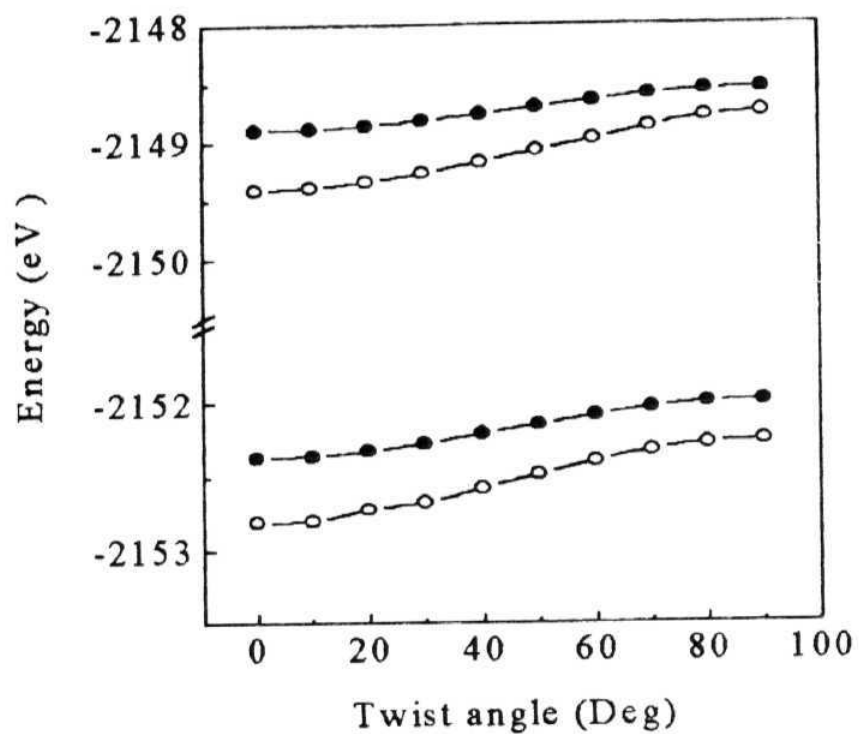
Fig. 6.6. Plot of the ground and lowest excited singlet state energies of C124 as a function of the twist angle of the amino group with the adjoining ring in the gas phase (•) and in acetonitrile (O).
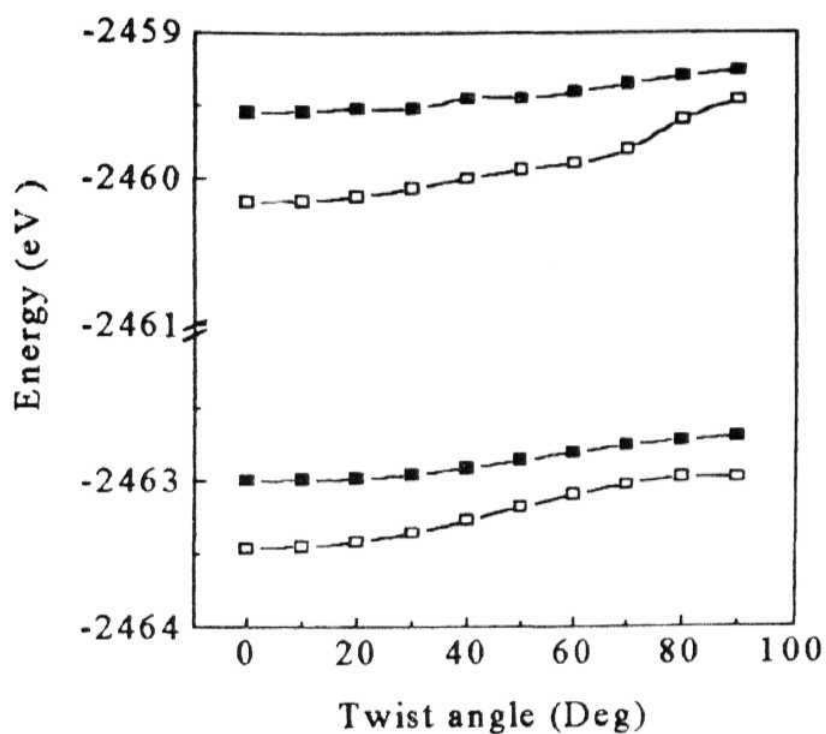
Fig. 6.7. Plot of the ground and lowest excited singlet state energies of C165 as a function of the twist angle of the amino group with the adjoining ring in the gas phase (•) and in acetonitrile (□)

It is evident from the figures that the planar form is most stable for both the compounds. The gas phase energy differences between the 90° twisted form and the planar one in the ground sate are 0.39 and 0.29 eV for C124 and C165, respectively. As the energy gap is much higher than the available thermal energy

187

at room temperature (0.026 eV at 27°C) the planar form is expected to be predominant in the ground state. The twisting in the excited state involves barriers of 0.36 and 0.28 eV, respectively, in the gas phase. Therefore, the barriers to twisting do not change significantly on electronic excitation. Further, as seen from the energy profiles in acetonitrile (calculated using equn. 2.9), the twisting becomes more difficult in polar media. These results suggest an unfavourable energetics for the rotary decay process in Carbostyrils both in the ground and excited states.

Two sets of molecules with similar structure and electron distribution behaving differently with respect to twisting is rather unusual. Since the rotary decay is governed by the energetics of the excited state, one expects the relative spacing and ordering of the energy states of the coumarins (Cl, in particular) to be different from those in Carbostyrils. However, a recent study on coumarins suggests that twisting of the a dialkylamino group in Cl is unfavourable.[8] In a more recent paper, Rechathaler and Kohler concluded that the rotary decay process in coumarins is significant only when the methyl hydrogens at C4 are replaced by electronegative fluorine atoms.[1c] There has been an instance when dual amplified spontaneous emission has been reported for C1[15] and C120[16] in polar solvents, but this was later disproved.[17] Thus we are led to conclude that as far as twisting in the excited state is concerned, the behaviour of Carbostyrils and coumarins should be similar. We believe that the reduction of ϕ_f of C1 in water, which was considered as an evidence of TICT decay[1a], is actually due to

the specific hydrogen bonding interaction of the probe and the solvent molecules. On careful examination of the data of Cl presented in ref. la, one finds no reduction of ϕ_f with increase in the polarity of the solvents in aprotic media. Therefore, the present results suggest that further studies on coumarins, Cl in particular, taking into consideration of the hydrogen bonding effect, is necessary. It is shown clearly that the rotation of the amino or dimethylamino group of the Carbostyrils does not play any significant role in determining the fluorescence yield and lifetimes of the compounds.

6.]. 6. Likely Application of Carbostyrils in Studying the Organised Media

In view of the solvent sensitive fluorescence response of the Carbostyrils we thought that it might be appropriate to examine the potential of the Carbostyrils as probe molecules for the organised media. The results of the preliminary investigation carried out with C165 and C124 in SDS and CTAB micelles are not very encouraging and hence, no studies were attempted in Triton-X.

The absorption spectra of C165 in *aq* SDS are shown in Fig. 6.8. Increase in surfactant concentration leads to a small shift of the absorption band indicating the passage of the probe molecules into a less polar micellar environment. A similar observation has been made in CTAB micelles. The absorption spectral behaviour of C124 in SDS and CTAB is quite similar to that
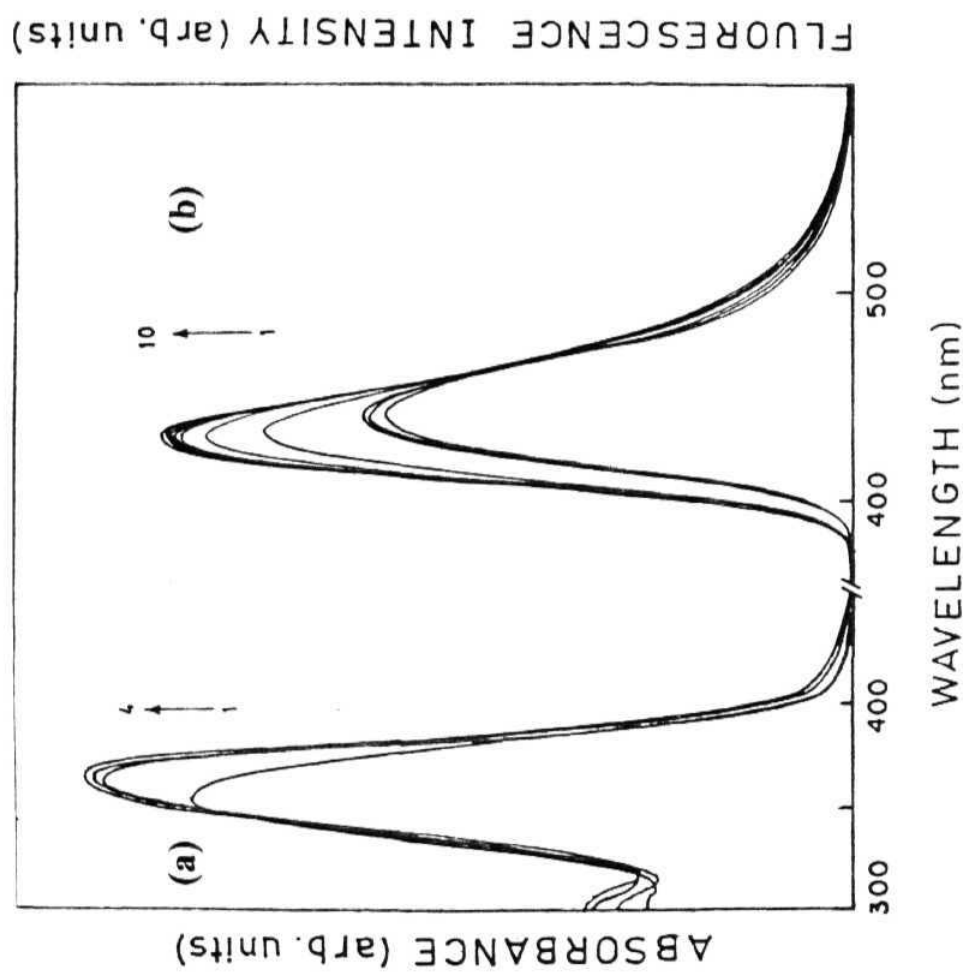
Fig. 6.8. Absorption (a) and fluorescence spectra (b) of C165 in aqueous solution with different amounts of SDS. The concentrations of SDS (mM) are (a) for spectra labelled 1 - 4 are 0, 5.6, 60, 98 respectively; (b) in increasing order of intensity, 0, 2.0, 5.6, 9.2, 13, 16, 22, 27, 60, 98, respectively. $\lambda_{exc} = 340$ nm.

190

The fluorescence spectra of C165 as a function of SDS concentration is shown in Fig. 6.8 The fluorescence intensity and the position of the fluorescence maximum remain constant initially. Beyond a certain concentration of the surfactant, the fluorescence intensity starts increasing with a blue shift of λ_{flu}^{max}. At very high SDS concentration, as expected, the saturation values are reached. The plot of the variation of the relative fluorescence intensity as a function of SDS concentration for C165 is shown in Fig. 6.9. The inflection point corresponds to the CMC. The changes in spectral data of C165 in the presence of micelles, the measured CMC values and the binding constants with the micelles (calculated using equn. 3.3) are given in Table 6.7. A good agreement of the measured CMC values with the literature values of the micelles has been observed.
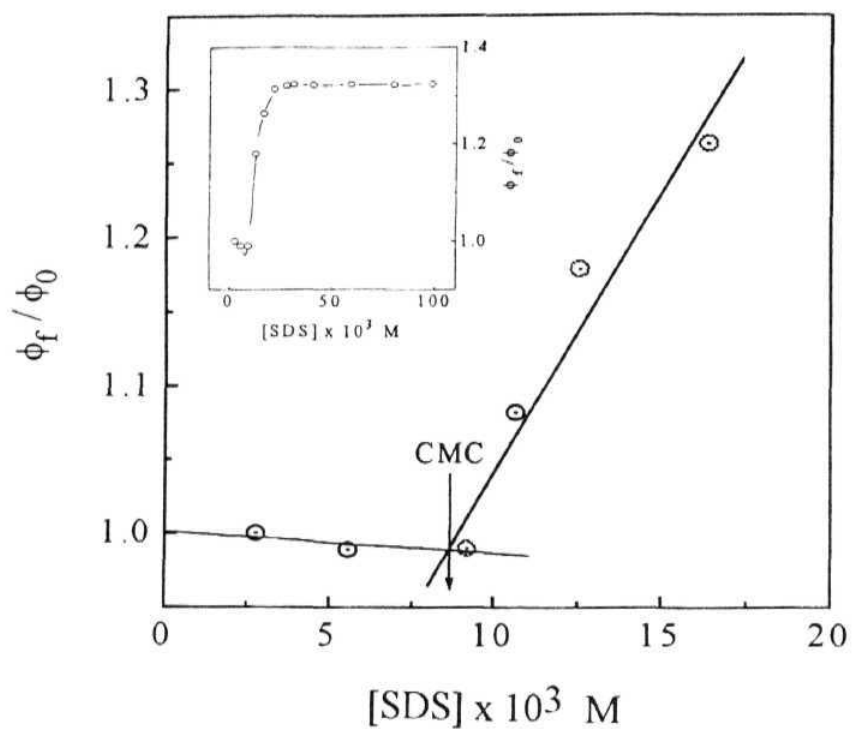
Fig. 6.9. A plot of ϕ_f/ϕ_0 of C165 against SDS concentration in aqueous medium. The insert shows the variation of the ratio over a larger concentration range.

Table 6.7 Fluorescence Spectral Data, Estimated CMC Values and Binding Constants of C165 in Aqueous Micelles.

Surfactant	Concentration (mM)	Maximum		CMC (mM)		Binding constant (M^{-1})
		Enhancement	Shift (nm)	Literature[a]	Measured	
SDS	79	1.32	11	8.00	8.5 ± 0.5	21300 ($\pm$2000)
CTAB	56	1.14	12.5	0.92	0.84 ± 0.06	51600 ($\pm$5000)

a From ref. [20]

193

The maximum shift of the fluorescence maximum observed for C124 at very high concentration surfactant concentrations is relatively lower; 6 and 6.5 nm in SDS and CTAB, respectively. The fluorescence enhancement was not high enough to allow the measurement of CMC values or the binding constants with any reasonable accuracy. However, the CMC values of the micelles could be determined from the variation of λ_{flu}^{max} of C124 for SDS and CTAB are (8i5 ± 0.5) x 10^{-3} M and (0.92 ± 05) x 10^{-3} M, respectively.

The changes in the fluorescence properties of both the dyes in aqueous solutions of surfactants suggest the binding of the Carbostyrils to a relatively less polar micellar site than the bulk aqueous phase. The spectral shift and enhancement values of C165 in *aq* micelles show that the probe molecule is bound to a site which is more polar than MeOH but less polar than the *aq* phase. The estimated polarities of the binding sites of C165 are 58.1 and 57.4 (in $E_T(30)$[18] scale) for SDS and CTAB, respectively. A lower surface polarity obtained for CTAB than SDS is consistent with the literature.[19] The data obtained for C124 could not be analysed precisely to estimate the polarity values of the binding sites because the surfactant induced changes were rather small.

The results presented above although show that the Carbostyrils are capable of following micellisation, the fact that changes in the fluorescence properties are rather small do not make them very promising candidates.

6.2. Study of N,N'-bis(4-Carbomethoxyphenyl) piperazine

There has been a report on N,N'-bis(4-cyanophenyl)piperazine (BCCPZ, Chart 6.2), essentially a dimer of dimethylaminobenzonitrile (DMABN), that it displays fluorescence[-^] very similar to the long-wavelength fluorescence band of DMABN. Further, it is interesting to note that even though the excited state dipole moment of BCCPZ is expected to be less than that of the TICT state of DMABN (because of partial cancellation of moments in *Acceptor-Donor-Spacer-Donor-Acceptor* configuration of the molecule) the measured excited state dipole moment of BCCPZ is reported to be more than that of the TICT state of DMABN.[22] In order to find out whether other derivatives of this class show similar behaviour. we have examined the fluorescence behaviour of the symmetrical, molecule N,N'-bis(4-carbomethoxyphenyl)piperazine (BIMBP, Chart 6.2).
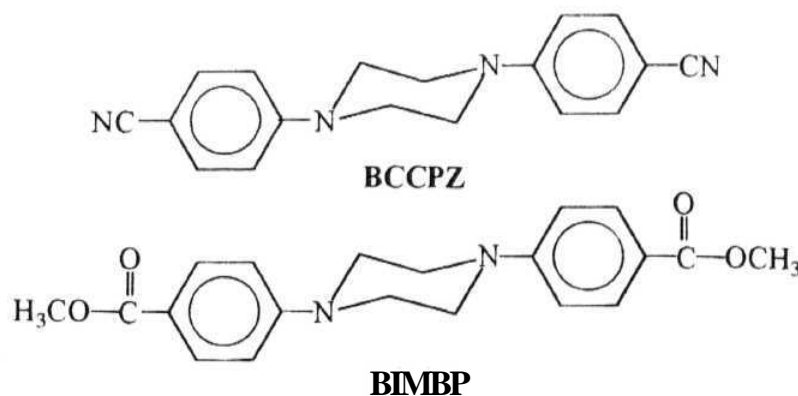
CHART 6.2

6.2.1. *Structure of the Molecule*

The molecular structure of BIMBP as determined by X-ray crystallography, is shown in Fig. 6.10. The structure of this molecule is found to
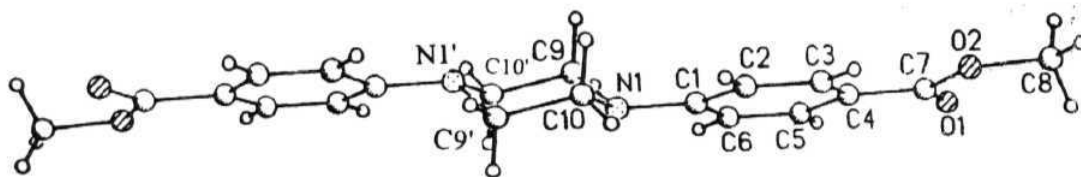
Fig. 6.10. Molecular structure of BIMBP. The atoms with a prime are related to those without prime through the inversion center.

very similar to that reported for BCCPZ.[21] The two protons of the piperazine have been replaced by 4-carbomethoxyphenyl group and the piperazine is shown to adopt a chair conformation. The two halves of the molecules are related by a crystallographic centre of symmetry; hence the phenyl rings can be said to be parallel. The nitrogens are seen to be slightly above the planes of the respective phenyl rings and can be described as flattened pyramid as in the case ofBCCPZ. The important bond lengths and angles are shown in Table 6.8.

Table 6.8 Some Selected Distances and Angles in the Molecular Structure of BIMBP (estimated standard deviations in parentheses referring to the last digit).

Distances (A)		Angles (deg)	
N(1)-C(1)	1.404(3)	C(1)-N(1)-C(9)	116.4 (2)
N(1)-C(9)	1.464(3)	C(1)-N(1)-C(10)	117.8 (2)
N(1)-C(9)	1.457(3)	C(10)-N(1)-C(9)	110.3 (2)
C(10)-C(9)# 1ᵃ	1.502(3)	C(2)-N(1)-C(10)	122.5(2)
C(9)-C(10)# 1	1.502(3)	N(1)-C(10)-C(9)# 1	111.7 (2)
		N(1)-C(9)-C(10)# 1	112.2 (2)

ᵃ Refer to the appendix. Table 3.

6.2.2. Spectral Features of BIMBP

The representative absorption and emission spectra are shown in Fig. 6.11 and the spectral data in various solvents are given in Table 6.9. That the emitting state of the molecule is more polar than the ground state is evident from large Stokes shift of the fluorescence maximum. Further, large Stokes shift between the λ_{abs}^{max} and λ_{flu}^{max} in any given solvent is indicative of the fact that emission originates from a low-lying state that is different from the locally excited (LE) state. The solvent polarity dependent shift of the emission maxima and a comparison of the fluorescence data of BIMBP and DMABN[23] indicate that the emission takes place from a highly polar state, which could be either a
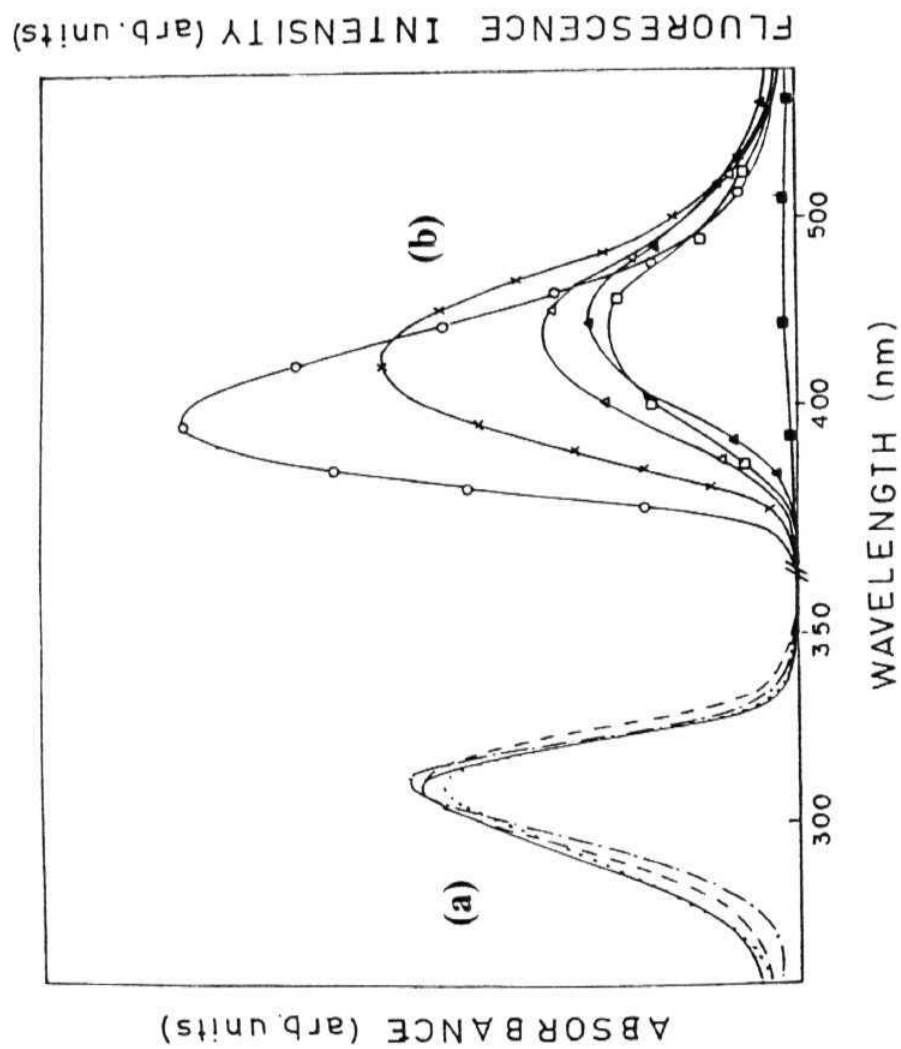
Fig. 6.11. Absorption (a) and fluorescence (b) spectra of BIMBP in various solvents at room temperature: (a) (——) 1,4-dioxane; (·····) tetrahydrofuran; (-·-·-) dichloromethane; (-·-·-) acetonitrile; (b) (-○-○-) toluene; (-×-×-) 1,4-dioxane; (-△-△-) tetrahydrofuran; (-□-□-) dichloromethane; (-▲-▲-) ethyl acetate; (-■-■-) acetonitrile. $\lambda_{exc} = 300$ nm.

Table 6.9 Absorption and Fluorescence Spectral Data of BIMBP at Room Temperature in Different Solvents.

Solvent	ε^a	$f - \frac{1}{2}f'^b$	$\bar{\nu}_{abs}^{max}$ (cm^{-1})	$\bar{\nu}_{flu}^{max\,c}$ (cm^{-1})	ϕ_f	τ_f	k_{nr} (10^7 s^{-1})
Toluene	2.38	0.1264	32563	25381	0.240	4.6	16.4
1,4-dioxane	2.21	0.1219	32573	23557	0.180	5.9	13.8
Tetrahydrofuran	7.58	0.3094	32573	22624	0.110	4.8	18.3
Ethyl acetate	6.02	0.2923	32573	22650	0.080	3.8	23.6
Dichloromethane	8.93	0.3188	32573	22371	0.090	4.2	21.5
Acetonitrile	35.94	0.3919	32468	21299	0.004	0.6	169.4

a Taken from ref. [18]. b As defined in sec. 2.1.5. c Excited at 310 nm.

199

TICT state[23] or a state involving more pyramidal nitrogen (PICT).[24] The similarity of the spectral behaviour of BCCPZ and BIMBP also points to the same conclusion. The measured ϕ_f and τ_f of BIMBP are also indicated in Table 6.9. It can be seen that with increase in polarity of the medium both ϕ_f and τ_f decrease. This is indicative of an enhancement of the nonradiative rate with increase in polarity of the medium.

6.2.3. Excited State Dipole Moment

In order to establish the nature of the emitting state (whether LE or TICT) the excited state dipole moment of BIMBP has been estimated from the fluorescence spectral data, using the equn. 2.4. The use of the this equation over the commonly used Lippert-Mataga equn. for the measurement of the excited state dipole moment is based on the fact that the emitting state in the present case can not be directly populated and hence it resembles more the emitting state of exciplexes.[23b, 25] The plot of $\bar{\nu}_f$ vs $(f - \frac{1}{2}f')$ is shown in Fig. 6.12, from the slope of which μ_e of BIMBP has been calculated. We adopted the following procedure to obtain a reasonable estimate of the Onsager cavity radius of BIMBP for the estimation of μ_e using equn. 2.4. Since the dipole moment of the BCCPZ has been determined by time-resolved microwave conductivity method that is considered to be accurate,[22] we have analysed first the fluorescence spectral data of BCCPZ in terms of equn. 2.4 to determine the representative cavity radius for BCCPZ. Such an analysis (using μ_e of 16D)[22] leads to a cavity radius of 6.94 A that corresponds closely to **the** distance

between one of the piperazine ring nitrogen to the terminal nitrogen atom of the cyano group (6.82 A) of the fully optimised (AM1) ground state of BCCPZ. Therefore, μ_e of BIMBP is estimated using the distance between the ring nitrogen to the terminal carbon atom of the -OCH3 group.
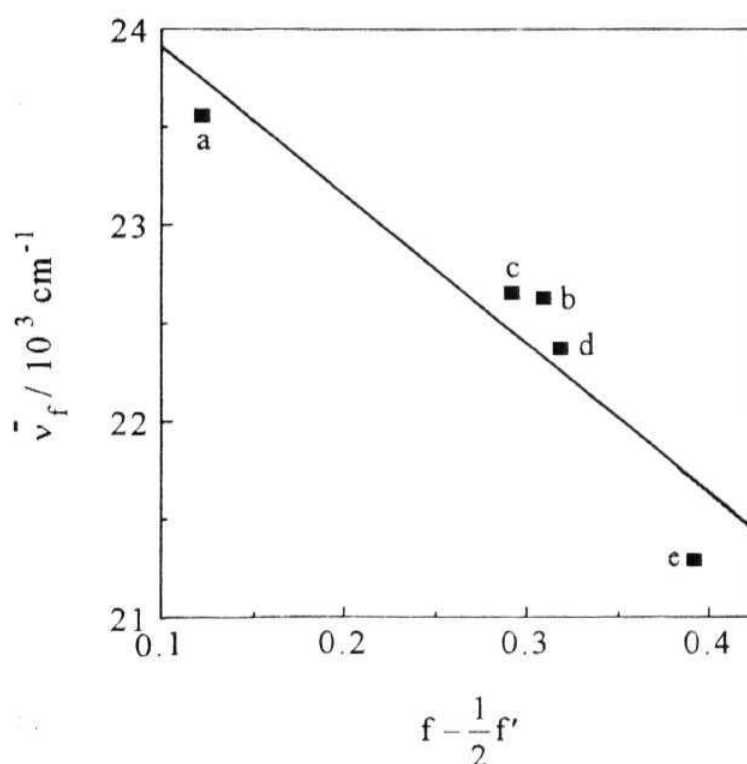
Fig. 6.12. Variation of $\overline{\nu}_f$ (cm^{-1}) of BIMBP as a function of the solvent polarity function $(f - \frac{1}{2}f')$(sec. 2.1.5) according to equn 2.4. a. 1,4-dioxane; b. tetrahydrofuran; c. ethyl acetate; d. dichloromethane and e. acetonitrile.

From the plot based on equn. 2.4 (Fig. 6.12), μ_e of BIMBP is obtained as 18.9 D. Thus the excited state dipole moment of BIMBP is quite similar to that of BCCPZ. Even though the value may not be accurate, it clearly suggests that the emitting state of BIMBP is more polar than the TICT[23] or PICT[24] state of DMABN. The ground state dipole moment of BIMBP, as is evident fInfrrn the crystal structure or AM1 calculated (0.64 D) structure is close to zero, indicating the cancellation of the dipole moments of the two halves of the molecule. Obviously, if the chair form of the piperazine ring is retained in the excited state, a dipole moment larger than that of the TICT of DMABN can not be explained. The structural restraints in the present system do not allow a twist of dialkylamino group, as commonly observed for this class of systems. Even if it is assumed that one of the carbomethoxyphenyl moieties twists relative to the rest of the molecule, the resulting dipole moment of BIMBP in the excited state would be less than that of DMABN because of partial cancellation of the dipole moment. Therefore, a structural change of the piperazine ring (most likely from a chair to a boat transformation) takes place in the excited state.

6.3. **References**

1. a) G. Jones II, W. R. Jackson and C. -Y. Choi, W. R. Bergmark, *J. Phys, Chem.*, <u>89</u>, 294, **1985;** b) J. A. V. Gompel, K. B. Schuster, *J. Phys. Chem.*, <u>93</u>, 1292, **1989;** c) K. Rechthaler, G. Kohler, *Chem. Phys.,* <u>189</u>, 99, **1994**.

2. B. B. Raju, *J. Phys. Chem.,* <u>101</u>,981, **1997.**

3. T. L. Arbeloa, F. L. Arbeloa, M. J. Tapia, I. L. Arbeloa, *J. Phys. Chem.*, 97, 4704, **1993.**

4. a) M. Maeda, In: *Laser dyes*, Academic Press: New York, **1984;** b) J. M. Yarborough, *Appl. Phys. Lett.*, 24, 629, **1974;** c) J. B. Marling, J. G. ftawley, E. M. Liston, W. B. Grant, *Appl Optics*, 13, 2317, **1974.**

5. M. R. Nimlos, D. F. Kelly, E. R. Bernstein, *J. Phys. Chem.*, 91, 6610, **1987.**

6. S. Mukherjee, A. Chattopadhay, A. Samanta, T. Soujanya,./. *Phys. Chem.*, 98, 2809, **1994.**

7. R. Nakagaki, N. Kitamura, I. Aoyama, H. Ohtsubo, *J Photochem. Photobiol,* 80, 113, 1994.

8. P. K. McCarthy, C. J. Blanchard, *J. Phys. Chem.,* 97, 12205, **1993.**

9. S. F. Mason, *J. Chem. Soc,* 5010, **1957.**

10. P. R. Hammond, A. N. Fletcher, R. A. Henry, R L Atkins, *Appl Phys.,* 8, 311, 1975.

11. J. F. Ireland, P. A. H Wyatt, *Adv. Phys. Org. Chem.,* 12, 131, **1976.**

12. W. Rettig, V. Bonancic-koutecky, *Chem. Phys. Lett.,* 62, 115, 1979.

13. A. D. Gorse, M. Pesquer,./. *Phys. Chem.,* 99, 4039, 1995.

14. T. Soujanya, G. Saroja, A. Samanta, *Chem. Phys. Lett.,* 236, 503, **1995.**

15. V. Masilamani, V. Chandrashekhar, B. M. Sivaram, B. Sivasankar, S. Natarajan, *Opt. Commun.,* 59, 203, 1986.

16. A. Ramalingam, P. K. Palanisamy, V. Masilamani, B. M. Sivaram, *J. Photochem. Phtobiol, A: Chem.,* 49, 89, **1989.**

17. R. W. Yip, Y. X. Wen, J. *Photochem. Photobiol., A: Chem.,* <u>54</u>, 263, **1990.**

18. C. Reichardt, *Solvent and Solvent Effects in Organic Chemistry,* VCH: Weinheim, **1988.**

19. K. Kalyanasundaram, J. K. Thomas,./. *Phys. Chem.,* <u>81</u>, 2176, **1977.**

20. K. Kalyanasundaram, *Photochemistry in Microheterogeneous Systems,* Academic Press: Orlando, **1987.**

21. J. **P.** Launay, M. Sowinska, L. Leydier, A. Gourdon, E. Amouyal, M. L. Boillot, F. Heisel, J. A. Miehe, *Chem. Phys. Lett.,* <u>160</u>, 89, **1989.**

22. S. A. Jonker, J. M. Warman, *Chem. Phys. Lett.,* <u>185</u>, 36, **1991.**

23. a) K. Bhattacharyya, M. Chowdhury, *Chem. Rev.,* <u>93</u>, 507, **1993;** b) W. Rettig, *Angew. Chem. Int. Ed. Engl.,* <u>25</u>, 971, **1986.**

24. **a)** K A Zachariasse, T. von der Haar, A. Hebecker, U. Leinhos, W. Kuhnle, *Pure Appl. Chem.,* <u>65</u>, 1745, **1993;** b) W. Schuddeboom, S. A. Jonker, J. M. Warman, U. Leinhos, W. Kuhnle, K. A. Zachariasse, *J. Phys. Chem.,* <u>96</u>, 10809, **1992;** c) K.A Zacharisse, M. Grobys, T. von der Haar, A. Hebecker, Y. V. Il'ichev, Y. -B. Jiang, O. Morawski, W. Kuhnle, ./. *Photochem. Photobiol. A: Chem.,* <u>102</u>, 59, **1996.**

25. U. Leinhos, W. Kuhnle, K. A. Zachariasse, *J. Phys. Chem.,* <u>95</u>, 2013, **1991.**

CONCLUDING REMARKS

The conclusions drawn from the investigations reported in the thesis are presented in this chapter. The scope of further work that could be carried out based on the present findings is also briefly discussed.

The work embodied in the thesis describes the Photophysical behaviour of some fluorescent electron donor - acceptor (EDA) systems in homogeneous and micellar media. The highly sensitive fluorescence properties of 4-aminophthalimide (AP) and 4-N,N-dimcthylaminophthalimide (DAP) on the polarity of the surrounding environment have been made use of in studying the microenvironments of the simplest membrane mimetic systems, micellar media, It has been shown that the aggregation of the surfactant molecules in aqueous solution can be very conveniently followed by monitoring any one of the following emission parameters of AP, fluorescence intensity, lifetime or position of the band maximum. It is of interest to note in this context that the ability of the AP derivatives to follow the micellar aggregation is not limited by the micellar charge. In this respect, the AP derivatives are found to be superior to many ionic EDA fluorescent systems. One of the several parameters that characterises a micellar aggregate, critical micelle concentration (CMC), has

been evaluated for three types of micelles using AP. The measured values are found to be in excellent agreement with the literature values. It has been unambiguously established that AP can always be located at the micelle-water' interfacial region. This preferential location of the fluorescence probe-molecule at the interface is found to be the result of a combination of hydrogen bonding interaction of AP with the water molecules and its hydrophobic interaction with' the micelles. The interfacial polarities of the anionic, cationic and neutral micelles, quantitatively measured using AP as fluorescent probe, in terms of microscopic polarity parameter, $E_T(30)$, show a rather small variation with the charge of the micelles.

A new amphiphilic fluorophore, APL has been developed, in which the AP fluorophore is covalently labelled to the nonpolar terminal group of a fatty acid, in an attempt to design fluorescence probe for the deeper core region of the micelles. The Photophysical properties of this system in homogeneous media are found to be quite similar to those of AP. In micellar media, however, APL shows stronger binding with the micelles. Even though the binding of APL with the micelles is found to be stronger than with AP, interestingly, the changes of the fluorescence properties of APL on micellisation are not found to be drastically different from those observed with AP. Fluorescence quenching studies suggest that despite its covalent attachment with the nonpola tail of the surfactant molecule, the fluorescing moiety of APL can still be located at the interface. Chain folding of the polymethylene spacer of APL has been proposed

in micellar media to account for this observation. Strong hydrogen-bonding affinity of the carbonyl groups of the fluorophore seems to be the driving force for this type of behaviour.

The studies involving DAP and DAPL reveal clearly the superiority of the DAP fluorophore compared to the AP fluorophore in sensing the hydrophobic regions of the micellar structure. The existence of a low-lying nonfluorescent TICT state below the fluorescent ICT state and enhanced hydrophobicity of the DAP fluorophore seem to account for the observed Photophysical behaviour of the compounds. Chain folding, as observed in the case of APL, has also been demonstrated in the case of DAPL.

A series of new n-(4-aminophthalimido)alkane derivatives have been synthesised and fully characterised with a view to understand their Photophysical behaviour in homogeneous media. Studies on these systems have led to some interesting observations particularly in aqueous media. For systems with large alkyl groups, the polarity sensed by the fluorophore in aqueous media is found to be considerably different from that of water. It has been shown that even at very low concentration, these molecules readily aggregate in aqueous solutions. The emission observed from these aggregates is found to be considerably different from that of the bare fluorophore in the same medium.

The photophysics of two Carbostyril laser dyes, Cl 24 and Cl65, which are structurally and electronically similar to extensively studied coumarin dyes, has been studies as a function of the solvent polarity to find out whether keto-

enol tautomerism and internal rotation (twisting) of the amino or dialkylamino group plays any role in influencing the Photophysical behaviour of these systems. The experimental studies have been supplemented by semi-empirical theoretical calculations. The results of this investigation reveal that the keto form of the Carbostyrils is the only dominant form, both in the ground and excited state. Further, unlike in coumarins, twisting of the dialkylamino group is found have no influence on the photophysics of the Carbostyrils. A reinvestigation of the fluorescence properties of a few coumarin dyes seems to be necessary based on the present findings. The preliminary investigation carried out to investigate the potential of the Carbostyrils as fluorescence sensors for micellar media reveals that although these systems can be used to follow the microheterogeneous environments, the fact that the magnitudes of the changes of the fluorescence properties are not very appreciable suggest that the Carbostyrils are not very promising systems among the EDA molecules.

The fluorescence behaviour of a dimeric species N,N'-bis(4-carbomethoxyphenyl)piperazine has been investigated in media of different polarities to determine the excited state dipole moment of this kind of highly symmetrical systems. The X-ray diffraction studies confirmed a highly symmetrical structure of the system in the ground state. On the other hand, the fluorescence data clearly indicate that the ground state symmetry of the molecule is lost in the excited state. It is argued that twisting alone can not account for extremely high dipole moment of the molecule in the excited state. Structural

changes in the piperazine ring seem to be necessary to account for the experimental findings.

Since hydrogen bonding interaction with water molecules is primarily responsible for the location of the fluorescent AP moiety at the micelle-water interface the development of AP-based fluorescence probe molecules for the nonpolar micellar core region requires development of systems where the hydrogen bonding interaction of the fluorophore with the solvent is prevented. Since the carbonyl groups of AP are found to be involved in hydrogen bonding interaction with water molecules, one can probably achieve this objective by designing systems in which the carbonyl groups are engaged in intramolecular hydrogen bonding interaction with appropriate groups (such as -OH group) at 3 and 6 positions of AP. This is one direction where further studies are to be made.

As hydrogen bonding interaction is also responsible for chain-folding in surfactant-linked systems, APL and DAPL; the structural modification as stated above might also help preventing such folding of the polymethylene groups. This aspect needs to be studied.

The investigations have been carried out only in membrane mimetic simple model systems. The present results will be useful in understanding more complex media of biological relevance such as membranes and proteins. Such studies are required to be undertaken.

The TICT model has recently been criticised and a new model has been proposed according to which a change in the hybridisation of the amino nitrogen is responsible for the nonradiative decay of the fluorescent LE state and long-wavelength fluorescence band of DMABN. It is therefore necessary to re investigate the Photophysical behaviour of dimethylamino derivative of AP to find out whether it can be understood in terms of the newly-proposed mechanism.

The results obtained with the dimeric molecule raises interesting possibilities. Further studies are necessary to find out the exact nature of the structural changes associated with the electronic excitation of the system.

APPENDIX

Table Al Atomic coordiantes [x 10^4] and equivalent isotropic displacement parameters [A x 10^3]. U(eq) is defined as one third of the trace of the orthogonalized U_{ij} tensor.

	x	y	z	U(eq)
0(1)	12622(2)	-255(3)	9334(2)	81(1)
0(2)	13203(2)	1035(3)	7849(2)	68(1)
N(l)	6365(2)	302(3)	5811(2)	44(1)
C(1)	7827(3)	330(3)	6425(2)	42(1)
C(2)	8922(3)	1106(4)	6006(2)	56(1)
C(3)	10352(3)	1123(4)	6630(2)	55(1)
C(4)	10746(3)	375(3)	7700(2)	45(1)
C(5)	9647(3)	-353(4)	8138(2)	51(1)
C(6)	8227(3)	-379(4)	7523(2)	50(1)
C(7)	12256(3)	325(4)	8388(3)	52(1)
C(8)	14732(3)	1018(5)	8445(3)	73(1)
C(9)	5613(3)	-1280(4)	5754(3)	56(1)
C(10)	6007(3)	1113(4)	4689(2)	58(1)

Table A2 Bond lengths [A] and angles [°].

O(1)-C(7)	1.197(3)	O(2)-C(7)	1.340(3)
O(2)-C(8)	1.452(3)	N(1)-C(1)	1.404(3)
N(1)-C(10)	1.457(3)	N(1)-C(9)	1.464(3)
C(1)-C(2)	1.391(4)	C(1)-C(6)	1.399(4)
C(2)-C(3)	1.383(4)	C(3)-C(4)	1.383(4)
C(4)-C(5)	1.390(4)	C(4)-C(7)	1.471(4)
C(5)-C(6)	1.371(4)	C(9)-C(10)#1	1.502(3)
C(10)-C(9) #1	1.502(3)		
C(7)-O(2)-C(8)	117.0(2)	C(1)-N(1)-C(10)	117.8(2)
C(1)-N(1)-C(9)	116.4(2)	C(10)-N(1)-C(9)	110.3(2)
C(2)-C(1)-C(6)	117.1(2)	C(2)-C(1)-N(1)	122.5(2)
C(6)-C(1)-N(1)	120.3(2)	C(3)-C(2)-C(1)	121.5(3)
C(2)-C(3)-C(4)	121.0(3)	C(3)-C(4)-C(5)	117.7(2)
C(3)-C(4)-C(7)	123.3(3)	C(5)-C(4)-C(7)	119.0(2)
C(6)-C(5)-C(4)	121.5(3)	C(5)-C(6)-C(1)	121.1(2)
O(1)-C(7)-O(2)	122.5(3)	O(1)-C(7)-C(4)	124.8(3)
O(2)-C(7)-C(4)	112.6(3)	N(1)-C(9)-C(10)#1	112.2(2)
N(1)-C(10)-C(9) #1	111.7(2)		

Symmetry transformations used to generate equivalent atoms: #1 -x+1, -y, -z+1.

212

Table A3 Anisotropic displacement parameters [A^2 x 10^3]. The anisotropic displacement factor exponent takes the form: $-2n^2 [(ha^*)^2 U_{11} + \ldots + 2hka^*b^*U_{12}]$.

	U11	U22	U33	U23	U13	U12
O(1)	47(1)	124(2)	62(2)	23(1)	-5(1)	0(1)
O(2)	35(1)	96(2)	67(1)	12(1)	0(1)	-5(1)
N(1)	39(1)	45(1)	44(1)	5(1)	-1(1)	-7(1)
C(1)	32(1)	43(2)	48(2)	-1(1)	3(1)	0(1)
C(2)	45(2)	72(2)	48(2)	13(2)	2(1)	-7(2)
C(3)	42(2)	66(2)	54(2)	6(2)	7(1)	-9(1)
C(4)	38(2)	48(2)	48(2)	-4(1)	5(1)	4(1)
C(5)	44(2)	60(2)	44(2)	6(1)	0(1)	3(1)
C(6)	41(2)	59(2)	50(2)	10(1)	9(1)	-4(1)
C(7)	40(2)	60(2)	53(2)	-7(2)	4(1)	4(1)
C(8)	36(2)	96(3)	80(2)	2(2)	0(2)	1(2)
C(9)	45(2)	54(2)	60(2)	12(2)	-5(1)	-8(1)
C(10)	45(2)	65(2)	56(2)	14(2)	-4(1)	-12(2)

Table A4   Hydrogen coordinates (x 10^4) and isotropic displacement parameters (A°2×103).

	x	y	z	U(eq)
H(2)	8686(3)	1624(4)	291(2)	68
H(3)	11062(3)	1646(4)	6326(2)	65
H(5)	9881(3)	-834(4)	8866(2)	61
H(6)	7517(3)	-876(4)	7841(2)	60
H(8A)	15301(3)	1558(5)	7978(3)	109
H(8B)	15056(3)	-98(5)	8580(3)	109
H(8C)	14848(3)	1581(5)	9169(3)	109
H(9A)	5807(3)	-1765(4)	6519(2)	67
H(9B)	5998(3)	-2015(4)	5253(2)	67
H(10A)	6410(3)	483(4)	4141(2)	69
H(10B)	6451(3)	2194(4)	4755(2)	69